PolyPublie
Polytechnique Montréal

POLYTECHNIQUE MONTRÉAL
UNIVERSITÉ D'INGÉNIERIE

Titre: Title:	Chemical Recycling of Meta-Aramid Fibres Into Nanofiber for Particulate Blocking Firefighter Hood
Auteur: Author:	Joseph-Émile Laquerre
Date:	2023
Type:	Mémoire ou thèse / Dissertation or Thesis
Référence: Citation:	Laquerre, J.-É. (2023). Chemical Recycling of Meta-Aramid Fibres Into Nanofiber for Particulate Blocking Firefighter Hood [Mémoire de maîtrise, Polytechnique Montréal]. PolyPublie. https://publications.polymtl.ca/57115/

Document en libre accès dans PolyPublie
Open Access document in PolyPublie

URL de PolyPublie: PolyPublie URL:	https://publications.polymtl.ca/57115/
Directeurs de recherche: Advisors:	Abdellah Ajji, & Ahmad Ibrahim
Programme: Program:	Génie chimique

Ce fichier a été téléchargé à partir de PolyPublie, le dépôt institutionnel de Polytechnique Montréal
This file has been downloaded from PolyPublie, the institutional repository of Polytechnique Montréal

https://publications.polymtl.ca

POLYTECHNIQUE MONTRÉAL

affiliée à l'Université de Montréal

Chemical recycling of meta-aramid fibres into nanofiber for particulate blocking firefighter hood

JOSEPH-ÉMILE LAQUERRE

Département de génie chimique

Mémoire présenté en vue de l'obtention du diplôme de *Maîtrise ès sciences appliquées*

Génie chimique

Décembre 2023

© Joseph-Émile Laquerre, 2023.

POLYTECHNIQUE MONTRÉAL

affiliée à l'Université de Montréal

Ce mémoire intitulé :

Chemical recycling of meta-aramid fibres into nanofiber for particulate blocking firefighter hood

présenté par **Joseph-Émile LAQUERRE**

en vue de l'obtention du diplôme de *Maîtrise ès sciences appliquées*

a été dûment accepté par le jury d'examen constitué de :

Jason Robert TAVARES, président
Abdellah AJJI, membre et directeur de recherche
Ahmad IBRAHIM, membre et codirecteur de recherche
Sampada BODKHE, membre

ACKNOWLEDGEMENTS

The work in this master results from the collaboration of Polytechnique Montreal, CTT Group, and an industrial partner. The master was pursued while working full time at CTT group as a project leader. I would like to thank my research director Prof. AJJI Abdellah (Polytechnique), my co-director IBRAHIM Ahmad (CTT) and DECAENS Justine (CTT) for their generous access to equipment and expertise, allowing me to work on this project and supporting me during this work.

Additionally, I am grateful for the financial support. I acknowledge the support of the Natural Sciences and Engineering Research Council of Canada (NSERC), [funding reference number RDA 571060-21 and RGPIN-2021-03902]. This project is also supported by Investissement Québec through the innovation programs support for innovation projects, [reference number SQRI51446].

RÉSUMÉ

L'exposition des pompiers aux produits chimiques et aux particules par voie cutanée est problématique pour leur santé; la zone de la mâchoire et du cou est particulièrement mal protégée et sensible à l'absorption (Stec et al., 2018). Afin d'améliorer la protection de cette zone, une membrane de filtration est ajoutée dans les cagoules. Depuis 2018, la norme du National Fire Protection Agency (NFPA) 1971 décrit les exigences pour la membrane de protection (NFPA1971, 2018). La membrane doit balancer entre des critères de protection contre les particules et de confort par l'évacuation de la sueur.

Les barrières actuelles sont basées sur des films expansés de polytétrafluoroéthylène (ePTFE) ou de nanofibre de polyimide (Nomex® Nanoflex) produit par W.L. Gore & Associates et DuPont (Barbeau, Lozier, & Rousse, 2018; Blake et al., 2021; Sonntag, 2020). L'utilisation des substances perfluorée et polyfluoroalkylées (SPFA) dans les habits sont potentiellement problématiques pour la santé des pompiers et pour l'approvisionnement de l'industriel avec la proposition de bannir leur usage non essentiel par REACH. Le développement d'un nouveau filtre à particules sans SPFA se basera sur les principes établis de filtrations des gaz, des micros aérosols et de nano aérosols (Leung, 2021). Deux méthodes de fabrication seront évaluées.

Le ratio de surface élevée des nanofibres augmente l'efficacité de filtration, sans réduire le débit d'air. Étant donné cet effet unique, la première méthode de fabrication sélectionnée est l'électrofilage (Li, Shang, Li, & Yang, 2017a; T. Lu et al., 2021). Un défi du projet est la sélection d'un polymère pour satisfaire les critères de résistance thermique tout en étant soluble et stable à l'électrofilage.

L'électrofilage est comparé à une membrane hydrophile à base de polyuréthane et de nanofibre d'aramide. La membrane non poreuse offre une meilleure protection contre les composés organiques volatils et hydrocarbonés aromatiques polycycliques. Les propriétés de confort, de protection et de durabilité sont jugées acceptables selon les critères établis. Une efficacité de filtration de 99.8% à 0.3 micron et une efficacité de protection aux composés organiques volatils supérieures aux produits commerciaux sont obtenues.

ABSTRACT

Exposure of firefighters to chemicals and particles through the skin is problematic for their health; the jaw and neck area are particularly poorly protected and sensitive to absorption (Stec, Dickens et al. 2018). To improve the protection of this area, a filtration membrane is added to the hoods. Since 2018, the National Fire Protection Agency (NFPA) 1971 standard describes the requirements for the hood protective membrane (NFPA1971, 2018). The membrane must balance between criteria of protection against particles and comfort through the evacuation of sweat.

Current barriers are based on expanded polytetrafluoroethylene (ePTFE) or polyimide nanofiber nonwoven (Nomex® Nanoflex) produced by W.L. Gore & Associates and DuPont (Barbeau, Lozier et al. 2018, Sonntag 2020, Blake, Harper et al. 2021). The use of per-fluoro and polyfluoroalkyl substances (PFAS) in turnout gear are potentially problematic for the health of firefighters and with the proposal to ban their non-essential use by REACH. The development of a new PFAS-free particle filter will be based on the established principles of filtration of gases, micro aerosols and nano aerosols (Leung, 2021). Electrospun membrane and a knife coated membrane are evaluated for the application. The high surface area ratio of the nanofibres increases filtration efficiency, without reducing air flow(Li et al., 2017a; T. Lu et al., 2021). A challenge of the project is the selection of a polymer to meet the thermal resistance criteria while being stable to electrospinning. A hydrophilic membrane of polyurethane and aramid was prepared by knife-over-roll coating method. The non-porous membrane by knife coating offers a better protection against volatile organic compounds and polycyclic aromatic hydrocarbons. The comfort, protection and durability properties are considered acceptable according to established criteria. A filtration efficiency of 99.8% at 0.3 microns and a superior protection against volatile organic compounds to commercial products are obtained.

TABLE OF CONTENT

ACKNOWLEDGEMENTS iii

RÉSUMÉ iv

ABSTRACT v

TABLE OF CONTENT vi

LIST OF TABLES ix

LIST OF FIGURES x

LIST OF SYMBOLS AND ABBREVIATIONS xii

LIST OF APPENDICES xiv

CHAPTER 1 INTRODUCTION 1

CHAPTER 2 LITERATURE REVIEW 3

2.1 Regulatory changes and problematics 3

2.2 High Performance Polymers 5

2.3 Commercial product of aramid 8

2.4 Processing of aramid 8

2.5 Aramid recycling 8

2.6 Hood filtration media 14

2.7 Filtration mechanism 20

2.8 Heat Loss for Thermal Comfort and Heat Stress 23

2.9 Conclusion and perspectives 23

2.10 General objective 24

2.11 Specific objectives 24

CHAPTER 3 MATERIALS AND CHARACTERIZATION METHODS 25

3.1 Materials 25

3.2 Polymer Characterization 25
3.3 Characterization of fibrous media 26
3.4 Hood characterization 27
CHAPTER 4 ELECTROSPUN NANOFIBER 30
4.1 Electrospinning rationale 30
4.2 Preparation of Solution 30
4.3 Preparation of electrospun mats 31
4.4 Evaluation of Solvent for Solution Preparation 32
4.5 Evaluation of adhesion to nonwoven fabric 34
4.6 Evaluation of Flame Retardancy 37
4.7 Conclusion 39
CHAPTER 5 NANOFIBER BY DEPROTONATION 40
5.1 Nanofiber by deprotonation justification 40
5.2 Pre-treatment 40
5.3 Kinetic study 41
5.4 Nanofiber Morphology 45
5.5 Nanofiber Thermal Stability 46
5.6 Scale Up 47
5.7 Coating on Fabric 47
5.8 Conclusion 48
CHAPTER 6 DEVELOPMENT OF COATING 49
6.1 Feed preparation 49
6.2 Optimization of the Coating 51
6.3 Evaluation of the coated textile 55

6.4 Evaluation of the Handle 58
6.5 Wash Durability 59
6.6 Flame Resistance 60
6.7 Particulate Blocking Efficiency 61
6.8 Permeation to VOC 62
6.9 Conclusion and perspectives 64
CHAPTER 7 ARTICLE 1: DOES THE NFPA 1971-2018 PARTICULATE-BLOCKING HOOD PROTECT AGAINST VOC? AN EVALUATION OF FIREFIGHTER'S HOOD WITH PARTICULATE-BLOCKING BARRIER AGAINST VOC 66
7.1 Abstract 66
7.2 Introduction 67
7.3 Material 69
7.4 Method 69
7.5 Results and discussion 71
7.6 Conclusion 77
CHAPTER 8 CONCLUSION AND PERSPECTIVES 79
REFERENCES 82
APPENDIX 89

LIST OF TABLES

Table 2-1. Typical properties of high-performance fibre (Horrocks, 2016) 6

Table 5-1. Summary of progress in deprotonation reaction 13

Table 2-2. Summary of aramid recycling method 14

Table 2-3. Airborne particles categories 20

Table 3-1. Characterization method of polymers and fibre 27

Table 3-2. Method of testing hoods according to the NFPA (NFPA1971, 2018) 28

Table 4-1. Comparison of solvent properties (A.Chandrasekaran) 33

Table 4-2. Evaluation of flame retardancy of nanofiber coated fabric 38

Table 5-2. Scouring solutions for aramid 40

Table 5-3. Approximation of length over diameter ratio of neat fibre and chemical nanofiber ... 46

Table 6-1. Initial polyurethane-aramid coating formulation 49

Table 6-2. Observation of wetting on release paper 52

Table 6-3. Final formulation of polyurethane with aramid 54

Table 6-4. Water permeability of hydrophilic polyurethane aramid film 56

Table 6-5. Comparison of total heat loss of barriers and hood composite 57

Table 6-6. Evaluation of the bending rigidity on the Kawabata 58

Table 6-7. Vertical flame test of coated fabric 61

Table 6-8. Evaluation of the particulate blocking efficiency 62

Table 6-9. Evaluation of the permeation of coated textiles 64

Table 7-1. Evaluation of permeation of the hood and hood barrier against Tetralin 75

Table 7-2. Evaluation of hood barriers air permeation and water resistance. 77

LIST OF FIGURES

Figure 1-1. Schematic of a composite structure of the garment 1

Figure 2-1. Examples of a NFPA 1971 2018 Edition firefighter hood 3

Figure 2-2. Chemical structure of para-aramid and meta-aramids 7

Figure 2-3. Production of drylaid webs with carding and take-off (Brydon, Pourmohammadi, & Russell, 2022) 16

Figure 2-4. Wet-laid web formation (Koukoulas, 2022) 17

Figure 2-5. Electrospinning process(Inovenso, 2022) 18

Figure 2-6. Filtration efficiency of different mechanisms (Thomas et al., 2018) 22

Figure 3-1. Schematic of the filtration apparatus (NFPA1971, 2018) 29

Figure 4-1. Dissolving apparatus 31

Figure 4-2. Electrospinning apparatus 32

Figure 4-3. Fiber degradation after surface treatment 35

Figure 4-4. SEM observation of fabric after 0.6 kV corona treatment, before electrospinning. .. 35

Figure 4-5. Adhesive dot on the nanofiber and nonwoven 36

Figure 4-6. Evaluation of adhesion by basis weight of the peeled tape 37

Figure 4-7. Specimens with a coating (left) and without a coating (right) 38

Figure 5-1. Wetting of aramid before (left) and after pretreatment (right) 41

Figure 5-2. Kinetic study of alkali ratio on formation of aramid nanofiber 42

Figure 5-3. Reaction rate in function of water content 43

Figure 5-4. Effect of temperature on reaction kinetics of aramid nanofiber 44

Figure 5-5. Effect of temperature on reaction rate natural logarithms 45

Figure 5-6. Effect of the chemical treatment compared to the original fibre (top left) 45

Figure 6-1. Aramid particle before dispersion 50

Figure 6-2. Top view of the coated knit defects and defect-free observed by SEM 53

Figure 6-3. Coated knit (coated side) 54

Figure 6-4. Schematic of test cell 63

Figure 6-5. Schematic of the photoionization detector (Science, 2021) 63

Figure 7-1. Cross-section (left) and top view (right) of Stedair Prevent tri-laminate. 72

Figure 7-2. Hood composite (left) and nanoflex barrier (right) cross-section view. 73

Figure A-1. PID PPB Calibration against Isobutylene 89

Figure B-1. Aramid deprotonation in function of time 92

Figure B-2. Nonwoven before and after scouring 92

Figure B-3. FTIR of aramid before (black) and after (red) scouring 93

LIST OF SYMBOLS AND ABBREVIATIONS

AATCC	Association of Textile Chemists and Colorists
Abs.	Absorbance
ASTM	American Society for Testing and Materials International
CAN/CGSB	Canadian General Standards Board Catalogue
CAS	Chemical Abstracts Service
DMAc	Dimethylacetamide
DMF	Dimethylformamide
DMSO	Dimethyl sulfoxide
ECHA	Enregistrement, évaluation et autorisation des produits chimiques
ePTFE	expanded Polytetrafluoroethylene
FTIR	Fourier transform infrared spectrometer
IAFF	International association of fire fighters
LiCl	Lithium Chloride
LOD	Loss on drying
Min.	Minute
mol	mole
MPPS	Most penetrating particle size
mV	millivolt
NFPA	National Fire Protection Association
NIOSH	National Institute for Occupational Safety and Health, U.S. Department of Health and Human Services
nm	nanometre
PAH	Polycyclic aromatic hydrocarbon

PBI	Polybenzimidazole
PFAS	Per- and polyfluoroalkyl substances
pH	potential of hydrogen
PID	Photoionization Detectors
PM	Particulate matter
PMTA	polymetaphenylene isophthalamide
ppb	part per billion
ppm	part per million
PU	Polyurethane
REACH	Registration, Evaluation, Authorization and restriction of CHemicals
SCBA	Self-contained breathing apparatus
SEM	Scanning electron microscope
SPFA	Substances per-fluoro et polyfluoroalkylés
TFE	2,2,2-Trifluoroethanol
TGA	Thermogravimetric analysis
TOP	Test Operations Procedure, U.S. Army Developmental Test Command
Uv-vis	Ultraviolet and visible light
VOC	Volatile organic compound

LIST OF APPENDICES

APPENDIX A : VALIDATION METHOD FOR VOC ANALYSIS 89

APPENDIX B : SEM, UV-VIS AND FTIR SPECTRUM 93

CHAPTER 1 INTRODUCTION

Protective equipment used in firefighting must balance between properties of comfort and protection. The garment should protect against the convective, conductive and radiant heat from fire to prevent burn, while allowing sufficient cooling by evaporation of the sweat to avoid excessive heat burden. Moreover, the permeability to sweat should be balanced with the barrier properties against harmful chemicals released during combustion. Finally, the material should be durable in the used condition; the material should be stable to heat, flame, washing, drying and repeated uses. The National Fire Protection Association (NFPA) 1971: Standard on Protective Ensemble for Structural Fire Fighting and Proximity Fire Fighting 2018 Edition is responsible for establishing the minimal performance requirements of firefighting protective equipment (NFPA1971, 2018).

Multiples personal protective equipment (PPE) are worn by firefighters to protect against chemicals found in structural firefighting situation (Park, Park, Lin, & Boorady, 2014). Self-contained breathing apparatus (SCBA) are worn by firefighters to protect from exposure by inhalation, and have proven efficient. Turnout gear such as hood, jacket and pants are worn to prevent exposure to chemicals. Garments and pants are equipped with a moisture barrier to protect against liquid chemicals penetration (NFPA1971, 2018) such as hydraulic fluid, gasoline, battery acid and other. A multiple layer structure is used to obtain the protection properties required for the firefighter gear. The garment layers can be composed of woven, non-woven, knit, coating and film. A general garment structure is composed of an outer shell, a barrier and a thermal liner (NFPA1971, 2018) (Corbett, 2009).

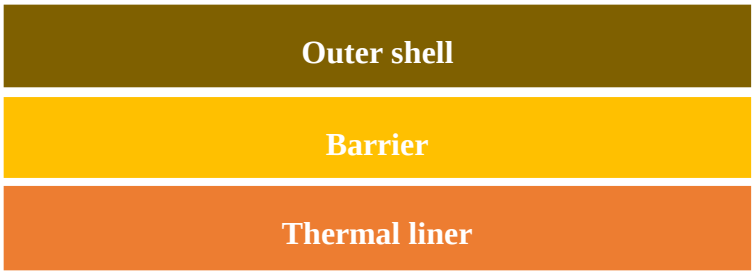

Figure 1-1. Schematic of a composite structure of the garment

The outer shell is a rugged layer designed to protect against the outside environment as flame and abrasion (Corbett, 2009). The barrier layer is used to protect against chemical liquid, bloodborne

pathogen, volatile organic compound (VOC) and particulate penetration (Corbett, 2009). The thermal layer is the innermost layer. The inner layer must protect against heat, be comfortable and ease the donning and doffing of the equipment(Corbett, 2009). The layers of the composite can be combined or assembled in the final garment by laminating or quilting for example(Corbett, 2009).

Since 2018, an optional particulate barrier is available on hoods to protect against particulates and chemicals (NFPA1971, 2018). This project will treat of the development and evaluation of a barrier for firefighter's hood to meet the requirement of the NFPA 1971 edition 2024.

In this document containing 7 chapters, the first chapter introduced the subject of the firefighting gear and the hood barrier. In the second chapter, the literature review presented the polymer used in firefighting, the fabrication method of the filtration media, air filtration and heat loss mechanism. The polymer and barrier developed in this project will be characterized and tested. The characterization method of the polymer, barrier and hood used for the development of an improved barrier are presented in the section material and method in the third chapter.

To improve on the design of the hood barrier, two methods of fabrication will be evaluated for hood barriers. The first method of fabrication is a nonwoven of nanofiber by electrospinning with a bottom-up approach presented in the chapter 4. The second method of preparation of nanofiber by deprotonation, or top-down approach, will be presented in the fifth chapter. The nanofibers are used in the preparation of a hydrophilic coating. The chapter 6 presents the results and characterization of the developed hydrophilic membrane for hood barriers. To address the issue around VOC and PAH permeation in firefighting hood, a submitted publication about the permeation to VOC of the developed barrier is presented. The publication reviews the current certified hood and compare it to the developed hydrophilic barrier.

The appendix A explains the design choices and validation of the method to evaluate permeation of chemicals in the hood barrier. The appendix B is supplementary spectrum, thermogravimetric analysis and microscope image of the scoured aramid.

CHAPTER 2 LITERATURE REVIEW

The hoods became a standard part of the firefighters' ensemble about 30 years ago. They are one of the least protected parts of the ensemble, due to the construction. The hood is fitted over the head to seal the SCBA and protect the head-neck interface, a bib is tucked under the collar of the jacket.

Figure 2-1. Examples of a NFPA 1971 2018 Edition firefighter hood

Until the 2018 edition of NFPA 1971, the construction lacked a barrier membrane required to protect against chemical hazards and fine particles, leaving the skin exposed to carcinogens. The development of a new particulate blocking layer for hood will have to tackle the presented challenges in firefighter ensemble.

The industrial partner uses an expanded polytetrafluoroethylene (ePTFE) membrane as the current chemical protection membrane for hood barriers. Fluorinated polymers are resistant to many chemicals and heat due to the strong covalent bonding and high crystallinity of the material. The porous structure obtained by stretching the PTFE film gives the membrane permeability to gas, vapour and humidity required to evaporate the sweat. The fine fibrillated structure of ePTFE protects against fine particles. Despite the material properties, the use of PFAS in firefighters' gear has been criticized.

2.1 Regulatory changes and problematics

The European Chemicals Agency (ECHA) has published the regulation registration, Evaluation, Authorization and Restriction of Chemicals (REACH) Restriction Proposal for Per- and Polyfluoroalkyl Substances (PFAS) to restrict its manufacture and uses due to its negative impact on environment and human health. PFAS are known to be persistent in the environment, toxic,

harmful to reproduction, may harm the unborn child, may cause several cancers and is suspected of interfering with the hormonal system (Paris-Davila, Gaines, Lucas, & Nylander-French, 2023; Peaslee et al., 2020). PFAS has been used in a variety of firefighting products, and is still used in some applications for foam, textile finish and garment barriers. The firefighting foam is used to extinguish fuels based fires by armed forces, aviation, municipal and industries (Peshoria, Nandini, Tanwar, & Narang, 2020). Its uses are a concern for environmental pollution and health issue. PFAS are also used in oil and water-repellent finishing used in the garment to protect against chemical and water and to improve drying of the fabric. Finally, PFAS are used in the barrier membrane in the form of ePTFE.

The high level of PFAS found in turnout gear (Peaslee et al., 2020) could be one of the pathways of exposure. The international association of firefighters (IAFF) is working with three law firms to modify regulatory standards, demand PFAS-free gear, and seek compensation for PFAS-related illness for members and families. The current draft of NFPA 1971: 2024 Edition has addressed the raising concern around PFAS with the possibility of a PFAS FREE label for protective equipment without the intentional addition of PFAS to facilitate identification.

The chemical particles generated during combustion can be of volatile organic compounds (VOC), polycyclic aromatic hydrocarbons (PAH) and fine particulate matter (PM) (Sjöström, Julander, Strandberg, Lewné, & Bigert, 2019). It has been demonstrated that the firefighters are exposed to increased concentrations of chemicals and have higher rates of cancers compared to the general population (Lee et al., 2020; Stec et al., 2018). An increase in concentration of chemicals in air from inside the garment was noted, additionally, an increase in metabolites of VOC and PAH was observed in biological samples taken before and after the firefighting situation. (Fent et al., 2022; Fent et al., 2020; Mayer et al., 2022; Mayer et al., 2023; Sjöström et al., 2019; Stec et al., 2018).

Studies on firefighter conducted by trained professional using analytical method demonstrated the penetration of VOC and increase in metabolites of VOC (Mayer et al., 2023). In the study, the firefighting equipment was worn, including the SCBA to protect against inhalation of chemicals and doffing best practice were used to avoid self-contamination. The dermal absorption is the most plausible exposure route to rationalize the increased chemicals in biological samples after firefighting (Mayer et al., 2023; Stec et al., 2018). VOC and PAH can penetrate the garment and could penetrate the skin to increase the metabolite of VOC and PAH. The penetration rate could

be higher in the jaw and neck region where the skin is thinner and important blood vessels are present (Fent et al., 2013; Mayer et al., 2023) and where the skin is less protected by the personal protective gear (Stec et al., 2018). Ideally, the hood barrier should protect the wearer against VOC and PAH.

In summary, the development of firefighting gear should consider those problems: uses of PFAS in firefighters' gear, exposure to VOC and PAH, and balancing protection, comfort and durability. The hood and the hood barrier will require material resistant in the conditions of uses. High performance polymers are required to support the intense temperature and chemical resistance for the application. Those polymers can be processed to prepare the hood barrier in the form of a nonwoven, porous membrane or hydrophilic coating to obtain a sufficient permeability to water vapour and protection against non-polar chemicals and particles. This literature review will present the fabrication of a barrier for hood by presenting the high-performance polymers available for firefighting gear, recycling, the method of fabrication of a barrier and the mechanism of filtration.

2.2 High Performance Polymers

High performance polymers and fibres are required due to the high temperature environment of the firefighting situation. The selected material for hood barriers should not melt, should be stable at the maximum operating temperature and should not ignite.

The stability of high-performance fibre is mostly based on the aromatic backbone of the polymer, as seen in the table 2-1. The high crystallinity of these fibres gives high mechanical properties. The fully aromatics polymers shown in the table 2-1 do not exhibit a melting point. This property is desirable for the protection of the wearer against drip or shrinkage. However, it restricts the method of processing to solvent-based processes. In the table 2-1, the limiting oxygen index indicates the concentration of oxygen required to maintain combustion of the polymer. As oxygen concentration is about 21% in atmospheric condition, a greater value indicates the material as nonflammable (Horrocks, 2016). The decomposition temperature indicates the temperature at which the material begins to carbonize. A high degradation temperature shows a thermal stability of the fibre.

Table 2-1. Typical properties of high-performance fibre (Horrocks, 2016)

Polymer	Trade name	Structure	Decomposition temperature (°C)	Limiting oxygen index (%)	Melting
Meta-aramid	Nomex, Tejinconex	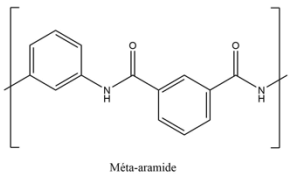 Méta-aramide	375-430	29-30	No
Para-aramid	Kevlar, Twaron, Technora	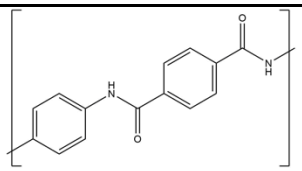 Para-aramide	560	29	No
Polyamide-imide	Kermel	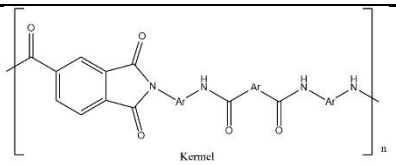 Kermel	400	30-32	
Aromatic polyimide (Evonik)	P84	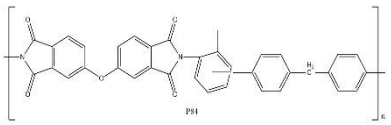 P84	≥ 370	38	No
Polybenzimidazole (Shiels, Copeland, & Qin, 2017)	PBI	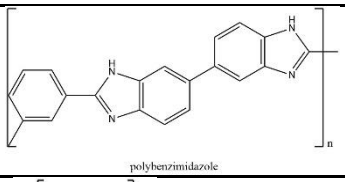 polybenzimidazole	≥ 555	> 50	No
Polytetrafluoroethylene	Gore-Tex	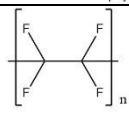 polytetrafluoroethylene	400	> 95	Yes

This project will focus on aramid for the development of the hood barrier. The meta-aramid was selected due to the large availability, low cost and proven use in firefighting garments.

Aramids are a subcategory of polymers from the polyamide family. They have a characteristic aromatic function between the amides moieties. There are two configurations at the aromatic branching, either in position 1,4 (para) or in position 1,3 (meta).

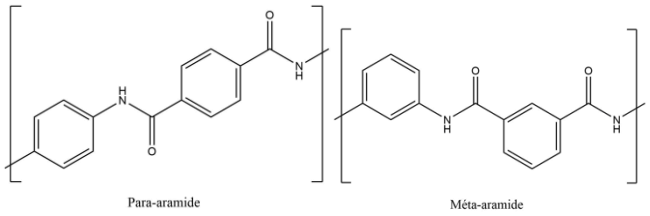

Figure 2-2. Chemical structure of para-aramid and meta-aramids

Both chemical structures have stiff and stable aromatic function. Intermolecular interactions, in particular through hydrogen bonds, confer high mechanical properties. The structure of para-aramid promotes high crystallinity, which results in superior mechanical properties compared to the meta-aramid. The thermal resistance of the material is high; the glass transition of aramid is of about 280 °C (Godwin & Kutz, 2017), the degradation is at about 375°C (Mather, Rana, & Wardman, 2023) and the material does not melt. The decomposition of the material occurs before the melting point; therefore, the aramid cannot be processed by conventional melt process. The aramid is a specific thermoplastic named liquid crystal polymer (LCP) (Dupont, 2019) (Dupont, 2017). The preparation of the LCP from aramid requires the uses of solvents. This implies specialized equipment for processing and solvent recuperation, which is reflected in the high price of the aramid fibre (Godwin & Kutz, 2017). Another disadvantage of the aramid fibre is the poor stability to ultraviolet and visible rays from 300-400 nm, and the moisture absorption, which limits the use of aramids in certain applications (Mather et al., 2023). The aromatic nature of the aramid is responsible for the absorption of the UV light (Godwin & Kutz, 2017). The polarity of the amide is responsible for the absorption of water.

Another type of polyamide is the partially aromatic polyamide. Partially aromatic polyamide bridges the processability of aliphatic amid (nylon) and the mechanical and thermal performance of aramid. Partially aromatic polyamide can be processed in melt phase and with easier polymerization technique (Fink, 2014). Aromatic polyamide will be covered in this project.

2.3 Commercial product of aramid

Aramids are supplied in forms powder, yarns, fibres, and pulp to be used in material such as composites, films, textiles and papers. This report will focus on aramid fibres, which is produced almost exclusively by the company DuPont and Teijin. The development and the commercialization of aramid materials were done by DuPont. Aramid fibres are sold under the trade name Nomex® for meta-aramid and Kevlar® for para-aramid material. Teijin produce meta-aramid fibre Tejinconex® and the para-aramid Twaron® and Technora® (Bhattacharyya & Fakirov, 2012).

2.4 Processing of aramid

Aramid fibres are produced via solution spinning. The meta-aramid is dissolved in an organic solvent. Para-aramid is much more difficult to dissolve. It can be dissolved in concentrated sulfuric acid. The solution is extruded through a spinneret and stretched in air or liquid. The solvent can be eliminated by dry spinning by drying in air or in contact with a hot roll or in a non-solvent bath for wet spinning. The drawing of the fibre increases the orientation of the polymer. Heat treatment can enhance the orientation of the fibre and further improve the mechanical properties of the fibre (Mather et al., 2023). The fibre can be washed and dried to remove residual solvent and impurity.

Fibrids and pulps are used in the manufacturing of aramid paper. Fibrids are small particles of aramid formed by coagulation under high shears. The fibrids can be used to reinforce aramid paper, composite, coating and elastomer. The fibrids has a high surface area, therefore mixing can be challenging.

Pulp is also used in the manufacturing of paper. Pulp is formed by cutting yarns in small fibres. The small fibres are suspended in water with fibrid to form a mixture referred as floc. The floc is used in the fabrication of aramid paper. Production scraps such as broken paper in mill is considered as a waste and can be sent to the landfill (B. Yang et al., 2018).

2.5 Aramid recycling

Global production is around 80,000 tonnes per year (H.-J. Chen, Bai, Liu, Wu, & Wang, 2021), and therefore waste management is important given the cost, and the need for preventive replacement in PPE applications. Aramid waste is not biodegradable. Thus, recycling would be an

alternative solution over landfilling given the high value and non-biodegradability properties of aramid.

2.5.1 Mechanical recycling of aramid textile

Mechanical recycling uses mechanical energy to separate the aramid from other materials. The materials go through a preparation steps before the mechanical recycling. Usually, the preparation steps can include separation of the material, removing of foreign material, shredding or other means of size reduction, and cleaning. The mechanical recycling can be done by defibrillation or defibering, grinding, milling or other mechanical separation technique. Overall, the mechanical recycling is a simple method, and can be of lower-cost compared to other recycling methods.

However, the mechanical recycling is limited for highly contaminated post consumer material. The textile waste contains heavy contamination which cannot be completely removed by the pre-treatment. Contamination can foul, disrupt or interfere with the downstream process, resulting in lower-quality material and increased equipment maintenance. The purity of the starting material is important for mechanical recycling.

The mechanical recycling results in fibrillation of the fibres, where fibrils are exposed on the fibres surface. The fibres surface roughness is increased and the thickness of the fibre is reduced, which results in loss of mechanical properties of the fibre. The roughness of the fibrils can give an unpleasant handle and lower shine of the fibre. However, fibrillation can be advantageous in some applications. Fibrillation can also improve the adhesion (Karlsson, Gatenholm, Blachot, & Peguy, 1996), filtration (Nan, Xiang-yu, Chen, & Qin-fei, 2017; Xu et al., 2020) and insulation (Z. Lu et al., 2017) due to the increase of the surface. Overall, the mechanical recycling process will affect the properties of aramid fibre.

The defibrillation is carried by separating the fibre from the fabric by cutting, shredding and carding the fibre. Other mechanical process can be added. Cutting is done to size the material for the equipment and remove accessories such as fasteners, zipper, hook, loop, etc. Further resizing and the first opening of the fibre is accomplished by shredding. The shredding is followed by carding. The carding opens, separates and induces parallelization of the fibres. During the carding, the fibres bundles are held while a comb move, resulting in separation of the fibre. The fibre can be elongated and twisted to produce the yarn with conventional spinning equipment (PARKER & Kasper, 2020).

The fibre breakage during the mechanical recycling results in various fibre lengths and are separated into long fibre, short fibre and pulp (B. Yang, Li, Zhang, Wang, & Ding, 2021).

New materials are made from the recycled pulp and fibre. The pulp materials are used in the fabrication of aramid paper for applications. Aramid pulp can also be used in compound material such as rubber to improve the mechanical properties. Recycled pulp is used for lower performance composite applications in brake pads and gaskets. Recycled aramid pulp has been used friction material such as brake pads (Manoharan, Krishnaraj, Vijay, Singaravelu, & Suresha, 2017; Manoharan et al., 2019; Sloan, 2008). In 2013, 770 tons of used aramids were transformed into Twaron Eco advanced for applications in the form of pulp(Aramid).

Short fibre unsuitable for the fabrication of yarn can be converted in pulp. The material is first chopped into short fibre and suspended in water. The resulting slurry is then processed in a mill refiner in order to obtain a pulp with reduced size and increased surface area (Bhattacharyya & Fakirov, 2012).

Using end-of-life material with contamination from inflammable material (oil, fuel, solvents, dirt) can significantly reduce the performance of the aramid fibre(Crown & Batcheller, 2016). In recycled application, the soiled fabric should be pretreated to remove the contamination. Liquid detergent has been shown to restore flame retardancy of soiled fabric(Crown & Batcheller, 2016). Heavy hydrophobic contamination can be removed using organic solvents such as tetrachloroethylene to dry clean the fabric before processing the fabric (PARKER & Kasper, 2020). However, water cleaning is the preferred method due to the health and safety concern of chlorinated solvent.

2.5.2 Chemical Recycling

Chemical recycling can be used to convert aramid waste to raw material for the manufacturing of new material. The chemical recycling of aramid can be done by depolymerization, enzymatic separation, dissolution or solvent recycling.

- **Depolymerization**

Chemical recycling by depolymerization consists in degrading the polymer to recover the monomers. Once purified, the monomer is used to synthesize materials with the properties equivalent to that of a virgin monomer. Polycondensation-synthesized polymers are suitable for

chemical recycling by depolymerization due to their chemical structure, such as polyamides (Iwaya, Sasaki, & Goto, 2006) and polyester (Arai, Zenda, Hatakeyama, Yui, & Funazukuri, 2010; Shukla & Kulkarni, 2002).

- ## Enzymatic Recycling of Aramid

Enzymes have been used in the textile industry for selective dissolution. One common application is the desizing of cellulosic size applied to protect the yarn during the weaving. Enzyme has also found a use in chemical recycling of textile material.

In blend fibre, the synthetic aramid fibre can be recovered from the blend by using enzyme hydrolysis. The hydrolyzable fibre such as cotton, viscose, polyamide, polyester can be selectively degraded by enzymes (Xiang & Blankenbeckler, 2020). The fabric treated in a aqueous solution with the enzyme under the optimal condition of pH, temperature, salt concentration and time for optimal digestion. The hydrolyzable fibre can be selectively degraded by specific enzyme (Xiang & Blankenbeckler, 2020). The aramid is not affected by the enzyme. Therefore, the aramid fibre can be recovered in a gentle process without requiring solvent, harsh chemical or intensive mechanical separation. This method is limited to fabric containing hydrolyzable fibre by means of an enzymatic treatment. Moreover, polyamide and polyester digesting enzymes are not, yet, as efficient cellulose digesting enzymes.

- ## Solvent recycling

Chemical recycling can use solvents to dissolve the aramid or matrix.

For composite, the resin is dissolved in a solvent and the aramid fabric is recovered. This method is of interest in the case of a mixture of materials that are difficult to separate.

An interesting method at the laboratory scale is the deprotonation method to prepare nanofiber suspension from aramid. The deprotonation and regeneration of aramid nanofiber is a potential value-added recycling route through nanofiber fabrication. Nanofibers are of interest for filtration application, being small in diameter, they improve both the filtration efficiency and the pressure drop. Reducing the diameter of fibres in filters is a promising way to improve the quality of filter material.

Aramid nanofibres by deprotonation were first synthesized by the team of Kotov and al. (M. Yang et al., 2011) The method developed is inspired by the amide deprotonation method developed by

Takayanagi and al.(Takayanagi & Katayose, 1981) and cellulose process methods to develop a method for manufacturing aramid nanofibres in solution. The solution brings advantages in handling and application flexibility. The solution can be used for coating to form a film. Obtaining nanofibres increases the surface ratio, which is advantageous for filtration and composite reinforcement applications, among others. Finally, the energy consumption of nanofiber preparation with the solvent is potentially lower compared to mechanical recycling (B. Yang et al., 2021).

The deprotonation principle of Takayanagi and al. is based on the addition of sodium hydride to deprotonate the amide and form a polyanion dispersion (Koga, Ueta, & Takayanagi, 1988). Burch and al. developed the method with different hydrides in dimethylsulfoxide (DMSO) to prepare aramid solutions (Burch, Sweeny, Schmidt, & Kim, 1990). He notes that the addition of a protic polar co-solvent improves the solubility of aramid and that potassium hydride offers the best solubility. On the other hand, hydrides are partially soluble in most solvents and react violently with water. Thus, the solvents must be completely dry for the reaction and this must take place under an inert atmosphere. Kotov suggested replacing the hydride with a base with a lower pK_b , namely potassium hydroxide. The latter is relatively stable with water in addition to being soluble in water and several polar solvents that greatly simplify handling and reaction condition. He also notes that the mixture obtained would be a colloid rather than a solution (M. Yang et al., 2011).

The alkali deprotonates the amide functions of aramid, not leading to the dissolution of the polymer, but rather to a breakdown of the macro fibres into nanofibres (M. Yang et al., 2011). The fracture mechanism suggested is the reduction of attractive intermolecular forces by breaking π-π and Van der Waals interactions, in addition to creating an electrostatic repulsive force by deprotonation of the amide.

The choice of solvent and alkali is important to obtain the exfoliation of aramid nanofibres. DMSO is a polar aprotic solvent. It cannot receive the alkali charge. The choice of DMSO surely comes from the possibility of having positive dipoles and negative dipoles allowing a dipole-charge interaction or a dipole-dipole interaction. The solvent can therefore interact with the hydroxide ions, the amide anion, the proton and with the dipole of the amide and the aromatic.

Other dipolar aprotic solvents such as NMP, THF and sulfones are good solvents for aramid. The quality of DMSO is its ability to be a solvent for neutral aramid and for anionic aramid.

Different contributions were made to understand and improve the reaction.

Table 2-2. Summary of progress in deprotonation reaction

Publication	Fibre diameter (nm)	Fibre length (um)	Reaction condition	Variance	Process
(M. Yang et al., 2011)	3-30	10	168h, RT, 0.2%	-	LBL
(B. Yang, Wang, Zhang, Luo, & Ding, 2019)	10-12	-	4h, RT, 4% + Donneur proton	Fibrillation, Ultrasonication and protic solvent (water)	Vacuum filtration
(Miao et al., 2019)	14-15	>1	36h, RT, DMSO/potassium tert-butoxide, PEG	Potassium tert-butaoxide	
(Lv et al., 2021)	16	-	75 min., RT, 0,3%	Protic solvent study (IPA, EtOH, MeOH)	Vacuum filtration
(B. Yang et al., 2021)	10-12	10-15	5h, RT, RT, 2%	Protic solvent (water)	Recycling, filtration
(H.-J. Chen et al., 2021)	8	-	2h., RT, 4% 26 min, RT, 0,2%	Solvent exchange (aerogel)	Recycling, aerogel
(Tan et al., 2021)	-	-	1s to 10 min. impregnation	Textile coating	Coating
(Xu et al., 2022)	8-11	~15	8h, 60°C, 0,2% (KOH dissolved O.N. at 80°C)	Continuous sol-gel	Sol-gel coating
(L. Huang et al., 2022)	10-30		10 min., RT, 0,2%	Pretreatment	Pretreamtent and filtration

The reaction is noted to take about 7 days (M. Yang et al., 2011). One major contribution to reduce the reaction time is the addition of a pre-treatment. The nanofiber is prepared in 10 minutes by first

immersing the fibre in a concentrated alkaline solution for 15 seconds before adding the DMSO solvent. The concentration of the aramid is of 0.2%. A higher concentration is desirable to reduce the volume of solvents required.

In this project, an aramid nonwoven blend will be used to prepare the nanofiber dispersion. A pre-treatment will be evaluated to remove contamination from the reclaimed aramid. The deprotonation will be optimized by using UV-vis spectroscopy to follow the kinetics. Finally, the coating of the nanofiber dispersion will be evaluated for the hood barrier application.

In short, the current state of aramid recycling was presented. The advantages and disadvantages of recycling of aramid via mechanical and chemical method are presented in the table below:

Table 2-3. Summary of aramid recycling method

Method	Chemical recycling	Mechanical recycling
Advantages	• Wider variety of product • Novel and various technologies • Quality of the recycled material	• Simple • Lower-cost
Disadvantages	• Use of chemicals • Complexity	• Sensitive to contamination • Reduce properties by fibrillation

2.6 Hood filtration media

In order to improve the protection of the skin against particles and chemicals, a filtration membrane is added in the hoods. Since 2018, the National Fire Protection Agency (NFPA) 1971 standard describes the requirements for the protective membrane (NFPA1971 2018). The hood barrier must balance between protection against particles and comfort by evacuation of sweat.

The available air filtration technology in personal protective hoods are currently based on either nonwoven fabric or porous membrane. Recent hood patents describe a fibrous barrier based on ePTFE or polyimide nanofiber (Nomex® Nanoflex) produced by W.L. Gore & Associates and DuPont (Barbeau et al., 2018; Blake et al., 2021; Sonntag, 2020). Hydrophilic films are also used in some protective garment such as the moisture barrier where protection against gas and liquid

chemical is required. In short, the hood barrier could be made from porous film, hydrophilic film or nonwoven.

- **Porous Film**

Porous films can be formed by the extrusion of polymers with an incompatible organic or inorganic additive. The film is extruded on a cast roll and stretched in unidirectional or bidirectional direction to produce the final size of the pore (Wikol et al., 2007). A dryer can be used to remove the volatile organic pore forming additive prior to stretching. The temperature and stretching rate are controlled to avoid film breaking. Porous film is often laminated with a knit in hood application because the voids weaken the material (Wikol et al., 2007). The knit structure allows for flexibility and some stretching. The knit stretching is restricted to avoid permanent deformation of the laminated porous film. The flexibility and elasticity of the hood allow for ease of donning, better fit and comfort.

- **Hydrophilic Film**

Hydrophilic films are formed by extrusion or coating using a hydrophilic polymer. Most hydrophilic polymers are based on polyether polyurethane, polyether-ester, polyether-amide. The hydrophilic functions of the polymer such as ether, ester and amide provide intermolecular interaction with water and a wicking effect (Lomax, 2007). The water is evaporated through a sorption-diffusion-desorption mechanism. The diffusion mechanism is driven by the difference in humidity between the inside and the outside of the garment. Fick's first law of diffusion states that the high concentration will diffuse to the area of low concentration in water. (Chang & Liu, 2023) Therefore, the water permeation increases as the humidity increase inside the garment. The hydrophilic films are resistant to permeation of nonpolar gas. The specific permeability makes them ideal for protective garments. The film must be thin to allow sufficient water transmission by diffusion. Therefore, the hydrophilic film can be used in combination with porous film or laminated to a textile to avoid tearing, puncture or breaking of the film.

- **Nonwoven**

Nonwoven are predominantly used in filtration media. The nonwoven is a structure of textile fibre consolidated by mechanical interlocking or chemical bonding by fusion, solvents or adhesive bonding to form a web or a mat. The fibres can be oriented in one direction or randomly. The fabrication of a nonwoven is divided in three steps:

1. Veil formation
2. Consolidation
3. Finishing

Veil formation

Three methods of web formation are possible for the manufacture of nonwoven.

Drylaid process uses fibres of 10 to 500 microns to form a fibre layer. The drylaid veil can be prepared by carding or air laid.

By carding, the fibres are carded to separate the fine and parallelize the fibres. Fibre orientation can be reduced by using pre-needling jammers. The veils are superposed (napped), then consolidated by mechanical or thermal means.

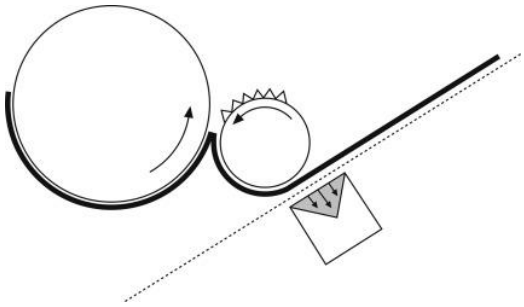

Figure 2-3. Production of drylaid webs with carding and take-off (Brydon, Pourmohammadi, & Russell, 2022)

Air laid uses a stream of air to disperse the fibres and convey it through a perforated rotating cylinder or conveyor to form a web on a conveyor belt. The veil uses shorter fibres and forms a random nonwoven, more flexible, and less dense than by carding. (Montefusco, 2005).

Wetlaid, or paper process uses fibres up to 12 mm in length, dispersed in a liquid. The dispersion is conveyed to a drip cloth to form a continuous veil. The liquid is recovered and recycled in the process. The resulting nonwoven has randomly aligned fibres. Thus, the nonwoven has an isotropic and uniform properties which allows use in high efficiency filters. Wet veil is dried in an oven to remove residual solvent before the finishing steps (Montefusco, 2005).

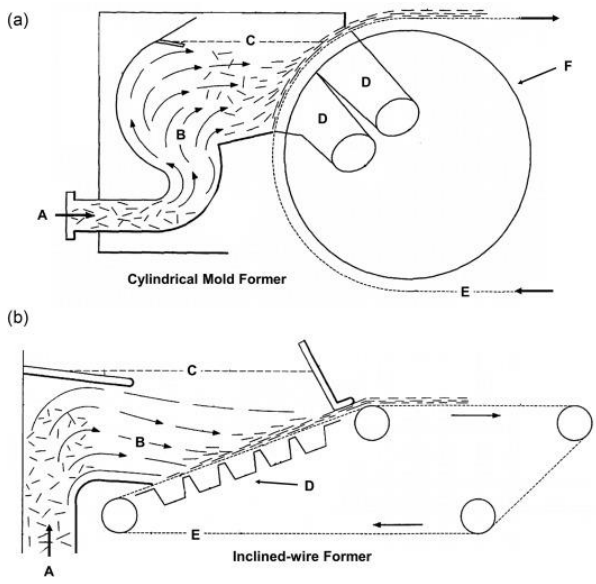

Figure 2-4. Wet-laid web formation (Koukoulas, 2022)

The main difference to the papermaking process comes from the length of the fibres which are higher in the textile. Wood, cellulose, viscose, polyester, polypropylene, glass, metal, aramid and carbon fibres are used in particular to manufacture nonwoven by this method.

Different combinations are possible by this technology to achieve temperature resistance, chemical resistance, porosity, strength, static and anti-static properties for various applications. This technology is less prevalent, and represents only 6% of the production of nonwoven (Thomas, Charvet, Bardin-Monnier, & Appert-Collin, 2018). The difficulty of this method mainly comes from the dispersion of fibres in a liquid and preventing the entanglement of fibres in dispersion to obtain a low viscosity liquid.

Melt process is divided into three categories, spunlaid, meltblown and electrospinning. The meltblown is the most widespread method for fabrication of filtration media.

Spunlaid consists of forming a filament from a thermoplastic (polypropylene, polyester, polyamide). The thermoplastic granules are extruded in a die to be cooled, hot stretched and deposited on a conveyor belt to form a veil. The fibre diameter is typically of 10 to 50 microns (Thomas et al., 2018). The stretching improves the mechanical properties.

Meltblown involves extruding the granules through a die, where hot air is blown to stretch, align and reduce the diameter of the fibres. Fibres of 0.6 to 10 microns in diameter are obtained by this

method (Thomas et al., 2018). The distance between the collector and the die, and the velocity of the air jet control the suspension time of the fibres in the air. Melt temperature, air velocity, air temperature and distance from the collector influence the solidification and crystallization of the polymer.

Electrospinning is carried out by the molten process or by the solution process. A jet of solution or melt is stretched by a sufficiently high electrical potential difference between the capillary and the collector to attract the filament to the collector.

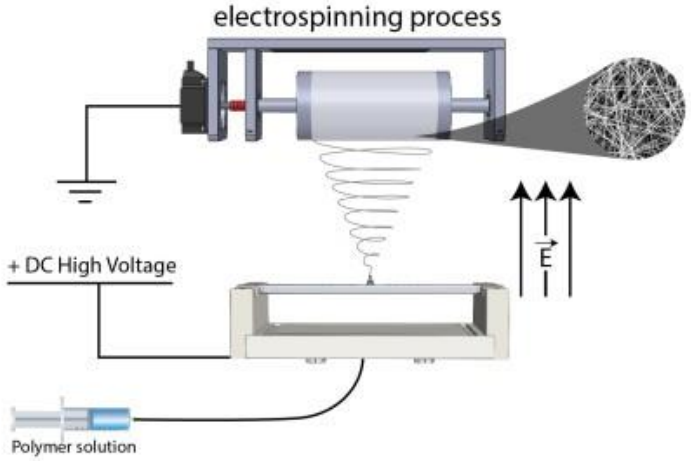

Figure 2-5. Electrospinning process(Inovenso, 2022)

In the solution route, the solvent is evaporated before the filament is deposited on the collector. The distance between capillary and collector, voltage, flow rate, solvent evaporation and polymer concentration influence the final properties. In filter, a fibrous support is added to ensure good mechanical strength (Thomas et al., 2018). Electrospinning has been a proven method to prepare nanofiber nonwoven mat for air filtration application with a variety of high-performance polymer (Faccini, Vaquero, & Amantia, 2012). PBI has been electrospun in nonwoven mats (Anandhan, Ponprapakaran, Senthil, & George, 2012; J. S. Kim & Reneker, 1999). Polyimide can be electrospun for the fabrication of high temperature filtration with 99.99% filtration efficiency for PM2.5 (Li, Shang, Li, & Yang, 2017b; Wang, Bai, Xie, Jiang, & Qiu, 2016). The uses of aramid as feed material has been demonstrated in the literature. The effect of different solvent was evaluated (H. B. Kim, Lee, Choi, Lee, & Lee, 2019; Yao, Lee, & Kim, 2010). Dimethylformamide with lithium chloride at 4% is the preferred solvent combination. The aramid concentration was evaluated from 6% to 16% in different papers. The uses of calcium chloride instead of lithium

chloride results in a spiderweb like structure (Oh et al., 2012). The reduction of the diameter has increased the filter quality by reducing the pressure drop and increasing the filtration efficiency (H. B. Kim et al., 2019).

The commercial application of nanofiber for air filtration has been demonstrated by Donaldson Company (Grafe & Graham, 2003). Nevertheless, electrospinning has the disadvantage of a low throughput, difficult scale up, and the uses of organic solvents.

Consolidation

The consolidation of the web is necessary to improve the cohesion of the fibres. Consolidation is carried out by three methods; thermal, mechanical or chemical.

Thermal consolidation uses the plastic property of certain synthetic fibres to bind the fibres. Several heating methods can be used.

By calendering, the sheet is heated by passing it overheating cylinders or in an oven. The web is pressed between two heated rollers and consolidates the nonwoven. The surface of the nonwoven can be embossed at this stage to give a texture to the nonwoven, for example for texturized cleaning wipes. Lamination with another substrate is also possible at this stage.

The heat treatment can also be done by drying cylinders, air oven, infrared or other heating systems. Thermal annealing or heat setting increases the degree of crystallinity of the polymer for better dimensional stability. The annealing is typically done by heating between the glass transition temperature and the melting temperature of the polymer (Thomas et al., 2018).

In the **chemical consolidation** route, a polymer is applied by coating, impregnation or spraying to consolidate the fibres. The polymer is often in the form of a water-based emulsion, but application in powder or in solution in an organic solvent is also possible. After applying the polymer, the coated veil is conveyed in an oven to evaporate the water, then cross-link the polymers to consolidate the veil (Koukoulas, 2022).

The **mechanical consolidation** is done by needling or hydroentangling. Needling uses needles with barbs. The veil passes over a perforated plate, the needles drag the upper fibres towards the lower fibres to tangle the fibres (Brydon et al., 2022).

Hydroentanglement uses the turbulence of a high-pressure water jet to entangle the fibres. The formed nonwoven is more flexible and compact than by needling (Koukoulas, 2022).

The mechanical method does not contain additional resin, which is important for food and medical applications. For nonwoven used at high temperatures, the resin reduces the flame and heat resistance properties given the heat sensitivity of the resins used.

Finishing

Finishing is the last step to give the final properties to the nonwoven. Mechanical finishing treatments can be stretching, perforation, folding and crimping to give the web the final shape. The nonwoven can be laminated with different backing such as films, nonwoven, nets, etc.

Chemical treatments are applied on the surface of the fibre to functionalized the nonwoven. A conductive or anti-static treatment can be applied to dissipate charges or build static to trap charged particles. Flame retardants can be applied to reduce ignition and flame spread. A hydrophobic or oleophobic coating can be applied to protect against water or oil, or absorbent. Printing and dyeing are also possible to personalize the textile. Finally, the edge can be cut off, then the nonwoven is rolled up.

2.7 Filtration mechanism

Aerosols are a suspension of solid or liquid particles in a gaseous medium. (Thomas et al., 2018). Airborne particles are categorized into different classes according to their diameter. The hood barrier requires to block particulate of 0.1 to 1.0 microns in the categories PM 1 specified in NFPA 1971 will be based on the principle of gas filtration, micro aerosol and nano aerosol (Leung, 2021).

Table 2-4. Airborne particles categories

Class	Diameter
PM10	Below 10 µm
PM 2,5	Below 2,5 µm: Fine particle
PM 1	Below 1 µm: Very fine particle
PM 0,1	Below 0,1 µm: Ultrafine particle

Above all, air filtration differs from liquid media filtration, which is mainly based on the pore size of the substrate to retain the particle. For air filter, the particle capture mechanisms are different, the size exclusion mechanism is still present, but the filtration can also be achieved by diffusion, interception or inertial impact.

Screening, or **size exclusion**, occurs when particles are larger in diameter than the filter pore diameter. This mechanism happens at the surface of the membrane. In the case of sizes of 0.1 to 1.0 microns required for NFPA 1971 filtration, the pore size of the membrane would be less than 0.1 microns to capture particles by this mechanism. However, this filtration mechanism is not the only mechanisms of air filtration, which explains why an ePTFE membrane with 5-micron pores can achieve a filtration efficiency of 99.99% for particles of 0.1. microns (Wikol et al., 2008).

Once the particles penetrate the filter, several capture mechanisms are possible through the interaction between the particle and the filter. In fact, small particles (<0.2 microns) move rapidly and randomly in the airflow like the Brownian motion of colloids suspended in a liquid. Thus, the collision of particles with the matrix **by diffusion** is high for small particles (Thomas et al., 2018). **Interception** occurs when the particle comes into direct contact with a fibre or substrate. The particle is fixed on the substrate by Van der Waals forces (Thomas et al., 2018). In the case of a fibrous media, the fibre density increases this phenomenon. In the case of a porous filter, a reduction in the pore density increases this capture mechanism. **Inertial impact** is an important mechanism for larger particles. The airflow deflects around the fibres while the heavy aerosols continue in the straight direction with inertia due to the density and size of the particle (Thomas et al., 2018). A high fibre density rapidly increases the capture rate by this method. In short, the particle capture efficiency of different mechanisms varies with particle size. The filtration efficiency according to the size of the particles, and can be optimized based on these principles.

The cumulation of the different filtration mechanism gives for a most penetrating particle (MPPS) where the filtration efficiency is the lowest which varies depending on the test condition such as particle velocity, air flow rate, pressure, temperature, humidity and the filter (Thomas et al., 2018).

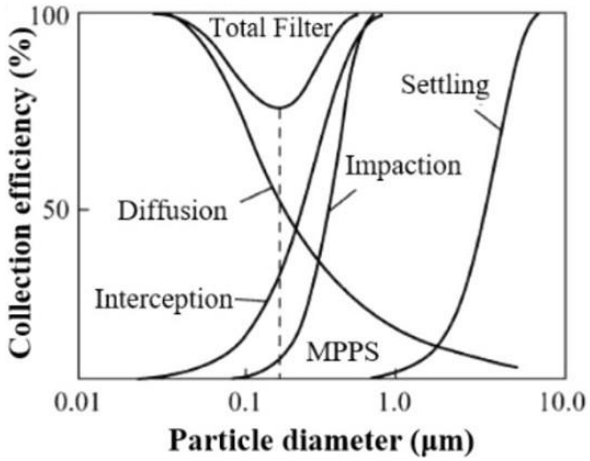

Figure 2-6. Filtration efficiency of different mechanisms (Thomas et al., 2018)

Fibre diameter: The advantage of reducing the fibre diameter by nanofibres comes from the increase in the ratio of fibre surface area to filter volume for the same fibre density. For example, reducing the size from 1 micron to 0.1 microns increases the surface area by a factor of 10.

Fibre density: An increase in the fibre density in a filter improves the filtration efficiency, on the other hand, the pressure differential increases proportionally. By reducing the fibre density with nanometre fibres, the pressure differential is reduced for efficiency similar to the conventional filter (Thomas et al., 2018).

Filter Thickness: Filter thickness can also improve particle retention; however, the pressure differential will also increase significantly. The filter should be thin to maintain a low-pressure differential with acceptable efficiency (Thomas et al., 2018).

In the hood application, the filtration on the surface of the material can be advantageously compared to in depth filtration. The advantage of blocking the particles on the surface is the ease of particle removal; the filter can thus be cleaned and regain its initial airflow, which is an advantage for hoods that are frequently cleaned. Washing is recommended after use of the hoods according to NFPA 1971, which appears to favour-surface filtration. The washing procedure corresponds to 5 washes. Dimensional stability, flame resistance, heat resistance, thermal protection performance and breaking strength are evaluated before and after washing.

2.8 Heat Loss for Thermal Comfort and Heat Stress

Under the extreme environmental temperature of the firefighting, the hood composite should provide protection against conductive, convective and radiating heat transfer to prevent burn and heat stress. The material should have a high thermal resistance. The thermal protection properties should be balanced with the thermal comfort (Song & Wang, 2018).

The thermal comfort can be described as the condition of an individual that express satisfaction with the thermal environment. The thermal comfort is critical to prevent heat stress condition during work in hot environment. The body's response to heat stress is the heat strain. It can cause injury such as heat stroke, heat exhaustion, heat cramps and rashes as the body cannot maintain a normal internal temperature (Eisenberg, Methner, Dowell, & Mueller, 2015). The heat stress is the sum of heat generated by the body (metabolic heat) and the heat gained from the environment minus the heat loss to the environment (Shults, Noonan, Turner, & Ronk, 1992; Smith, Horn, Goldstein, & Petruzzello, 2008).

The hood properties should allow heat loss to the environment to reduce the possibility of heat stress condition. The hood resistance to permeation to heat, air and water can restrict the heat loss to the environment. The permeation to water will be evaluated according to the method ASTM E96 and the total heat loss will be tested according to the method ASTM F1868 presented at the chapter 3.

The evaporation of sweat also contributes to the comfort as a lack of permeability can result in water vapour condensation which creates a discomfort sensation (Song & Wang, 2018).

2.9 Conclusion and perspectives

In summary, a rationale for recycling of aramid was presented. The characterization method for the polymer, filter and hood were presented. For the hood barrier, the requirement of the standard NFPA 1971 were presented. Other characterizations of the hood that can be complementary to the NFPA 1971 standard were assessed in the literature, which includes the stability to UV, the decontamination efficiency and on field testing.

The NFPA 1971 standard does not require the hood to be tested against ultraviolet light ageing (NFPA1971, 2018). However, the aromatic polymers used in the construction of hood are typically sensitive to degradation by UV light. The durability of the hood to light was evaluated by Gaskill

and al. (A Kasebi, Gaskill, & Ormond, 2020) for ASTM. The efficiency of filtration of the hood membrane is not influenced by light, only a slight reduction of mechanical properties is observed. The durability to different conditions was evaluated such as the combinations of laundering, donning, and thermal exposures (Arash Kasebi, 2022). The efficiency of the washing and durability was evaluated (Horn et al., 2021; Mayer et al., 2019). The washing of hood reduces the load of contaminants, while some contaminant can be difficult to remove.

The protection against VOC and PAH in the situation was evaluated by NIOSH and other. A high concentration of VOC is observed through the hood and garment (Fent et al., 2022; Fent et al., 2020; Mayer et al., 2022; Mayer et al., 2023; Sjöström et al., 2019; Stec et al., 2018). The evaluation of VOC permeability in a testing laboratory environment has not been done yet.

2.10 General objective

The regulatory change and problematics around firefighting gear discussed in the introduction makes for the right moment to revise the design of the hood barrier. The barrier of the hood will be revised to meet the new regulation and to address the current problematics around firefighting gear. The general objective is to develop a PFAS free membrane for firefighters used in hood application.

2.11 Specific objectives

1. Evaluate the electrospinning of reclaimed aramid for hood barrier application
2. Develop a hydrophilic barrier with reclaimed aramid using conventional knife coating method
3. Evaluate the resistance of permeation to chemicals to which firefighters are exposed

CHAPTER 3 MATERIALS AND CHARACTERIZATION METHODS

A polymer will be used to fabricate a barrier against particulate matter. This barrier will be included in a hood, and this hood will be used as a part of the firefighting ensemble. Therefore, there is a need for characterization method for polymers, barriers and of firefighter hood in this project.

3.1 Materials

The polyurethane and additives used for the coating were supplied as sample by Azelis Canada and Dempsey Corporation.

Nomex E89 nonwoven, knit and other textiles were supplied by the industrial partner.

Commercially available hood LION's RedZone™ with STEDAIR® PREVENT barrier (model: HD395142-10+U) and PGI BarriAire™ Gold with Nomex® Nano Flex barrier (style no. 39700-00-194071, LOT #022123) were purchased from Safedesign.

Solvents and reagent chemical were purchased from MilliporeSigma. >99.9% Dimethyl sulfoxide (CAS 67-68-5), ≥99.8% Dimethylformamide (CAS 68-12-2), ≥99% Lithium chloride (CAS 7447-41-8), ≥99% Dimethyacetamide (CAS 127-19-5), Anhydrous, +99%, 1,2,3,4-Tetrahydronaphthalene, Tetralin™ (CAS 119-64-2), HPLC, 99.9% Methanol (CAS 67-56-1) were purchased from MilliporeSigma. Ultra-high purity nitrogen 5.0 is purchased from Linde Canada. Products were used as received.

3.2 Polymer Characterization

The particulate barrier will consist of at least one polymer. The material should be characterized.

Thermogravimetric Analysis

Thermogravimetric analysis measures the change in mass as a function of a temperature profile, which makes it possible to determine the temperature of polymer degradation, the level of humidity, volatile compound, and other gas-solid reactions. The thermal stability of polymers is important for the final application. The hood must be stable in an oven at 260°C for 5 minutes. Thermogravimetric analysis will be used to determine if the stability of the polymers is suitable for the final application.

Fourier Transforms Infrared Spectroscopy

Fourier transforms infrared spectroscopy measures the energies of molecular vibrations. It makes it possible to identify certain functions to confirm the molecular structure of the polymer. The presence of contamination or degradation can also be observed by comparing the peaks to the reference polymer.

3.3 Characterization of fibrous media

Basis weight

The basis weight of the textile corresponds to weight per surface, typically expressed in grams per square metre or in ounces per square yard. A low grammage is desired to obtain a light and comfortable final product. The ISO 9073-1 and ASTM D3776-96 methods are used to determine the basis weight of nonwoven.

Thickness

The thickness is an important characteristic for filtration properties, especially for depth filters where thickness is used to retain particles in the medium. The compression of the nonwoven causes a variation of the measurement according to the structure of the nonwoven. The thickness can be determined microscopically by sectional view to eliminate the compression effect. However, the manipulation is delicate. One micrometer with a presser foot is used for all the thickness measurement in this project because of the simplicity.

Fibre Diameter

Fibre diameter, typically reported in micrometres, is an important parameter for filters. Thickness relative to mass is more often used in textiles, known as linear density. The linear density is the ratio between the mass and the length of yarn, generally expressed in tex, representing the mass in grams per 1000 metres of yarn.

Kawabata bending rigidity

The Kawabata evaluation system is a series of instruments used to measure the touch and feel quality of textiles. One method the evaluate the flexibility of a coated textile is the bending rigidity from the Kawabata evaluation system. The bending rigidity is the force applied to bend the fabric at an angle of 150°.

Permeation

The permeation relates to the rate of penetration of a liquid, gas or vapour through a solid (i.e. textile). The permeation to air is evaluated against the test method ASTM F737-18, where the air flow is measured at a fixed pressure differential. The water vapor permeation rate is evaluated by the standard ASTM E96 B, where a cup of water covered by the barrier in standard condition is weighted periodically. The rate of weight loss is reported over the exposed area. A method to evaluate the permeation of chemical was developed in this project and will be presented in details at the section 6.7. Other general method of polymer and fiber characterization are summarized in the following table.

Table 3-1. Characterization method of polymers and fibre

Instrument	Property	Description
Thermogravimetric analysis (TGA)	Decomposition temperature	The sample is heated and weighted under air or nitrogen. The decomposition temperature and weight loss at different temperatures can be evaluated.
Precision weighting scale	Basis weight	The material is weighted over a known surface. The weight over the surface is reported in grams per square metres.
Micrometer	Thickness	Thickness of the material in compression
Fourier transforms infrared spectrometer (FTIR)	Molecular vibration	Confirm the molecular structure from the specific wavelength of the covalent bond. The spectra can be confirmed using database.
Scanning electron microscope (SEM)	Cross-section and top view of fibre, nonwoven	Compare the size of the fibre and evaluate the pore size

3.4 Hood characterization

The NFPA 1971 describes the Standard on Protective Ensembles for Structural Fire Fighting and Proximity Fire Fighting. The standard refers to methods from various standards organizations, including ASTM International (ASTM), the American Association of Textile Chemists and

Colorists (AATCC) and the International Organization for Standardization (ISO). The NFPA standard requires minimum performance thresholds for different products in protective ensembles.

In the 2018 edition of NFPA 1971, an optional particulate barrier was added for hoods. The optional barrier requires a particle filtration efficiency test for protection and a total heat loss test for comfort to the requirement for hood.

Table 3-2. Method of testing hoods according to the NFPA (NFPA1971, 2018)

Test	Method	Description
Vertical flame resistance	ASTM D6413/D6413M	Five 75x305 mm specimens are exposed to a vertical flame. Flames should leave < 4 inches of charred specimens from the bottom, < 2 seconds of self-extinguishing and no melt or drip.
Heat resistance	ASTM F2894/F2894M	The hood is put on a mannequin, before and after washing. Donning should be easy, shrinkage should be less than 5%. The dummy is placed in an oven at 260° C. for 5 minutes. The hood must not show any fade, separation or ignite.
Thermal protective performance (TPP)	ISO 17492	The hood is exposed to a source of radiant and convective heat. The time to obtain a heat transfer equivalent to a second-degree burn is recorded. The thermal protection performance must be at least 20. This evaluates the thermal insulation performance of the hood.
Burst strength	ASTM D6797	Evaluates the mechanical strength of the hood by measuring the burst strength.
Dimensional stability	AATCC 135	The hood is placed on a dummy head. Size should vary less than 5% after washing.
Particulate blocking efficiency	ASTM F2299/F2299M	The filtration efficiency must be greater than 90% for particles of 0.1 to 1.0 microns.
Total heat loss (THL)	ASTM F1868	Evaluates the heat transferred through the hood in dry and wet conditions to reflect perspiration and thermal conductivity. The value is reported in clo – a unit of thermal resistance (insulation) equivalent to 0.155 K m^2/W.

Conditioning	AATCC 135	Each test is done before and after 5 wash cycles with a load of 1.8 kg.

The filtration efficiency is of great importance for the development of a barrier with protection against smoke particles. The laboratory test uses a filter tester equipment. The aerosol is generated from a latex solution of standardized size. The solid latex particles are dispersed in the air to form a solid particle aerosol. The aerosol is routed to the test specimen. The upstream aerosol concentration is measured by an optical detector. The average concentration downstream of the filter is measured to determine the filtration efficiency according to the following equation:

$$\eta = \left(1 - \frac{average\ downstream\ count}{average\ upstream\ count}\right) \tag{2.1}$$

Where η is the filtration efficiency express in percent. The measurement is carried from sizes 0.1 to 1.0 microns with an increment of 0.1.

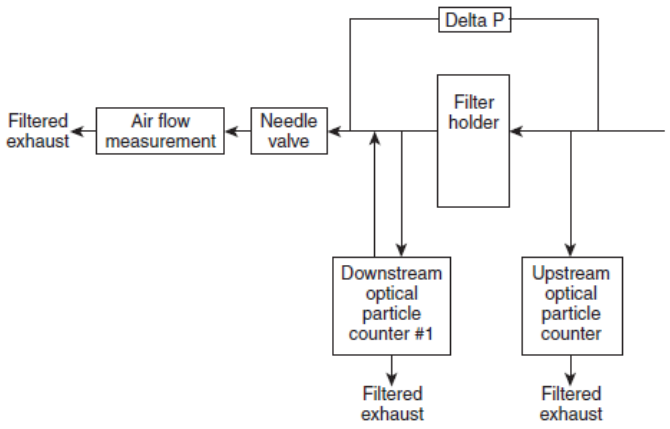

Figure 3-1. Schematic of the filtration apparatus (NFPA1971, 2018)

A pressure differential of 249 Pa is maintained and a flow rate of 1.7L/min is maintained during testing. The flow rate is low compared to medical masks, to represent the airflow next to the skin.

In conclusion, polymers, barriers and of firefighter hood will require characterization. For the evaluation of polymer and fibres, general test method will be used. For the evaluation of the hood barrier, the specific test method described in the NFPA 1971 edition 2018 standard will be used.

CHAPTER 4 ELECTROSPUN NANOFIBER

4.1 Electrospinning rationale

The reduction of fibre diameter improves both filtration efficiency and airflow or pressure drop. Therefore, it is desirable to reduce the diameter of the fibre in the hood barrier. One method to produce nanofiber is electrospinning.

The uses of electrospinning are limited due to the low throughput, difficult scale up and uses of solvents. The electrospinning of aramid fibre is still of interest:

- The uses of organic solvents are inherent to processing of aramid fibre
- Low throughput and low tenacity can be improved by coating a conventional nonwoven

To lessen those problems, the electrospun mat was deposited on a nonwoven. The nonwoven has a sufficient strength for the application and protect the nanofiber from excessive stretching. The nonwoven is also expected to act as a prefilter, remove large particles, increase filtration depth and prevent clogging of the nanofiber filter. Finally, the improved mechanical strength of the composite structure should allow for a lower coating weight of nanofiber to improve the throughput.

Aramid blend nonwoven is commercially available and has been proven for multiple high temperature applications for firefighter gear. A Nomex III blend is used for the nonwoven to collect the nanofiber coating. The lamination method and adhesion of the nanofiber and the nonwoven will be evaluated in this project.

4.2 Preparation of Solution

Scoured aramid fabric is cut in 1x1 cm pieces to prepare 4 grams of cut fabric. The fabric is cut in sized of 1x1 cm to simulate the shredding of the fabric at the laboratory scale. The size was selected based on the vats and stirrer size. A fabric sizes smaller to the impeller or stirrer blade size prevent ragging and fouling of the impeller. In the same way, square piece is less susceptible to wrap around the stirrer shaft to blade.

The fabric pieces are immersed in 120 grams of room temperature dimethylformamide in a tricol. The tricol is connected to a condenser with cold water circulating, a mechanical stirrer equipped with a scrapping stirrer and a thermometer. The thermometer is used to monitor the reflux

temperature. The mixture is heated with a Glass col round-bottom flask heater to reflux while under agitation. Lithium chloride is slowly added after 1 hour to the mixture.

The dissolution of the aramid is carried in steps to prevent gelling of the polymer. The aramid is first mixed in room temperature solvent. The temperature is increased to increase gradually the solubility of the material. Finally, the lithium chloride is added slowly to further increase the solubility of the aramid.

The mixture is stirred for at least 4 days to solubilize the meta-aramid from the fabric. The mixture is collected.

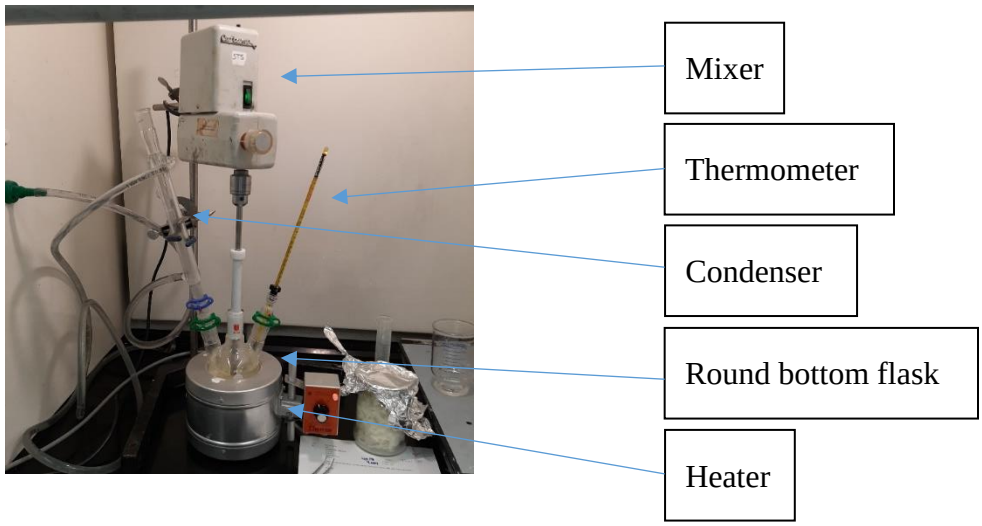

Figure 4-1. Dissolving apparatus

The remaining undissolved material (para-aramid, undissolved meta-aramid) is removed from the solution by centrifugation. The solution is recovered and weighted. The undissolved material is recovered by centrifugation, dried under vacuum and weighted. The dissolved fibre is calculated by subtracting the undissolved fibre from the total weight of fibre. The excess solvent is evaporated to obtain the final concentration of 6% aramid. A small amount of lithium chloride is added to obtain the exact required concentration of 4% by weight.

4.3 Preparation of electrospun mats

A fabric is placed on the collector to collect the electrospun material. For non-woven material, the electrospun material is collected on the “smooth” side. The machine direction of the fabric is placed in the machine direction of the collector.

The solution is pumped by a syringe pump. The syringe is connected to a capillary silicon tubing. It is used to minimize dead volume and good chemical resistance to LiCl/DMF solvent.

The tubing is connected to a needle, using PFA fitting.

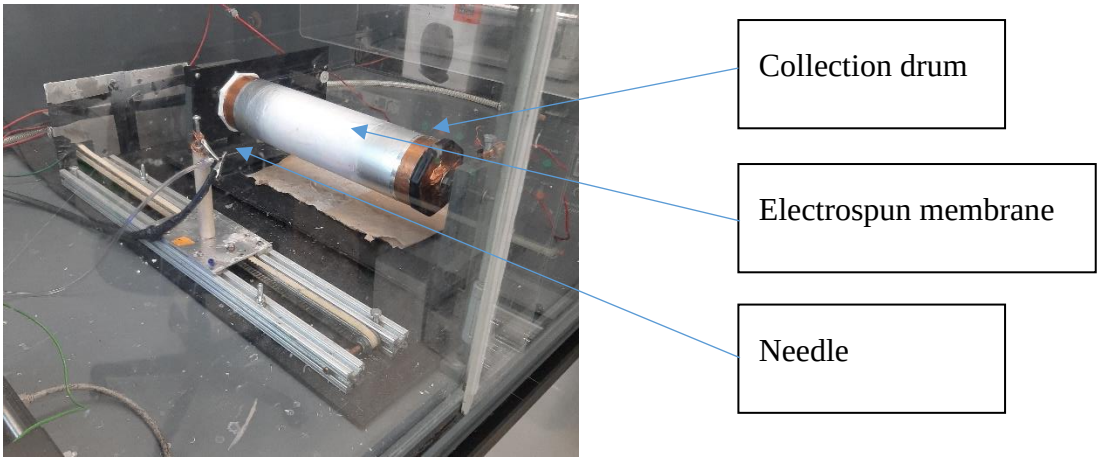

Figure 4-2. Electrospinning apparatus at Polytechnique Montreal

The feed rate, potential and collector distance are varied to obtain a uniform electrospun mat. The final parameter is a feed rate of 350 µL/h, a potential of 11 kV and a distance between the needle and the collector of 12 cm. The collector is under rotation and the needle under translation to form a uniform mat. The speed of the translation and collection is adjusted to form a mat with aligned fibre in the transverse and machine direction to obtain three rotations for 1 translation of 30 cm each.

4.4 Evaluation of Solvent for Solution Preparation

At first, the solvent Tetrahydrofuran (THF), 2,2,2-Trifluoroethanol (TFE), N-methyl-2-pyrrolidone (NMP), dimethyl sulfoxide (DMSO), dimethylformamide (DMF) and dimethylacetamide (DMAc) were evaluated for dissolution by visual observation. TFE and THF showed no solubility. DMF, DMAc NMP and DMSO shows partial solubility. DMF and DMAc showed the best solubility. However, the obtainable solid concentration was too low to prepare nanofiber nonwoven by electrospinning. The solution should be in concentration of around 6% by weight. To increase the solubility, the addition of a co-solvent lithium chloride was done. The lithium chloride forms a salt complex with the solvent to increase the polarity of the solvent and the solubility. The high

crystallinity of the aramid fibre makes for challenging dissolution. Dimethyl formamide was selected for the good solubility of aramid and volatility.

Table 4-1. Comparison of solvent properties (A.Chandrasekaran)

Parameter	Dimethylformamide (DMF)	Dimethylacetamide (DMAc)
Polarity Index	6.4	6.5
Boiling point (°C)	153	166
Vapor pressure (Pa)	516	300

For the electrospinning, a low boiling solvent with a high vapour pressure is desired to evaporate the solvent before the fibre hitting the collector.

For the dissolution, a high polarity, low molecular weight and high boiling point is desired. For entropy driven dissolution, a high boiling point can favour the dissolution of the polymer. A high polarity can increase the interaction with polymer solvent. A low molecular weight solvent can penetrate in the polymer structure and dissolve the polymer.

The DMF/LiCl solvent blend is commonly used for the spinning of aramid fibre. However, for electrospinning, the high conductivity of the DMF/LiCl solution has shown to be difficult to process. The high conductivity of the solution can short the circuit, causing current spike and unstable electrospinning in certain conditions. The conductivity of the solution could explain the tendency to short. The conductivity of the solution was measured with a conductivity meter. The formation of the Taylor Cone required for stable electrospinning can be disrupted by a solution with very high conductivity. The DMF/LiCl/Aramid has a conductivity of 4.61 mS/cm and the DMAc/LiCl/Aramid of 2.61 mS/cm. Similar conductivity is reported for aramid DMF/LiCl at a concentration of 6% (H. B. Kim et al., 2019), where fibres were spun successfully. This deviation from the literature could come from the equipment used for electrospinning. Difference in the feed material is also plausible. The feed material requires to remove undissolved Kevlar fibre and the supplementary manipulation could also create variation and error. Multiple samples were prepared from the same material lot to rule out this possibility.

Due to the narrow processing condition and poor repeatability of the results, a limited amount of electrospun mats were prepared and tested.

4.5 Evaluation of adhesion to nonwoven fabric

The addition of a substrate to the nonwoven is required for hood application to obtain the required resistance to burst strength and durability to washing. A good adhesion between the two layer is required to avoid the substrate rubbing through the nanofiber nonwoven during washing or usage. The method of lamination of the nanofiber nonwoven was evaluated. The mats are spun directly on the substrate to bound the wet nanofiber to the substrate with the residual solvent. Three method to improve the bonding of the substrate was evaluated;

- Plasma pretreatment
- Solvent bonding
- Chemical bonding

Corona pretreatment: Surface modification by corona discharge is used to modify the surface of the electrospun mats substrate. The goal is to achieve an increase in adhesion of the mat to the substrate. The corona surface treatment remove contamination, increase surface roughness and imparts a chemical modification to the fabric. The new chemicals can increase the surface energy of the fabric to improve the wettability of the electrospun fibre. The new chemicals on the substrate could increase the interaction with the solvent and increase the diffusive bonding by polymer entanglement.

The fabric sample is guided on a film to the corona lamp. The potential is varied from 0,2 to 0,8 kV, the fabric linear speed is kept constant at 1.5 m/minute and for one pass.

Brown specs are observed at 0,7 kV and 0,8 kV could be due to degradation of the polymer. The energy is reduced to prevent colour change of the polymer. At lower energy, a change of gloss is observed on the fabric, with a rougher surface fibrillated surface. The sample at 0.6 kV is selected for further analysis. Samples are stored in a plastic bag and tested under 24h after the Corona treatment, spinning on the substrate is done immediately after the corona.

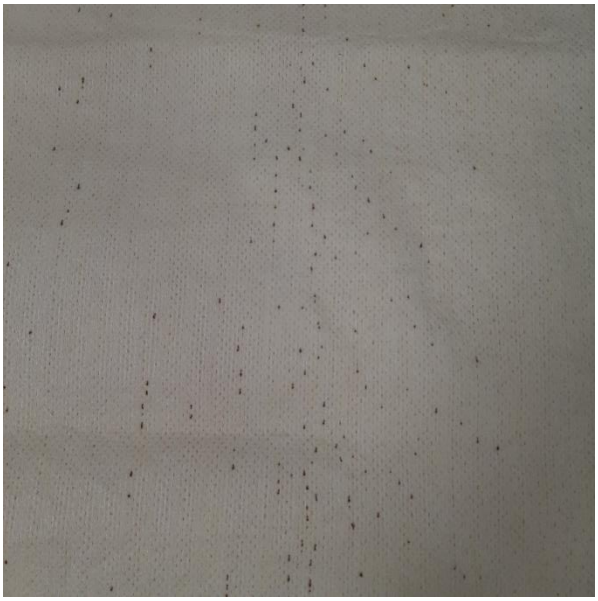

Figure 4-3. Fiber degradation after surface treatment

SEM is performed to assess the roughness of the surface or the fibrillation of the fibre.

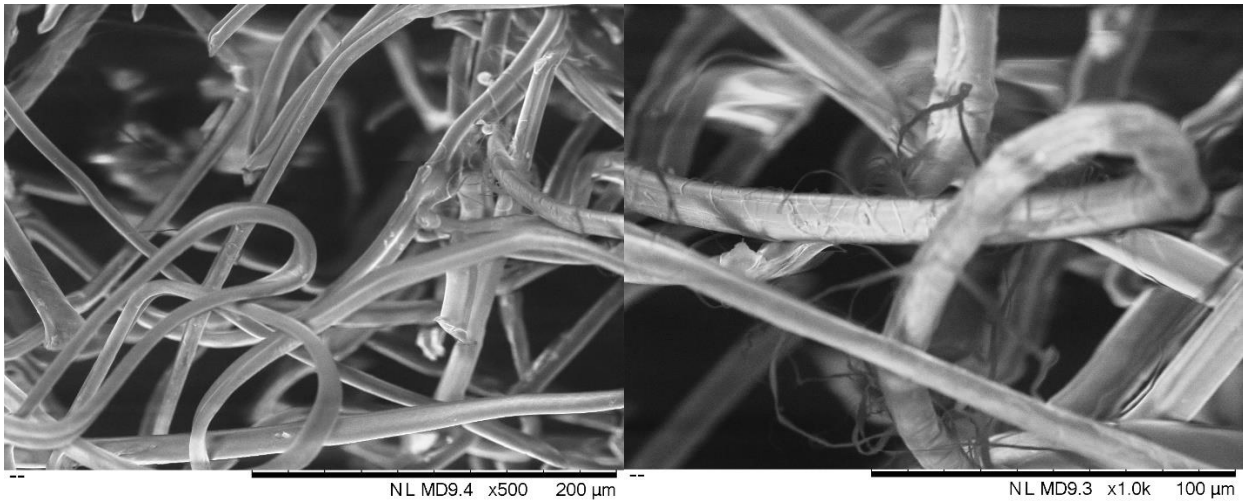

Figure 4-4. SEM observation of fabric after 0.6 kV corona treatment, before electrospinning.

An increase in fibre end and an increase in overall fibre roughness is observed by comparing the corona treated fabric against the reference fabric.

Chemical bonding: A water-based solution of acrylic copolymer emulsion is sprayed to obtain a concentration 5% on weight of the fabric before and after electrospinnning. The acrylic is selected due to the good adhesion, antifraying properties and consolidation of the coating. The adhesive is

self-cross-linking, avoiding the use of sensitizing cross linkers. The glass transition of the polymer is close to the room temperature, the tacky surface could improve particle retention in the filter. The fabric is dried and cured after the electrospinning. The fabric has a glossier finish and stiffer, but acceptable handle or quality of touch after applying the adhesive. The addition of adhesive should be minimal to obtain good adhesion, without clogging the pores.

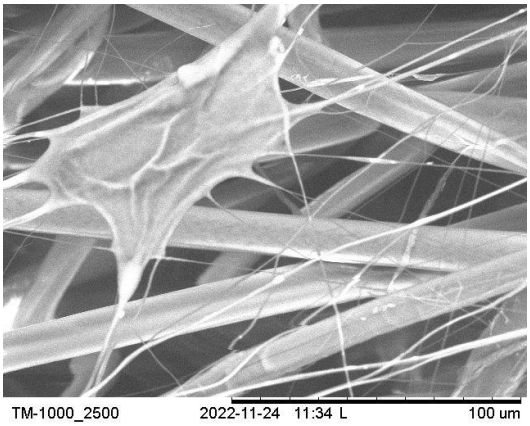

Figure 4-5. Adhesive dot on the nanofiber and nonwoven

Solvent bonding: Dimethylformamide (DMF) is electrosprayed on the fabric at the collector to reduce the glass transition, increase chain mobility to improve adhesion by diffusion of the nanofiber. A dimensional change and increase of the fabric rigidity are observed. This method is not pursued due to unacceptable handle and dimensional change.

To assess rapidly the effect of the surface treatment on the adhesion of the electrospun an adapted version of the tape test ASTM F2252 was used. Clear packaging tape is used for the testing. The adhesive tape is applied on electrospun coated fabric, and pressure is applied by roll. The tape is peeled by hand at 120 to 150 degrees at moderate speeds of 305 to 460 mm/s. The surface of the tape is examined for removed material.

To quantify the removal of material, the basis weight of the peeled tape is calculated. A surface of the tape is weighted and the area measured.

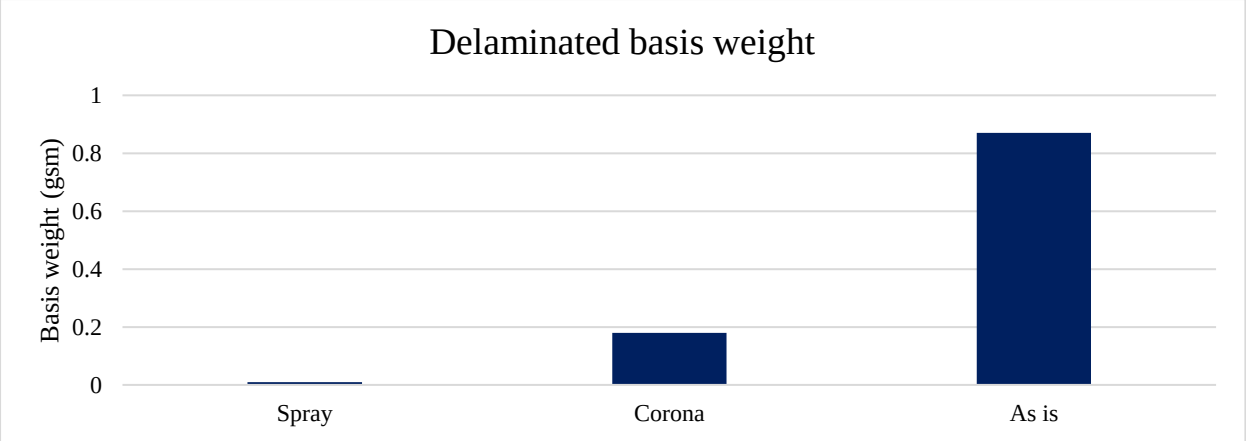

Figure 4-6. Evaluation of adhesion by basis weight of the peeled tape

The basis weight of the electrospun material is expected to be of 0.13 gsm. The substrate as is delaminated completely under the peeling zone and around the peeling zone.

The surface treated corona delaminates only around the peeling zone and stay laminated around the peeling zone. The basis weight of the electropsun mat is close to the basis weight of the peeled surface. The adhesion of the electrospun is expected to be higher than the cohesion of the nanofiber. The adhesion of the mat is improved, but judged too low to be durable to 5 wash cycles as required for the application.

The spray treated electrospun, or chemical consolidation, fabric creates very little loss of fibre after peeling. To further improve the lamination, the adhesive could be electrosprayed to reduce the droplet size and reduce filter clogging by the adhesive, which has been used by other researchers (Li, Shang, Li, & Yang, 2017)(Cloupeau & Prunet-Foch, 1990; Jaworek & Sobczyk, 2008).

The consolidation by adhesive is selected for further testing against filtration efficiency and flame retardancy. The addition of a chemical consolidation could impact the properties of the aramid. Does the addition of a chemical consolidation reduce the resistance to flame of the composite?

4.6 Evaluation of Flame Retardancy

The flame retardancy of the nanofiber composite was evaluated by vertical flames from the standard NFPA 1971, using the test method ASTM D6413. The sample was both tested in the machine direction only due to lack of specimens. The coated nonwoven needed an extension at the top of the sample to obtain the required length.

Table 4-2. Evaluation of flame retardancy of nanofiber coated fabric

Parameter	Specification	Nonwoven	Nonwoven with nanofiber
Afterflame (s)	< 2 s	0	0
Char length (mm)	< 100 mm	71±13	77±12
Melt, drip	No	No	No

The E89 nonwoven was evaluated without and with an electrospun coating to understand the effect of the electrospun with chemical consolidation on the flame retardancy. The electrospun coating is consolidated with an acrylic emulsion.

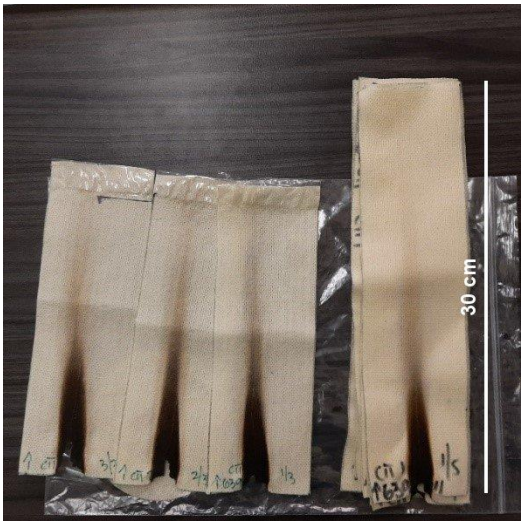

Figure 4-7. Specimens with a coating (left) and without a coating (right)

The filtration efficiency of the nanofiber was evaluated by using a particle size of 0.3 microns at the flow condition required by the NFPA1971. The filtration efficiency of the hood was of 11.93% for latex particles. A filtration efficiency of over 90% is required, it is not acceptable for the application. The filtration efficiency could be improved by increasing the coating weight and reducing the pore size. The basis weight obtained was around 0.13 gsm, where basis weight of around 0.5 gsm has been found to be effective for filtration (Zaarour, Tina, Zhu, & Jin, 2022). However, the difficult solubility and stability of the electrospinning of aramid solution did not allow for a stable electrospinning required for a longer time and thicker weight.

4.7 Conclusion

In conclusion, electrospun coated nonwoven were prepared in this project. The limited solubility of aramid and process stability restricted the amount of sample for testing. The sample size did not allow for evaluation of heat loss. It was possible to develop a lamination method for aramid nanofiber on aramid nonwoven with good adhesion with an acrylic binder and by the corona. The nanofiber bounded with the acrylic binder did not reduce significantly the flame resistance of the aramid nonwoven. The filtration efficiency was limited. A higher weight coating could improve the filtration efficiency. To obtain a higher coating weight, the process must be stable. The use of other polymer could provide a higher solubility and results in a more stable process.

CHAPTER 5 NANOFIBER BY DEPROTONATION

5.1 Nanofiber by deprotonation justification

Nanofibers are of interest to improve the filtration efficiency and heat protection in firefighters' hood. Deprotonation is a proposed method in the literature to prepare a nanofiber aramid dispersion. Aramid deprotonation can be categorized as a chemical recycling method; chemical solvent is used to prepare a new material from recycled aramid fibre. The dispersion can be applied by a coating on a fabric to prepare a filter with improved filtration efficiency, recovered on a filter to form a paper or film, or by the electro-deposition.

5.2 Pre-treatment

The aramid reclaimed material can have surface contamination from lubricants, water repellent or other finishing treatment. Those contamination can impact the quality of the nanofiber, wetting of the fibre, and repeatability. To remove those contamination, a water-based scouring solution is prepared.

Table 5-1. Scouring solutions for aramid

Function	Chemical	concentration (g/L)
Sequestring agent	Ethylenediamine Tetraacetic Acid (EDTA)	1
Wetting agent/detergent	Tergitol 15-S-15	1
Alkali	Sodium hydroxide (NaOH)	3

EDTA is used to counteract water hardness by chelating cations such as calcium and magnesium. Tergitol 15-S-15 is a secondary alcohol ethoxylate with a hydrophilic-lipophilic balance (HLB) of 15.4. It is used as a detergent and wetting agent. The reduction in surface tension from the surfactant improve the spreading and penetration of the liquid. In the textile industry, wetting is used to described the displacement of air in the textile structure by liquid, meaning the submersion of the textile. (Myers, 1999) Sodium hydroxide is used to catalyze the hydrolysis of oils, grease, coatings or other contamination on aramid.

The scouring solution is used at a liquor ratio of 50:1, meaning that 50 ml of the solution is used for 1 gram of textiles. The washing temperature is 60°C. 10 grams of tissue are treated in a 750 ml reactor with 500 ml. Tap water is used for cleaning.

The surface tension of the solution is measured with a K20 surface tensiometer equipped with a Noüy ring. A Harkins-Jordan (H&J) correction factor is applied. The surface tension of the cleaning solution is 34.5 mN/m which is consistent with the concentration of surfactants used. The pH of the cleaning solution is 12.7, which is expected with the concentration of alkali and EDTA used. The fabric is rinsed, spun by centrifugation and dried at 60°C for 20 minutes.

A FTIR and SEM are carried to verify that the material is not degraded, available in APPENDIX B. The SEM shows no surface defect from mechanical and chemical effect such as fibrillation or surface rugosity. The FTIR shows similar peaks, no intense hydrolysis or degradation of the fibre. The wetting of the fibre is significantly improved. The water contact angle is initially of 123±8° and of 0° after the scouring.

For the preparation of the nanofiber by dissolution, the aramid fabric is first wetted with water/KOH solutions for 30 seconds and the solvent is added. A complete wetting of the fibre was observed with the pretreated fibre, where untreated fibre showed dry spot.

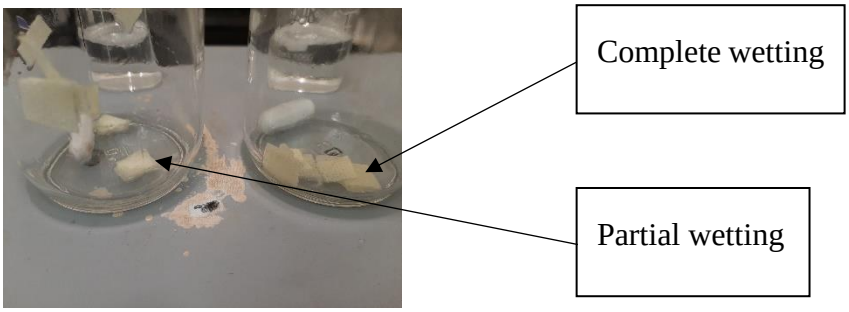

Figure 5-1. Wetting of aramid before (left) and after pretreatment (right)

A complete wetting improves the reaction time by visual observation. A light foaming is observed on the untreated fabric, and no foam is observed on the pretreated fabric. A reduction of foam formation is observed.

5.3 Kinetic study

The work on the reaction kinetics for para-aramid fibres made it possible to improve the reaction parameters from 1 week to 10 minutes with some optimizations of reaction conditions.

The addition order is based on the work of (L. Huang et al., 2022), where addition of an alkali and water before the solvent improved the reaction kinetic. The studied parameter is alkali to aramid concentration, DMSO to water ratio and reaction temperature.

The kinetic was studied by UV-vis spectroscopy by time-dependent sampling of the reaction. UV-vis is a simple and robust method to detect formation of chemicals in solution. For this reaction, the dispersion of aramid shows an increase in peak at around 300 nm, an example spectrum is available in the APPENDIX B. The colour shift is also observed visually, the reaction starts from transparent to an amber orange. The colour change is assumed to be from the formation of nanofiber. A dilution of 1:100 is done to follow the Beer-Lambert's law. A blank composed of the reaction solvent is done to obtain a baseline

5.3.1 Concentration of alkali

The concentration of the potassium hydroxide was studied by changing the ratio of solid potassium hydroxide to aramid fibre. The potassium hydroxide has better dissolution properties of aramid compared to other hydroxide such as sodium hydroxide. The following plot is obtained from the data processing of UV-vis spectrum.

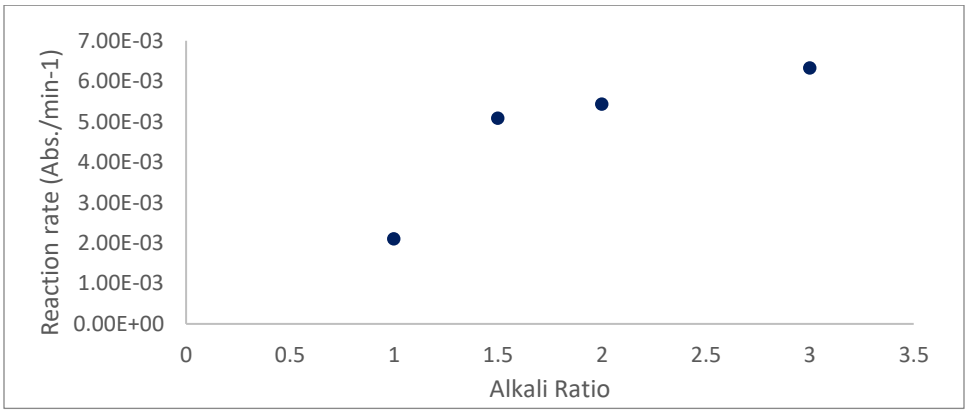

Figure 5-2. Kinetic study of alkali ratio on formation of aramid nanofiber

The kinetics of reaction was quickly increased between the ratio of 1 to 1.5 and increases slowly at ratio higher than 1.5. The increase of alkali concentration has a lower effect on the reaction kinetics at this point. At the end of the reaction, the alkali is considered a waste by-product, the concentration should be as low as possible with an acceptable reaction rate. A ratio of 1.5 is found to be ideal for this application.

5.3.2 Effect of Water Content on the Reaction Rate

The effect of water concentration on reaction kinetics is studied. Two phenomena in confrontation are expected.

1) Ionization of potassium hydroxide – increase reaction rate
2) Lower the aramid solubility – decreased reaction rate

Visually, the solvent ratio of 100:8 and 100:6 of DMSO to water seems to increase the kinetic of fabric digestion. Fabric pieces were dispersed in fibre in about 45 minutes.

The reaction kinetics were also followed by UV-vis spectroscopy to detect the optimal concentration. A solvent ratio 100:3, 100:8, 100:12 and 100:20 of water was evaluated.

The concentration of aramid in solution increase rapidly over the first 95 minutes. After 95 minutes, the concentration diminishes gradually for the solution with a ratio of 6 parts of water or higher. For the 3% solution after 95 minutes, the concentration maximum stabilizes quickly. The reaction rate over the first 95 minutes has a linear profile. The slope is taken as the reaction rate over this segment. The reaction rate in function of the water part is plotted.

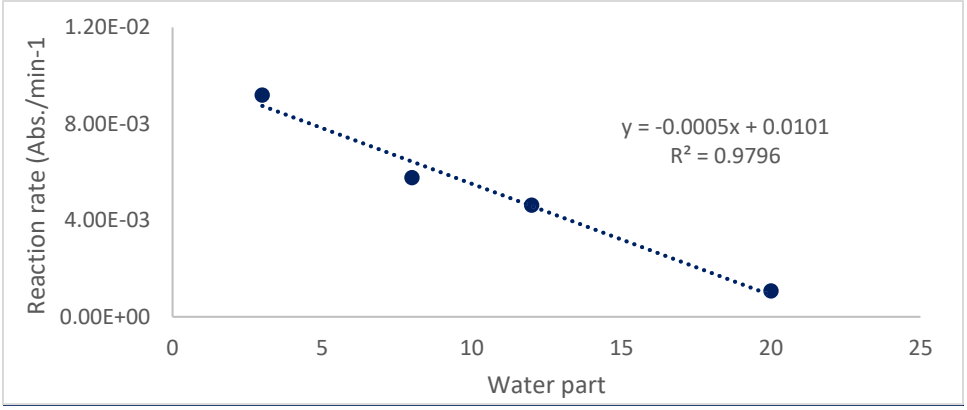

Figure 5-3. Deprotonation reaction rate in function of water content

The increase in water concentration decrease the reaction kinetics over 3 parts of water. However, the water concentration should be maximized because of the advantages:

1) Lower environmental impact compared to organic solvent
2) Lower cost
3) Easily removed by evaporation compared to DMSO

Water concentration can also have effect on the thermodynamic of the reaction. An increased of water concentration is noted to increase the size of the fibre. The effect of water concentration on fibre morphology and the fibre morphology during the reaction is studied by SEM.

5.3.3 Effect of Heat on Kinetic

The reaction temperature was increased from 24 to 45°C to study the effect of temperature on the reaction kinetics. The temperature was fixed by a heated oil bath. The solvent was fixed at 12:100 (water:DMSO) and the solid ratio was fixed at 3:2 (KOH:aramid). The reaction was followed by spectroscopy as described earlier.

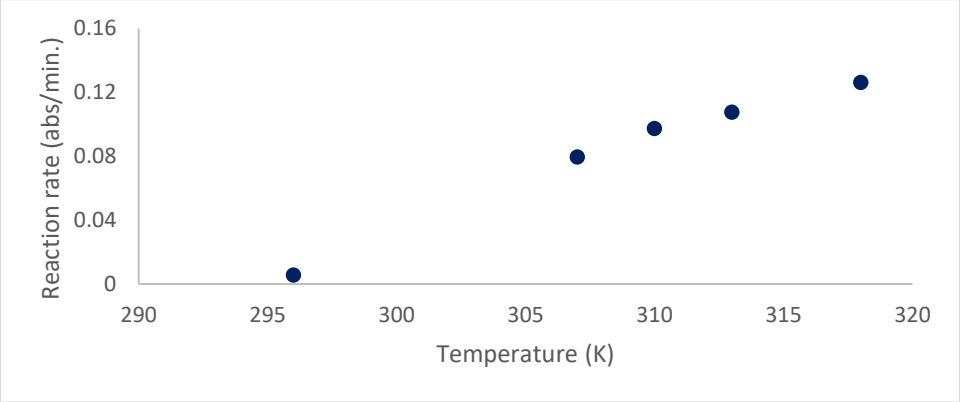

Figure 5-4. Effect of temperature on deprotonation reaction kinetics of aramid nanofiber

The reaction rate increases with the temperature as expected by the Arrhenius relationship. To linearize the relation, a natural logarithm is applied to the relation:

$$\ln k = -\frac{E_a}{R}\left(\frac{1}{T}\right) + \ln A \tag{5.1}$$

The natural logarithm of the reaction rate can be expressed in function of the temperature reciprocal to evaluate the activation energy.

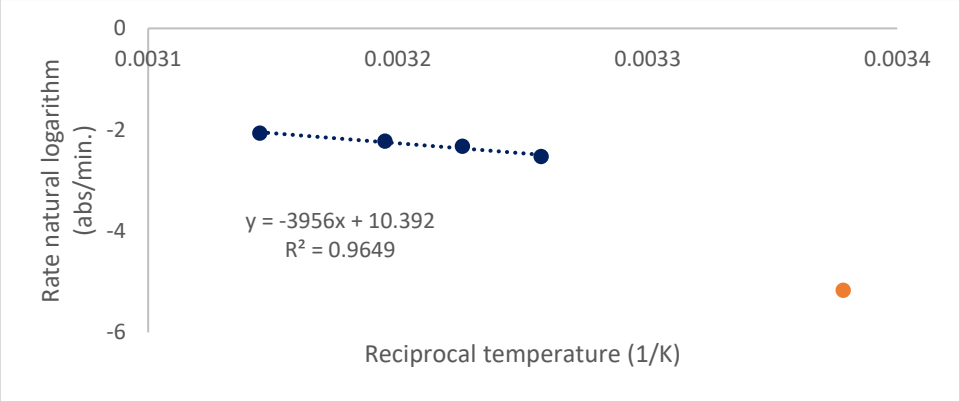

Figure 5-5. Effect of temperature on deprotonation reaction rate natural logarithms

The trend follows a linear path from 307 to 318 Kelvin, however, the initial temperature of 296 Kelvin does not follow the trend. The reaction roughly follows the Arrhenius model for most of the temperature. A limited range of temperature is studied, a larger range of temperature would be ideal to apply the model. The goal of this study was to improve the reaction kinetics for a fast reaction. The temperature can be used to increase the reaction kinetics. A larger range of temperature should be studied if one wishes to model the reaction to the Arrhenius model.

5.4 Nanofiber Morphology

A solid ratio and a solvent ratio were determined by the optimization of the kinetics. The resulting fibre was studied by SEM to evaluate the fibre morphology.

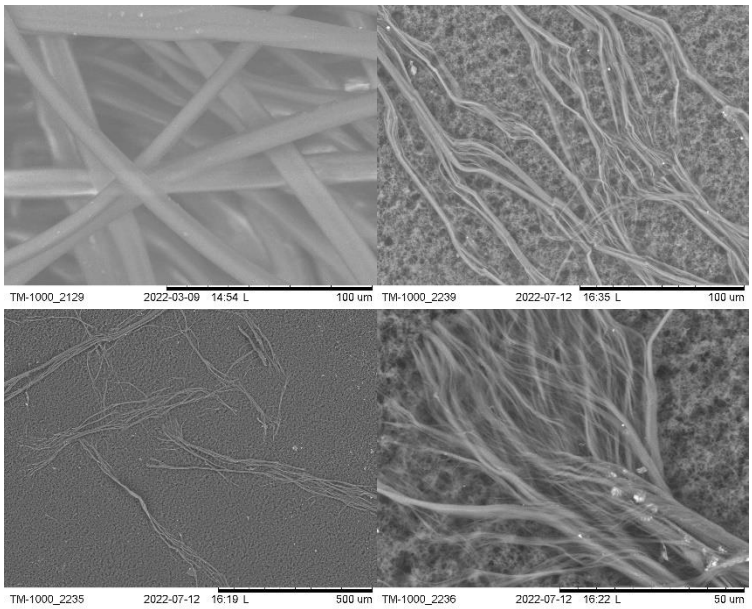

Figure 5-6. Effect of the chemical treatment compared to the original fibre (top left)

The SEM image taken during the reaction of deprotonation to understand the reaction. The fibre shows larger diameter at the middle, and smaller diameter fibre, with fraying at the end of the fibre. The separation reaction of the meta-aramid fibre starts at the end of the fibre to create a smaller diameter fibre in the length direction. In addition, fracture points are observed in the core of the fibre, in the perpendicular direction, where fibre starts to split. This observation is in conjunction with the observation of reduction of fibre length.

(L. Huang et al., 2022) also observed the formation of fibre parallel and perpendicular to the fibre direction in Para-aramid polymers. The separation of the fibres is observed by SEM towards the middle of the reaction. 2 ml of solutions are collected and filtered through a 4.5-micron nylon filter under vacuum. The filter is cleaned with deionized water and rinsed with acetone before being air dried.

Table 5-2. Approximation of length over diameter ratio of neat fibre and chemical nanofiber

Aramid	Length (mm)	Diameter (microns)	L/D ratio
After scouring	19	150	127
After chemical treatment	0.5	<25	20

The goal of the chemical treatment was to be reduced to the diameter of the fibre for an improved filtration efficiency. The diameter reduction was attained; however, the reduction in diameter also reduced the quality of the fibre. By comparing the L/D ratio between the fibre after scouring and after the chemical treatment, the chemical treatment reduces the length more than the diameter. This effect is undesirable as a high L/D is desired for higher mechanical property due to fibre entanglement. A low L/D fibre will also give a paper like aspect. Perhaps the reaction could be improved to the length of fibre after the chemical treatment.

5.5 Nanofiber Thermal Stability

A thermogravimetric analysis is carried out to evaluate thermal decomposition and the formation of volatile species. Thermal degradation produces volatile compounds, which is accompanied by a change in mass. Degradation is followed under nitrogen. The reference material has a weight shift at 412.12°C and the recovered nanofiber a degradation temperature of 411.85°C. The aramid

degradation temperature before and after deprotonation are similar. Thus, the thermal stability of aramid is preserved.

5.6 Scale Up

Higher concentration of the solution of 15% is prepared for coating. To improve the mixing, the magnetic stirrer is replaced by a mechanical mixer. Different impeller type was evaluated to limit ragging and fouling from the fabric piece. First, the fouling of the impeller and shaft create imbalances, which results in shaking and wear on the mixer component. Second, the impeller geometry is changed by the fouling, which reduced the mixing work. Between a pitch blade impeller, high shear disperser, a four-blade impeller with a low pitch ratio and large blade area was found to reduce the ragging.

5.7 Coating on Fabric

To form a coating of aramid, the solvent and alkali must be removed. The removal of DMSO by evaporation is challenging due to the low vapour pressure of the solvent. The alkali should be removed by rinsing the aramid.

The knife coating method is selected to apply a coating of aramid dispersion on the fabric before removing the solvent by coagulation in a non-solvent. The non-solvent used is water to remove the solvent and the alkali. The coated fabric is dried in an air oven. The knife coating method was preferred for the simplicity and ease of scale up.

The coating was applied on three nonwoven of different basis weight, composition and/or type. An aramid spunlace nonwoven of 20 gsm, an aramid spunlace nonwoven of 85 gsm and nylon 6,6 spunbond of 68 gsm. Spunlace nonwoven have good insulation properties for protection against heat and flame. Spunbond nonwoven is often used to support filter material. However, the nylon 6,6 will not have the required resistance to heat and flame. The nylon spunbond is used to demonstrate the possible filtration efficiency.

The coated fabrics are stiff and with poor adhesion between the fabric and the nonwoven. The flexion of the sample results in breaking and delamination of the film. The durability to washing is expected to be poor. To resolve the adhesion and flexibility problem, a new method of coating was evaluated. The aramid nanofibres are first recovered by phase separation by adding enough water to coagulate the aramid.

5.8 Conclusion

In summary, the deprotonation reaction of aramid was improved by first scouring the fabric and second by optimizing reaction parameters, the concentration of the alkali, aramid, water, DMSO and the temperature. The increase in temperature was found to greatly improve the reaction rate. SEM analysis of fibre during the reaction shows the splitting of the fibre in parallel and perpendicular direction. The L/D ratio of the fibre is diminished by the treatment, future work should be done to improve the L/D for fibre of higher quality. The thermal stability of the aramid was conserved according to the TGA. The stability of the coating to flame should be evaluated. The coating of aramid dispersion on nonwoven was not acceptable. The coated textiles are too stiff with poor adhesion between the coating and the nonwoven. To improve the barrier, a new method of coating will be evaluated in the next chapter.

CHAPTER 6 DEVELOPMENT OF COATING

Aramid has resistance to heat, flame, chemical and good char properties required for the end application. However, the aramid lacks the flexibility and adhesion required for the application. Flexibility and elasticity of the coating is required for ease of donning, fit and comfort for the wearer of the hood. Blending of polymers can be a solution to impart new properties to a polymer. By adding an elastomer, the flexibility of the barrier could be improved. The development of a flexible coating will be explained in the following structure:

1- Feed preparation – selection of material, dispersion of aramid and defoaming
2- Coating – optimization of the wetting and viscosity
3- Coated textile evaluation – evaluation of the barrier for hood applications

6.1 Feed preparation

Material selection

A hydrophilic polyurethane is selected for the flexibility and elasticity of elastomeric polyurethane, the high-water permeability for comfort and good adhesion to different fabrics for durability to washing. The polyurethane can lack resistance to heat and flame, where aramid can improve those properties. The coating will be based on aramid and polyurethane in waterborne form to reduce the environmental and health impact from VOC emission of solvent-based coating. The following formulation was first proposed for the application.

Table 6-1. Initial polyurethane-aramid coating formulation

Product	Function	Part per hundred of resins
Polyurethane water based dispersion	Flexibility, water permeability, adhesion to fabric, particulate blocking	100
Aramid filler	heat stability, flame retardancy, dimensional stability, mechanical strength	30
Wetting	Aramid wetting and dispersion	0.04

The wetting agent is used to improve the mixing of aramid in water. The material used in the formulation are mixed by first dispersing the aramid in water and by adding the polyurethane in a second step.

Dispersion of Aramid

The aramid should be well mixed to provide a homogeneous coating with a particle size appropriate for the processing by knife coating. Large aggregates of aramid during the knife coating results in defect such as streaks. Poor uniformity of the concentration or viscosity can lead to variation of thickness across the web (Gutoff & Cohen, 2006). In short, if the prepared coating formulation is not of high quality, a quality coating cannot be achieved.

The humidity of the fibre is of importance for ease of handling and mixing. For handling, the humidity reduces the volatility of the pulp and prevent static build up. Moreover, the presence of humidity facilitates the wetting and dispersion of aramid in water. Fully dried pulp is difficult to disperse in water – likely due to the strong bonding between the aggregate. The humidity of the pulp is measured by a moisture balance. The pulp is weighted, heated to 120°C and weighted until the constant. The humidity of the fibre is of about 50% by loss on drying (LOD) with a moisture balance.

Figure 6-1. Aramid particle before dispersion

The aramid is dispersed in water with a surfactant using a high shear sawtooth impeller at 1500 rpm for two hours. The mixing parameters are of D/T=1/3, C/T=1/3 H/T=1. A low form beaker without baffle is used to mix, an angle of about 10 degrees is used to prevent vortex formation. The impeller speed is adjusted to maximize shear without formation of the vortex. The high shear

sawtooth impeller is compared to a higher shear mixer, the rotor-stator mixer. Rotor stator is used to prepare dispersion at 12,000 rpm for 15 min.

The dispersion of the aramid is evaluated by coating aramid fibre with a blade on transfer paper. A streak-free coating is obtained with the rotor stator, while the sawtooth dispersion has streaks in the coating. The rotor-stator mixer is selected for the improved dispersion of the aramid.

Defoaming

The addition of filler and mixing a high shear results in some air entrapment in the formulation. The air between the aggregate of aramid is entrained in the formulation during mixing. The high shear mixer results in micro-foam, which can be difficult to remove. The foam forms in pinhole defects, which reduce the barrier properties of the membrane.

To prevent defect from foam such as pinholes, a defoamer was added to the mix. A polymeric defoamer is added during the grinding of the aramid and during the mixing of the resin. Moreover, the formulation was left at least 24 hours before applying the coating to complete the mixing and the defoaming.

6.2 Optimization of the Coating

The coating is applied by knife coating method, the formulation is fed to the substrate and removed by a metering blade to obtain the desired coating weight. The coating is applied on a release paper designed for water-based formulation to ensure a uniform and low coating thickness. The release paper is a Kraft paper with a release liner on one side. The release paper has a smooth uniform surface for the coating to dry and cure. The fabric is laminated on the wet coating and delaminated from the release paper to produce a coated textile.

Wetting

The formulation has shown poor wetting of the release paper. After coating the release paper with the formulation, the liquid crawl back in large droplets. The coating tends toward a state of lowest energy by minimizing the surface energy the systems by reducing the surface area between the coating and the release paper. A sphere will have the lowest surface for a given volume. The coated film tends to minimize the surface by forming droplets, close to the sphere (Gutoff & Cohen, 2006).

The coating shows acceptable wetting of the substrate initially. However, during conveying to the dryer or drying of the coating, dewetting or crawling occurs. The dewetting results in a coating of poor quality. Surface tension plays an important role in wetting of the coating. The release paper has a surface tension of 25.37 ± 0.80 mN/m measured by double sessile drop, where the coating has a surface tension of 45.86 ± 5.01 mN/m measured by DeNouy ring at room temperature. For good wetting, the release paper should have a high surface tension, and the coating a low surface tension (Gutoff & Cohen, 2006).

To improve the quality of the film, a surface additive is added to reduce the surface tension at the coating and substrate interface and improve the wetting of the substrate. The higher density of the additives compared to the other component of the formulation promotes migration of the additive to the substrate surface. The additives consist of a blend of succinic acid and esters. A loading of additive is optimized using different loading of surface wetting additive and observing the wetting condition after 30 seconds.

Table 6-2. Observation of wetting on release paper

Concentration of wetting agent (%w/w)	Observation after 30 seconds
0,0	Complete dewetting of the paper
1,0	Complete dewetting of the paper
2,0	Partial dewetting
3,0	Complete wetting, clean edge

As the coating needs to be released from the release paper, the wetting of the release paper should be high but the adhesion should be low.

The viscosity can also play a role in the wetting of the substrate. The liquid edge retraction during dewetting and progression during wetting happens at a slower rate for a higher viscosity liquid. The viscosity of the formulation is measured using a spindle viscosimeter Brookfield DV2T. The viscosity at room temperature is of 8 568±240 cP at 5 rpm (near zero shear rate), which is suitable for a knife coating application. A high viscosity can increase the wet film thickness, and should be controlled for reproducible and uniform thickness.

Optimization of Drying

The coating is dried in an air oven to remove water and cross link the polymer. The evaporation rates in the air-drying oven is mainly controlled by the air velocity and air temperature. High velocity removes humidity faster at the surface of the film by removing humidity at the surface of the coating and bringing dry air. High temperature increases the dew point. In other words, the air has more capacity to accept water molecules. The line speed and dwell time in the dryer are important parameters in continuous coating line operation. The coating wet weight, solid concentration, solid specific heat and density can affect the drying (Gutoff & Cohen, 2006). The release papers thickness, specific heat and density can affect the drying (Gutoff & Cohen, 2006).

The drying of the film was tested at 80°C first. Mudding or cracking defects were observed due to the rapid drying of under 2 minutes. The removal of water resulted in tension in the coating due to void (Tracton, 2005). The tension can wrap the substrate or cause crack in the film if the substrate cannot deform. The coating will crack as the release paper is rigid and fixed on a frame.

The temperature of the oven was reduced by intervals of 20 degrees Celsius. The temperature of the drying section was reduced to 40°C to prevent cracking or mudding defects. Still, some light cracking defects were observed on Figure 6-2. To further reduce the drying defect, a humectant was added to the formulation. The humectant is a polyethylene glycol of 400 g/mol. The humectant is partially miscible with the water-based coating formulation. The humectant has a lower vapour pressure than water, drying slower than water. The slower drying rate reduces the tension caused by the drying. This prevented formation of a skin and formation of cracks.

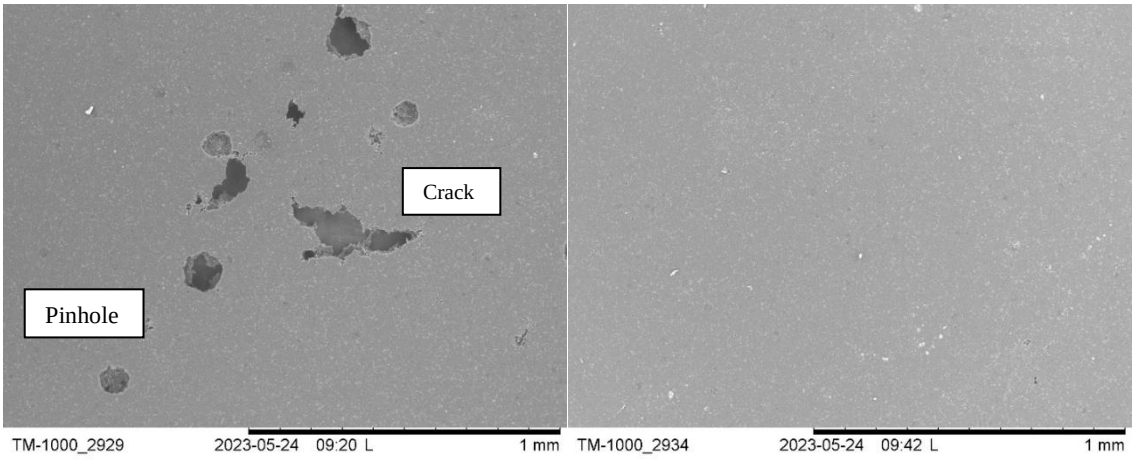

Figure 6-2. Top view of the coated knit defects and defect-free observed by SEM

The required time to dry the coating at the temperature and air velocity was of about 4 minutes at the laboratory scale. The uses of an infrared pre-dryer section at the industrial scale can improve the throughput. The infrared heater transmit heat directly from the emitter to the coating, resulting in a uniform and rapid heating of the coating (Gutoff & Cohen, 2006; Tracton, 2005).

A curing at 150 degrees Celsius is completed for 3 minutes to initiate cross-linking of the film from the self-cross-linking polymer and the carbodiimide cross linker. The carbodiimide can continue to crosslink slowly at room temperature in case the cross-linking is incomplete. The temperature and time were selected based on available technical data sheet from the supplier of the polymer and cross-linker.

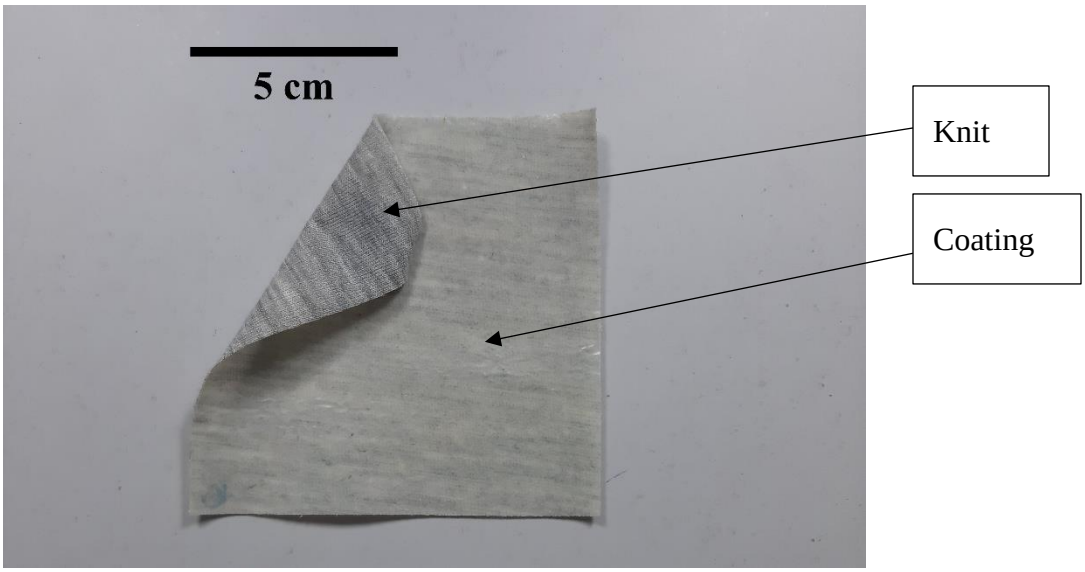

Figure 6-3. Coated knit (coated side)

The coated knit is a flexible, elastic film with good adhesion to the knit and glossy surface. The final formulation is the following.

Table 6-3. Final formulation of polyurethane with aramid

Product	Function	Part per hundred of resin
Polyurethane water based dispersion	Flexibility, water permeability, adhesion to fabric, particulate blocking	100
Aramid filler	heat stability, flame retardancy, dimensional stability, mechanical strength	30

Wetting	Aramid wetting and dispersion	0.04
Defoamer	Reduce foam during mixing, reduce coating defect	1.00
Humectant	Reduce drying defect	0.80
Substrate wetting	Provide wetting to release paper	4.00

6.3 Evaluation of the coated textile

Heat loss

The total heat loss (THL) of the hood barrier is evaluated by the test method ASTM F1868. A skin model simulates heat transfer between the skin/hood and the outside environment. The skin model consists of a heating plate to maintain the temperature of the skin. The heat input to maintain the plate at the set temperature is measured based on a 10x10 in the surface. The NFPA 1971 edition 2018 requires a minimum heat loss of 325 W/m^2 for comfort and heat stress management. Samples of 20x20 in. of coated fabric are tested in triplicate. The sample is maintained in a controlled temperature environment chamber with forced air circulation.

$$Q_t = \frac{10}{R_{cf} + 0.04} + \frac{3.57\ kPa}{R_{ef}^A + 0.0035} \tag{6.1}$$

Where Q_t is the indirect total heat loss in W/m^2, R_{cf} is the average intrinsic thermal resistance, and R_{ef}^A is the average apparent intrinsic evaporative resistance.

The first part of the equation corresponds to the dry heat loss which is a combination of convective, conductive and radiating heat transfer. The second part is tested in wet condition and is the heat loss associated with evaporation mainly.

The heat loss to the environment is accomplished mainly the passive body cooling by evaporation of the sweat. Therefore, the hood material should be permeable to water vapour. The evaporation of the humidity also depends on the environment condition such as temperature, humidity, forced and air convection. The heat loss is quite complex evaluate and measure as many factors can influence the results. The heat loss of the hood to the environment can be evaluated by using a simulated skin model in an environment chamber.

The use of a skin model is limited for laboratory scale specimens due to the requirement of 20x20 inch specimens, longer and complex test. Alternatively, the water vapour transmission rate can be tested quickly on multiple small samples by the test ASTM E96 method B. The hydrophilic films

are impermeable to air, the expected primary cooling of hydrophilic film is evaporative. Therefore, the permeability to water vapour is tested to develop the membrane and evaluate the comfort of the coated fabric. The method B with upright cup has a still air section, similar to the ASTM F1868.

Table 6-4. Water permeability of hydrophilic polyurethane aramid film

Characteristic	Method	Coated PU	AC-01	AC-02	AC-03
Variance	-	Reference	Aramid 30 parts	Reduced weight	Crosslinking
Water vapour transmission rates (WVTR), g/m^2/24h.	ASTM E96-B	383	331	509	499
Coating weight, g/m^2	ASTM D3776	220 (149)	196 (125)	140 (69)	126 (55)

The hydrophilic polyurethane is evaluated without the aramid but with additives. The viscosity is adjusted to 10 000 cP with an associative thickener. The coated fabric has a basis weight of 220 grams per square metre. By subtracting the basis weight of the fabric, the coating has an estimated weight of 149 grams per square metre.

To set in context the water vapour transmission rates, the healthy skin at rest permeates at a rate of 204 g/m^2/24h (Gupta, Agarwal, & Alam, 2010). However, during the firefighting exercise, the core temperature of the firefighter will increase until the heat production is equivalent to the heat loss, a steady state is reached (Sawka, Wenger, Young, & Pandolf, 1993). A heat loss by evaporation will be required to maintain the adequate body temperature. Therefore, the permeation rate of the clothing must be higher than the skin at rest. From the correlated data between the moisture vapor transmission rate and the total heat loss by a heated plate, the required moisture vapor transmission rate of the hydrophilic coating is estimated at around 500 g/m^2/24h (J. Huang, 2006; McCullough, Kwon, & Shim, 2003; Meena, Kerketta, Tripathi, Roy, & Jacob, 2022; Nazare, Madrzykowski, & Nazare, 2015).

The water vapour transmission rate of the reference sample is of 383 g/m^2/24h, which is below the target. The addition of aramid in the formulation reduced the permeation to water vapour, as expected. The aramid is less hydrophilic and more crystalline which reduce the permeability to water. To increase the permeation to water vapour, the coating weight is reduced. A 45% reduction

in thickness improved the water transmission rate by 34%. The reduction of the thickness follows the expected trend.

The cross-linking of the coating has no significant impact on the permeability. The permeation is expected to decrease with the increase of cross-linking density. However, the selected cross linker has a hydrophilic modification which could counterbalance the cross-linking effect on the water permeation rate.

The water permeation rate is estimated acceptable to generate enough cooling by evaporation. To validate the heat loss, a larger sample of coated knit is prepared on a pilot line, using similar technique to the laboratory coater. A basis weight of 158±6 gsm is obtained, which is higher than the target weight of 125 gsm. The control of the coating weight can be challenging when applying a second coat as the thickness and wetting behaviour varies from each applied coat. Despite the difference in coating weight, the behaviour of the coated textile can still be evaluated. The heat loss is tested according to the ASTM F1868 Part C specified in the NFPA 1971 standard.

The AC-03 coated knit is tested in the test chamber at CTT Group. The samples took about three hours to stabilize to a steady state condition, which is within the limit of 4 hours set by test standard. The steady state is reached when the heat loss is stable. The AC-03 has a high-water uptake and is humid after testing. The stabilization of the humidity inside the sample could explain the long time to reach the steady state in heat loss. After the test, the coating shows wrinkles upon water uptake and expansion.

Table 6-5. Comparison of total heat loss of barriers and hood composite

Property	**Specification**	**PGI BarriAire™ Gold with Nomex® Nano Flex barrier**	**LION RedZone™ with STEDAIR® PREVENT**	**ePTFE with knit**	**Coated knit AC-03**
Assembly condition	As hood composite, conditioned	As hood composite	As hood composite	As barrier	As barrier
Total heat loss (W/m^2)	>325	401	346	704	541±46

The value for the LION and PGI hood is taken from the available literature of the manufacturer. The LION RedZone™ uses roughly a similar ePTFE knit-hood barrier. The hood outer layer can have an impact on the THL, a barrier alone has a value of about 704 W/m^2, where the added outer layer reduces the value to about 346 W/m^2. The PGI hood has a better heat loss compared to the LION hood. The heat loss depends on the barrier, hood construction and lamination.

The developed barrier has an acceptable heat transfer to the environment. The coated knit cooling is of 541 W/m^2, which is over the requirement of NFPA 1971 of 325 W/m^2. To fully be in accordance with the specification, the barrier material should be tested in a hood composite construction. The addition of an outer layer for the composite hood can reduce the heat transfer, it has a high thermal resistance to insulate the wearer against conductive and radiating heat. The final lamination method will be by gravure coating of adhesive dots, which was not available at the laboratory scale. The prototype sample is laminated by bonding the knit to the coating. The gravure method should improve the flexibility and the permeability to water due to the increased available surface at the membrane for the evaporation of water. Overall, an improvement in heat loss is expected by the lamination method, and a reduction is expected from the added outer layer knit.

6.4 Evaluation of the Handle

The coated knit should have flexible and elastic handle for ease of fit and comfort. The bending rigidity was evaluated by a textile evaluation system named the Kawabata bending rigidity.

Table 6-6. Evaluation of the bending rigidity on the Kawabata

Bending rigidity (g cm^2/cm)	Prevent Barrier	AC-03
Length	0.0932 ± 0.0035	0.1749 ± 0.0558
Width	0.0464 ± 0.0065	0.0671 ± 0.0105

The bending rigidity of the coated knit is higher than the ePTFE. The developed coated knit is on average 66% stiffer, which would be less comfortable to wear. Nonetheless, the stiffness of the fabrics is in a similar range.

For perspective, the coated knit can also be compared with values from the literature from protective garment. A patent from WL Gore describe an insert for protective garment made from

ePTFE and aramid woven fabric. The bending rigidity in the same Kawabata testing method results in a bending rigidity of 0,1951 and 0,2275 g cm^2/cm (Dolan, Murphy, Minor, Shahkarami, & Krummel, 2016). An ergonomic study found a bending rigidity of 0.114 and 0.093 g cm^2/cm in warp and weft to be the best for protective fabric made of cotton and polyester (Bartkowiak, Frydrych, & Greszta, 2016). The coated knit developed in this work has a similar mean bending rigidity to a protective fabric made of polyester/cotton.

The polyurethane/aramid coating lamination method can increase the stiffness. The uses of dot glue by gravure coating can reduce the stiffness of the coated fabric. Additionally, a reduction of the coating thickness or cross linker concentration can be a solution to reduce the stiffness, however the protection would be lower.

6.5 Wash Durability

The decontamination of the hood includes a laundry wash. The hood barrier should be stable to laundering at mild condition (warm water with detergent and agitation). The NFPA 1971 requires durability to wash of five cycles in very hot condition. Commercial barrier manufacturers have reported over one hundred wash durability, but the washing condition is not reported. A new product should at least meet the standard requirement, and ideally be as durable if not better than the commercial products.

The hydrophilic polymer used in the coating is permeable to water by swelling and allowing water molecule to move in the film. The swelling can result in dimensional change and poor resistance to wash. The swelling can weaken the membrane, tear, puncture or delaminate the coating from the fabric.

The stability to laundering was first evaluated in the laboratory. The sample was immersed in a beaker with water and detergent at 40°C. The fabric did not delaminate from the coating, but a significant increase in weight and wrinkling of the coating is observed. The weight of the coated textile increased by 2.5 times after washing for 75 minutes.

To further evaluate the durability, the coated textile was assembled in a hood composite and tested for the 5 washing cycles in a washing machine. A mock outer layer interlock knit composed of 50/50 viscose/kermel is used to simulate the outer layer of the hood. The washing is completed according to AATCC 135 for five washing cycles. A fabric ballast is added to obtain a load of

1.8±0.1 kg. The wash cycle is at a normal cycle, using very hot water (60±3°C). The dimensional stability to washing of the coated fabric is evaluated as per the NFPA 1971-2018. The composite material is evaluated as a flat knit material instead of the assembled hood material. The average shrinkage is of -4.1% in length and of -3.8% in width, meaning the sample increased in size after washing. The dimensional change is lower than 5% which is acceptable to the standard.

The permeability to air of the coating is evaluated before and after washing. The permeability to air is below the equipment capacity before and after washing, meaning, no major break, rupture or pinhole is developed after washing.

Visually, the film has wrinkled from the washing and some beginning of delamination. The delamination can be resolved by improving the lamination method, such as adhesive dot gravure. The wrinkles are from expansion upon water absorption.

The future evaluation of durability of the composite should be in the hood composite laminated with glue dot with the commercial outer layer and assembled according to manufacturers' hood template, with all the accessories such as the elastics, labels, stitching and embroidery.

6.6 Flame Resistance

The coated fabric is composed of a polyurethane coating on an aramid knit. Polyurethane typically shows poor resistance to flame and heat, and can melt. Aramid does not melt and is proven to be resistant to heat and flame. The performance of the combined material to flame should be tested.

The flame retardant of the coated fabric was evaluated according to the test method ASTM D6413 with the NFPA 1971-2018 paragraph 8.2. Five specimens were tested in machine direction only due to the size of the sample. The char length corresponds to the length of the burned material, and should be below 100 mm. The after flame is the burning time of the sample after removing the burner, and should be below 2 seconds. The sample must not melt or drip. The specification requires all the layers of the hood to be tested, which is not the case for this evaluation. The goal of this test is not to obtain a specification, but to evaluate the flame retardancy of the coating and the variations.

Table 6-7. Vertical flame test of coated fabric

Test	Method	AC-00	AC-02	AC-03
Variance	-	Without aramid	With aramid	With aramid and Cross linking
MD – After-flame (s)	NFPA 1971-2018 par. 8.2. ASTM D6413 Vertical Flame Test	16.9±2.7	39.1±12.6	28.8±9.3
MD – Char length (mm)		305	305	305

All samples show no drip or melt during the testing. The combination of the polyurethane with a meta-aramid knit does not form a melt or a drip. The addition of a cross linker and of aramid in the polyurethane coating was evaluated. All the material shows a char length equivalent to the sample length. In other words, all the samples burn completely. The addition of aramid increased the after-flame time. The increase in after-flame shows a slower flame propagation, which is a desirable property for flame resistance. Perhaps the char formation characteristic of aramid improved the flame resistance.

The addition of a cross linker did not improve the flame retardant of the coated fabric. Overall, the aramid coated with polyurethane shows no melt or drip, and the addition of aramid slows the flame propagation. The flame resistance should be tested in a composite, including the outer layer knit, to evaluate the hood to obtain the NFPA1971 specification. To further improve the flame resistance, the addition of phosphorous by modification of the aramid could be explored by modification with phosphorous acid (X. Chen, Wang, & Jiao, 2017) or addition of ammonium polyphosphate (Wu, Wang, Xu, & Guo, 2020).

6.7 Particulate Blocking Efficiency

The efficiency of the particulate blocking was evaluated according to the NFPA 1971 edition 2018 with some modification; the filtration efficiency was only evaluated for 0.3 microns particulates size to reduce the testing length and cost. The most penetrating particle is around 0.3 microns for most filter.

Table 6-8. Evaluation of the particulate blocking efficiency

Parameter	Method	Coating without PU	Coating with PU	Commercial barrier
Base fabric identification	-	E89 Non-woven	Knit	Knit on both side
Filtration efficiency at 0.3 microns (%)	GCTTG 154	19 ± 5	99.98	99.99
Air permeability (CFM)	ASTM D737	2.1±0.6	<0.30	10
Basis weight (g/m^2)	ASTM D3776	136±4	196	210
Thickness (mm)	Digital micrometer	-	0.368 ± 0.009	0.428 ± 0.016

The aramid was coated on an aramid nonwoven blend E89. The aramid/polyurethane coating was applied on a meta-aramid knit. The commercial barrier uses viscose/aramid blend knit with an ePTFE barrier. The aramid coating shows poor filtration efficiency and low permeability to air. The aramid coating is stiff and brittle. A soft, elastic and flexible coated fabric is obtained by mixing the aramid with a polyurethane on a knit fabric. The filtration efficiency of the coated knit is similar to the ePTFE commercial barrier with a similar weight. The permeability to air is below the equipment capacity. The permeability to air of the coating is lower compared to the ePTFE. The lack of interconnected pores in the polyurethane coating blocks the air. The filtration mechanism of the polyurethane coating is expected to be by the size exclusion, as the pore size or defect size are smaller than the particulate size. In short, by blending the aramid with a polyurethane elastomer, a soft elastic coating with high-blocking efficiency was obtained.

6.8 Permeation to VOC

The objective of this study is to evaluate the performance level of protection against naphthalene vapour of hood barrier for the development of improved barriers. The test method should be simple, robust, with high time resolution and low concentration detection.

The permeation to volatile organic compounds (VOC) is evaluated using a custom permeation setup developed for this project. The apparatus is based on the 2-inch ASTM permeation cell from

At-mar glass product. The cell seals the specimen to only expose an area of 20.3 cm^2. The VOC is placed on the challenge side and must permeate through the sample to be collected to the test side.

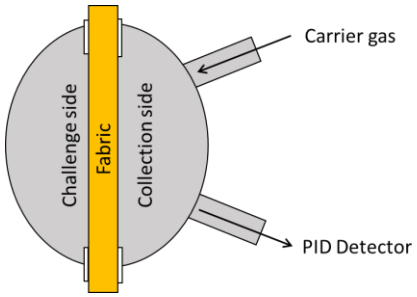

Figure 6-4. Schematic of test cell

The permeated gas is collected by a nitrogen sweep at 0.3 litres per minute for adequate mixing of the permeated gas. The gas is passed in a glass fibre filter before the detector. The VOC is detected by using a photoionization detection (PID) sensor MiniPID 2 PPB from Ions Science. The sensor has a detection range of 0 to 40 ppm and a minimal detection limit of 1 ppb. The lamp energy of 10.6 eV ionizes VOC for rapid detection without degradation of the chemical.

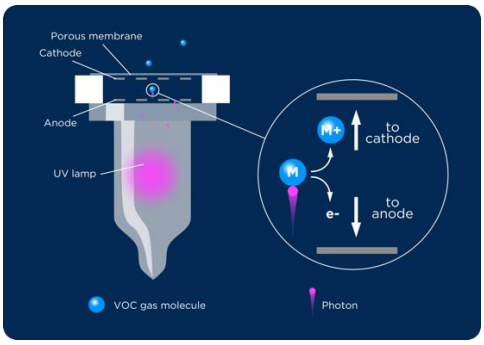

Figure 6-5. Schematic of the photoionization detector (Science, 2021)

More information on the method validation is available in the APPENDIX A. The permeability of the coatings is evaluated against tetralin. Two variances are evaluated; the reduction of coating thickness and the addition of a cross linker. The permeation rate is inversely proportional to the thickness. An increase in thickness is expected to decrease the permeation rate. The degree of cross-linking is inversely proportional to the permeation rate. An increase in the degree of cross-linking will reduce the permeability of the membrane. The sample is evaluated in as a coated textile with the inner knit. The effect of the outer layer used in the hood is not evaluated. The inner knit is

facing the detection side to represent chemical permeating to the wearer side and the coating is facing the chemical challenge side.

Table 6-9. Evaluation of the permeation of coated textiles

Parameter	AC-01	AC-02	AC-03
Variance	Reference	Reduced coating thickness	Addition of a cross linker
Thickness, mm	0.398	0.337	0.329
Basis weight, g/m2	196 (125)	140 (69)	126 (55)
Cumulative permeation, µg/cm^2/min.	0.093 ± 0.012	0.137 ± 0.055	0.139 ± 0.054
Breakthrough Time, hh:mm:ss	01:42:03 ± 00:09:50	00:16:03 ± 00:03:41	00:30:45 ± 00:09:19

The reduction of the thickness increased the cumulative permeation, meaning more chemical pass through the membrane. The breakthrough time correspond to the time required to obtain a cumulative permeation of >0.1 µg/cm^2/min. The breakthrough time is significantly reduced with the lowest coating weight.

The addition of a cross linker gives a similar cumulative permeation compared to the coating without crosslinker of the similar weight. The cross-linking increase by almost twice the breakthrough time. The time required for permeation of the chemical is higher for a cross-linked coating.

To obtain good barrier properties, the diffusion parameter for VOC should be as low as possible. On the coated fabric, defects such as pinholes, cracks, microporosity, uneven thickness can increase the permeation rate. A coating of high quality is required, which was achieved by carefully preparing the feed, applying, drying and curing the coating. During preparation, foam formation during mixing was avoided. A defoamer helped reduce foam and pinholes. The drying rate was controlled to prevent cracks, and a humectant reduced the drying rate at the surface of the coating. Finally, using a second coat improved the film by covering the pinhole and defect.

6.9 Conclusion and perspectives

The blending of polyurethane and aramid allowed for a flexible water vapour permeable coating with improved flame resistance and good barrier properties against VOC and particles.

The objective to develop a hood barrier with balanced protection and comfort is attained. The comfort in terms of flexibility and heat loss is similar to the commercially available barrier. The heat loss and flexibility are similar to the other material, and can be improved with a reduced coating weight. The protection against particulate matter is over the requirement of 90%. The protection against volatile organic compound is enhanced compared to others available hood barriers. The durability to washing is acceptable. The membrane did not shrink excessively and no break are observed from visual and air permeability evaluation. The formulation is prepared without the addition of PFAS and uses reclaimed aramid material.

The work in this project demonstrated a great potential alternative to the current offering on the market. An industrial trial should be done to go further. First, an industrial pilot trial will allow better precision of coating weight by the uses of precise equipment. Second, the pilot trial will allow to uses the lamination by gravure coating of adhesive dots to improve in flexibility and permeability. Third, the pilot trial could identify sticking point in the process and formulation. Finally, firefighting equipment manufacturers could be solicited to provide their external knit for evaluation in composites. The additional external knit will be used to confect a hood. The final assembly will influence the properties of the hood. The evaluation of the assembled hood will be a preparation for certification and commercialization.

CHAPTER 7 ARTICLE 1 : DOES THE NFPA 1971-2018 PARTICULATE-BLOCKING HOOD PROTECT AGAINST VOC? AN EVALUATION OF FIREFIGHTER'S HOOD WITH PARTICULATE-BLOCKING BARRIER AGAINST VOC

This manuscript of the article presented here was submitted on September 18, 2023 to the International Journal of Clothing Science and Technology. The authors are Laquerre, J., Ibrahim, A., Decaens, J., & Ajji, A.

I contributed to the design of experiments, conception and development of a test method, data processing, analysis, interpretation and redaction of this article submitted to the International Journal of Clothing Science and Technology.

7.1 Abstract

- **Purpose**

The International Agency for Research on Cancer classified firefighting as a known carcinogen to humans (Group 1) in 2022 (Mayer et al., 2023). In fact, fire generate many known carcinogens from particulate matter and volatile organic compound (VOC). The particulate-blocking hood provides some protection against particles; however, the field evaluation of the hood and garment has shown concerning permeation to VOC (Mayer et al., 2023). This paper aims to evaluate the permeation against VOC of commercialized firefighters' hood in a laboratory environment to improve the design of the barrier membrane.

- **Design/methodology/approach**

The permeation of commercial hoods barriers is measured in different configurations to investigate the effect of the design, used material nature and membranes structure on protection against VOC. A polyurethane hydrophilic coating was also developed and tested as an alternative material. The VOC permeation is explained based on analysis of the structure and composition.

- **Findings**

Stedair® Prevent ePTFE barrier has a better protection compared to Dupont Nomex® Nanoflex polyimide nanofiber. A novel hydrophilic barrier has an improved barrier property compared to

commercial barriers. The outward facing textile can have significant impact on the hood barrier property against VOC and should be studied.

- **Originality**

A simple evaluation method against VOC is proposed to study the permeation of the hood component and for the development of an improved firefighter hood barrier.

Keywords: Firefighter's Hood Barrier, Membrane, Nanofiber nonwoven, Personal Protective Garments, Occupational Health and Safety, VOC, PAH, PFAS, Measurement and Testing.

7.2 Introduction

Structural fires involve degradation by combustion of natural and synthetic material composed of various organic and inorganic chemicals. The degradation by combustion generates by-products such as volatile organic compounds (VOCs), Polycyclic aromatic hydrocarbons (PAHs), particulate matter (PM), acid gases, hydrogen cyanides, halogenated compounds and others (Fent et al., 2020). Volatile organic compound, polycyclic aromatic hydrocarbons and particulate matter are the main chemicals generated in structural fire. Volatile organic compounds (VOC) are a type of organic chemical in the air at room temperature. Polycyclic aromatic hydrocarbons (PAHs) are amongst the most damaging and most prominent VOC present during firefighting. During incomplete combustion of organic material, PAHs are released in the air (Sjöström et al., 2019). These compounds are known to be mutagenic, cytotoxic and classified as carcinogenic or suspected of causing cancer (M.-R. Chen, Tsai, & Wang, 2008; Mastrangelo, Fadda, & Marzia, 1996) by inhalation, dermal and oral exposure. Particulate matter (PM) is a type of particulate chemical generated in the fire situation from incomplete combustion, also commonly known as soot. Aerosol particulates are a suspension of fine particulates in air, which can penetrate the garment. Studies from National Institute for Occupational Safety and Health (NIOSH) and other research groups has shown an increase in exposure to chemicals and in cancer rates for firefighters compared to the general population (Fent et al., 2022; Fent et al., 2020; Mayer et al., 2022; Mayer et al., 2023; Sjöström et al., 2019; Stec et al., 2018). Moreover, the concentration of chemicals from biological samples of breath, urine and blood increased significantly after firefighting situation.

Possible exposure type to chemicals during firefighting is inhalation and dermal exposure (Fent et al., 2022; Fent et al., 2020; Mayer et al., 2023; Sjöström et al., 2019; Stec et al., 2018). Self-contained breathing apparatus (SCBA) are worn by firefighters to protect from exposure by inhalation. Turnout gear such as hood, jacket and pants are designed to prevent exposure to chemicals. Garments and pants are equipped with a moisture barrier to protect against chemicals (NFPA1971, 2018). Hoods have an optional particulate barrier to protect against particulates and chemicals (NFPA1971, 2018).

From the data available in the literature, dermal absorption is a conceivable route for exposure to chemicals. In fact, VOC and PAH can be absorbed through the skin (Mayer et al., 2022). Furthermore, skin on the head and neck regions show higher absorption due to skin thickness and important blood vessels (Mayer et al., 2023). Those areas should be covered by the hood and hood barrier protection (Mayer et al., 2022). However, hood shows an increased permeability to VOC compared to the jacket and pants (Mayer et al., 2023).

The National Fire Protection Association (NFPA) 1971: Standard on Protective Ensemble for Structural Fire Fighting and Proximity Fire Fighting 2018 Edition establish the minimal performance requirements of firefighting protective equipment. To protect from chemicals found in firefighting situation in the area covered by the hood, the blocking efficiency of particulates of 0.1 to 1.0 microns must be over 90% (NFPA1971, 2018). Particulate of those sizes are often the most difficult to block. In fact, the most penetrating particulate is often found between 0.2 and 0.4 microns depending on the testing condition and the filtration mechanism. The hood barrier testing is used to demonstrate some protection against liquid and particulate contaminant hazards. However, the NFPA 1971 standard lack specific testing against VOC and PAH to develop products with enhanced barrier properties. Due to the risk associated with VOC and PAH exposure in firefighting, new hood barriers should improve the protection against those chemicals.

The objective of this study is to evaluate the performance level of protection against chemical vapour found in firefighting of two certified hood barriers meeting the requirement of the NFPA 1971 for the development of improved barriers and to compare the performance with a new barrier material.

Regulatory changes at the global level for prohibition of chemicals, and the transition to a new Standard NFPA1970 in draft state gives an opportunity to make improvement in the material

chemistry, as well as the testing methods. This study could be an argument to establish VOC testing in the next NFPA standard.

7.3 Material

Commercially available hood LION's RedZone™ with STEDAIR® PREVENT barrier (model: HD395142-10+U) and PGI BarriAire™ Gold with Nomex® Nano Flex barrier (style no. 39700-00-194071, LOT #022123) were purchased for their evaluation. All hoods are compliant with NFPA1971 – 2018 edition. Prototypes hood barriers were developed at with a proprietary formulation. Two coats of a polyurethane emulsion are applied by knife coating on a release paper and a meta-aramid knit is laminated. The polyurethane formulation is a mix of a functional filler and crosslinker to impart heat, flame resistance and durability. A substrate wetting, dispersant and defoaming is added to obtain the required formulation behaviour.

Anhydrous, +99%, 1,2,3,4-Tetrahydronaphthalene, Tetralin™ (CAS 119-64-2), HPLC, 99.9% Methanol (CAS 67-56-1) were purchased from Millipore Sigma Canada. Ultra-high purity nitrogen 5.0 is purchased from Linde Canada. Products were used as received.

VOC permeation apparatus is a custom equipment composed of a photoionization detector (PID) sensor MiniPID 2 PPB from ION Science. The sample is held in glass permeation cells from At-Mar Glass. The gas is transported in Viton® tubing and connected with compression fitting. The detector signal is data logged and analyzed by computers. The temperature and humidity controller are used to condition the chemical, specimen and cell before and during testing.

7.4 Method

The method for evaluation of VOC permeation is inspired by ASTM F739 and TOP 8-2-501. The main modification to the ASTM method relates to the chemical exposure. The chemical is exposed at a low dosage in liquid to gas form instead of direct liquid contact due to the high permeation of the hood barrier. The test environment is at 32± 1°C and at a relative humidity of 80 ± 5 percent, for at least 24 hours prior to testing. The sensor is calibrated by using standard gas of isobutylene at 0, 0.1, 10 and 40 ppm of concentration at a constant flow rate of 0.3 litres per minute.

Naphthalene was found to be the predominant PAH in VOC and PAH airborne exposure at concentration around 40 ppm in structural fire (Austin, Wang, Ecobichon, & Dussault, 2001; Sjöström et al., 2019). For this study, a derivative of naphthalene, Tetralin™, was used to simulate

exposure to VOC and PAH of hood barriers. Tetralin™ has a similar chemical composition and a higher vapour pressure than naphthalene. The higher vapour pressure reduces the risk of condensation and error during testing. The initial concentration for testing was increased to 240 ppm to reduce testing time and have an acceptable signal for the detector.

CAN/CGSB-4.2 No. 14-2005 method was used to quantify the mixture of fibre by selective dissolution. The materials are dried at 105°C before analysis. The method was modified for polyimide. The polyimide was dissolved in concentrated nitric acid at 110°C. All using technical grade solvent at the temperature specified in the test method. Material was dried at 105°C before testing. The quantities are reported after moisture regain from the Canadian standard.

Hitachi Tabletop Microscope TM-3030 (SEM) was used to analyze the structure the textile and the barrier. The sample was sputtered coated in a vacuum with chromium using Quorum Q150T ES for higher resolution.

Basis weight and thickness were measured on conditioned specimens before testing. The weight per area is reported in grams per square metres. The thickness was measured with a digital micrometer from Fowler High Precision.

The infrared spectrums of the materials were acquired by using Fourier Transform Infrared Frontier Perkin Elmer. The spectrum was used to identify specific vibrations frequencies for identification of the material. Databases were used to validate the analysis.

The expanded polytetrafluoroethylene (ePTFE) membrane was separated from the laminated knit by selective dissolution of the adhesive in sodium hypchlorite at 12% under gentle reflux before FTIR analysis. The nanoflex membrane was recovered by carefully cutting the quilting tread with a seam ripper.

The water penetration resistance for hood composite was tested according to the Canadian General Standards Board (CGSB) 4.2 No. 26.3 with the hydrostatic column. A mobile surface analyzer (MSA) from Krüss was used to determine the water contact angle. The air permeation of the fabric is tested according to ASTM F737-18.

NFPA1971 specification was retrieved from available data sheet of the manufacturer. The most critical tests for this application were the thermal protection performance (TPP), total heat loss (THL) and particulate blocking test. The particulate blocking test is the filtration efficiency of

particle size from 0.1 to 1.0 microns at a flow rate of 1.7±0.1 LPM. The THL is the combination of cooling heat transfer by evaporation, convection and conduction in a simulated skin model. A high THL is desired for comfort of the wearer. The TPP exposes the outside of the specimen to radiant and convective heat and records the temperature inside the specimen. The Stoll curve is used to rate the onset of a second-degree burn. A high TPP indicates a higher protection against heat.

7.5 Results and discussion

Hood characterization

The LION's RedZone™ with STEDAIR® PREVENT barrier and PGI BarriAire™ Gold with Nomex® Nano Flex barrier was evaluated by SEM, FTIR, selective dissolution and visual observation to analyze the structure and composition of the hood.

LION RedZone™ with STEDAIR® PREVENT

The LION's RedZone hood with Prevent barrier is composed of one outer knit and the Prevent barrier at 210 g/m^2. The prevent barrier is black and grey knit with a thin white flexible membrane.

- Outer knit: 50/50 Viscose (regenerated cellulose)/Kermel (polyimide-amide) interlock knit according to the manufacturer
- Barrier: membrane laminated between two knit of 52.9% Polyimide-amide 47.1% regenerated cellulose by selective dissolution.

The membrane and knit are laminated with an adhesive. The knit used on the outside face is assembled with the barrier by stitching. The edges of the hood are also stitched.

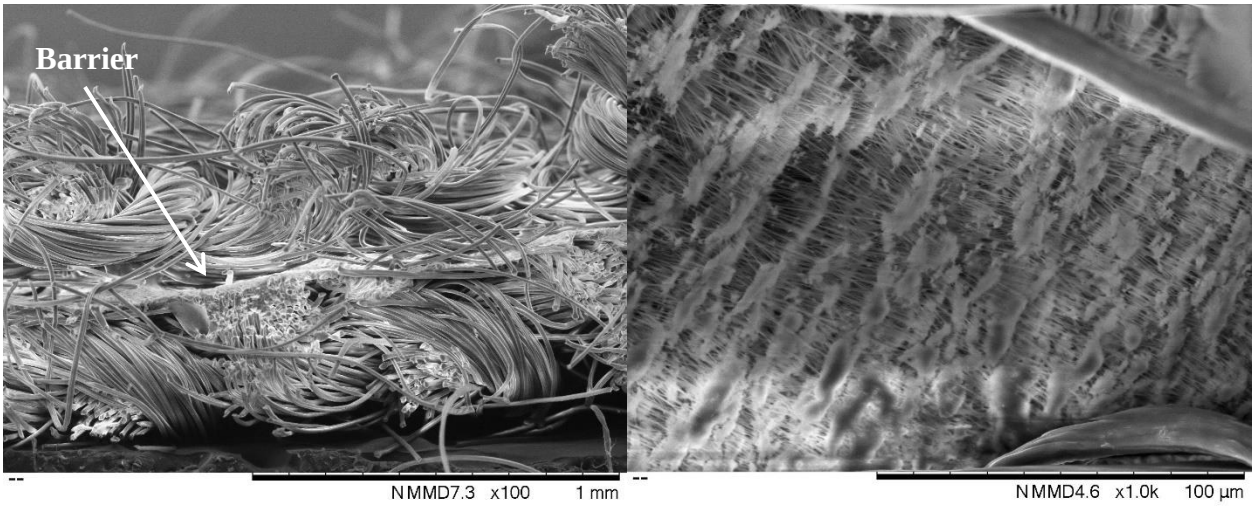

Figure 7-1. Cross-section (left) and top view (right) of Stedair Prevent tri-laminate.

The Stedair Prevent product commercialized by Stedfast is based on expanded polytetrafluoroethylene (ePTFE) membrane according to the FTIR and SEM. A strong peak overlapping around 1200 cm^{-1} corresponds to the asymmetric and symmetric stretching of the C-F bond. Other weak peaks and noise can be attributed to contamination such as adhesive and fibre. PTFE was invented by DuPont and ePTFE was created by Bill Gore who later founded W.L. Gore & Associates in 1958. PTFE resin is produced by emulsion polymerization. The fine powder is melted with a volatile lubricant and extruded in film on a calendaring roll. The lubricant is evaporated in a dryer before stretching the film at high temperature in uniaxial (machine direction) and biaxial (machine and transverse direction) to form an ePTFE membrane (Wikol et al., 2007). By expanding PTFE at a high rate, a porous structure with micron-size interconnected fibrils and nodes is created, which is observed on Figure 7-1. The formation of voids weakens the material. Hence, the ePTFE is laminated with two knit with an adhesive, as in the figure 1. The lamination enhances the mechanical properties and protect from tearing, puncture or rupture in the hood application. The porous structure can block liquids and particulate matters from entering giving protection to the wearer while allowing gas and humidity to pass through for comfort.

PGI BarriAire™ Gold with Nomex® Nano Flex barrier

The PGI Gold hood with Nomex Nanoflex barrier is composed of two kakhi colours knit facing the outside and the inside of the hood. The textile composition was quantified by selective dissolution.

- Inner and outer knit: 63.7% Meta-aramid, 18.1% of para-aramid, 13.8% of nylon and 4.4% of residual fibre identified as carbon anti-static fibres by microscopy
- Barrier: 100% polyimide nonwoven by selective dissolution and FTIR

The barrier has the characteristic orange colour of polyimide fibre. The knit and membrane are quilted in three layers. The quilting of the hood manufacturer puncture the membrane. In fact, our visual observations showed that light is visible through all three layers around the qulited yarn. The quilting defects could be a source of inward leakage of particles and VOCs. The quilting is used to increase the durability to the detriment of protection, it is preferred to the use of adhesives to avert clogging of the pore and reducing the comfort according to the manufacturer (Sonntag, 2020).

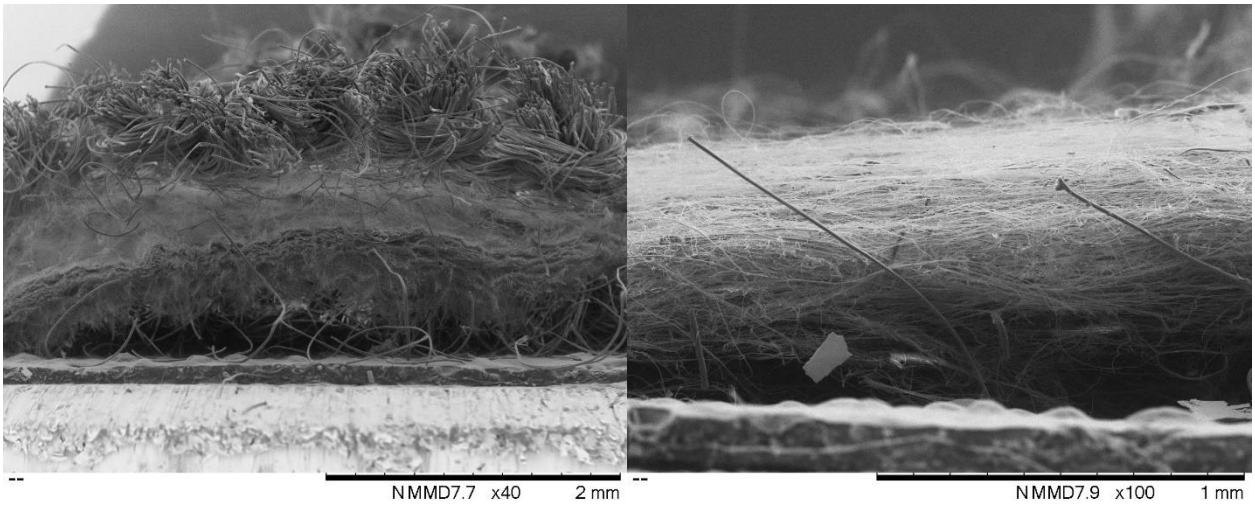

Figure 7-2. Hood composite (left) and nanoflex barrier (right) cross-section view.

Nomex Nano and Nanoflex marketed under DuPont trade name are a nanofiber nonwoven membrane material. Nanoflex nonwoven are a newer material from Dupont compared to ePTFE, less information is available.

The Nomex trade name is historically reserved for meta-aramid polymer commercialized by DuPont. However, the aromatic peak around 3000-3100 cm^{-1} and the strong N-H stretching at 3311 cm^{-1} which are characteristic of Nomex aramid are not present in the spectrum. Surprisingly, the Fourier Transform Infrared Spectroscopy (FTIR) spectrum shows the material to be polyimide (PI). A single peak is observed at 1776 cm^{-1} which is characteristic of carboxylic acid. A strong peak at 1715 cm^{-1} is characteristic of ketone. A peak at 1500 cm^{-1} which correspond to the aromatic carbon.

The overlapping peak at 1343 to 1242 cm^{-1} can be attributed to the C-N aromatic bond. The aromatic polymer with ketone and carbon amide function is most likely to be polyimide.

In fact, polyimide is seen as a replacement for aramid where higher fire and heat resistance, but lower chemical resistance, are required. Moreover, a patent from PGI also confirms the material barrier is polyimide (Sonntag, 2020).

Polyimide nanofiber nonwoven can be prepared by electroblowing, meltblowing or electrospinning by spinning polyamic acid in a nanofiber web. The polyamic acid is converted by evaporating the solvent and heating the web to imidize by a ring-closing reaction (Dennes, Simmonds, Arora, & Levit, 2013; Nakamori, Maeda, Kitagawa, Kobayashi, & Ohta, 2016). Various degrees of aromaticity, reaction conversion and crystallinity can be obtained from the material and processing method, which can make it difficult to characterize. The nanofiber web has visibly an important orientation in one direction; it can stretch in one direction, and is stiff in the other direction. This elongation behaviour is matched with the knit. Thus, the knit limit the deformation of the hood and protect the most delicate nanofiber.

Nanofiber structures are desirable for the increased filtration efficiency and reduced pressure drop due to the reduced diameter of the fibre. The increased filtration efficiency and thermal protection (TPP) of nanofibres allows to reduce the thickness of the material by up to 40% (DuPont, 2023). The thickness and basis weight of the nanofiber-based membrane and hood are much lower when compared to the laminated ePTFE as in table 7-1. The heat burden is reduced on the wearer; a THL of 401 W/m^2 was reported compared to 346 W/m^2 for ePTFE based barrier. The nanofiber nonwoven rupture very easily, and is supported by knits in a three-ply configuration for additional structural reinforcement as seen in the figure 2. (Sonntag, 2020). The nanofibres also allow for humidity and gas to permeate for comfort.

Dupont Nanoflex could be a replacement solution to fluorinated polymers in protective equipment clothing with a high temperature and flame resistance requirement. The European Chemicals Agency (ECHA) published the REACH restriction proposal for per- and polyfluoroalkyl substances (PFAS) to restrict its manufactures and uses due to the negative impact on health, environment and society impact. PFAS are known to be persistent in the environment. Consequently, humans and animals are exposed to the chemical by drinking water and food. The chemical has proven harmful effect such as toxicity for reproduction, can harm the unborn child,

may cause several cancers and is suspected to interfere with the hormonal system. For firefighters, their elevated level of PFAS in the blood (Mazumder et al., 2023) could be from the high level of PFAS found in turnout gear (Peaslee et al., 2020). PFAS free product must be used in the development of novel barrier. The current draft of the NFPA 1970 edition 2024 will allow a PFAS FREE label for protective equipment having no intentional addition of PFAS for ease of identification for those concerned.

VOC permeation evaluation

Both hood manufacturers claim particulate blocking efficiency, but no claim are made on the protection against VOC. Exposure of VOC through the hood has been shown to be a possible route. Therefore, the permeability of the hood was evaluated using a new method, inspired by ASTM F739 and TOP 8-2-501. A high time resolution was obtained to understand and compare the permeation of both membranes in a liquid to vapour diffusion assay. The detector allows real time monitoring compared to standard VOC test method using a sorbent tube with a low resolution time.

The efficacity of the barrier is judged by the cumulative permeability and the breakthrough time. The cumulative permeation corresponds to the summation of the detected chemicals, calculated according to ASTM F739 in open loop condition. The standard breakthrough time correspond to the time required to obtain a cumulative permeation of 0.1 µg/cm^2/min as per ASTM F739. Limited information is available on the exposure limit by dermal exposure for naphthalene. Moreover, a high skin temperature and humidity during firefighting can increase absorption. Therefore, these values cannot be used to determine safe exposure levels. Nonetheless, a high breakthrough time and low cumulative permeation are desirable characteristics for a barrier against chemicals.

Table 7-1. Evaluation of permeation of the hood and hood barrier against Tetralin

Configuration	Hood composite				Barrier only					
Material	PGI BarriAire™ Gold - Nomex® Nano Flex -		LION's RedZone™ - STEDAIR® PREVENT -		Nomex® Nano Flex		STEDAIR® PREVENT		Hydrophilic barrier	
Thickness, mm	0.848	±0.028	1.263	±0.089	0.146	±0.008	0.428	±0.016	0.329	±0.009
Basis weight, g/m^2	466	±23	802	±23	43	±3	210	±2	132	±23
Cumulative permeation, µg/cm^2/min.	0.182	±0.004	0.113	± 0.022	0.282	±0.042	0.153	±0.034	0.139	±0.054

Breakthrough Time, mm:ss	11:10	±00:17	22:37	± 06:11	08:10	±00:10	12:23	±01:47	30:45	±09:19

The permeation of the chemicals depends on the structure, thickness and composition of the material. Defects such as large pores, blister, crack, pinhole and sewing thread can increase the permeability. The ambient conditions are maintained during testing, as temperature and humidity can affect the gas diffusion. The permeation of hood material was compared in hood composite and in membrane only assembly. A hydrophilic membrane, used where high-protection and water vapour permeation are required, was added to the evaluated material to demonstrate a different membrane technology.

The Nanoflex membrane alone has the lowest thickness, basis weight and the highest permeation to tetralin. The membrane was recovered from a quilted hood. The defects from removing the quilt could explain the higher permeation. However, the hood composite with Nanoflex shows a minor improvement in protection. The breakthrough time is increased and the cumulative permeation is reduced which could be attributed to the added knits at the outermost layers.

The ePTFE membrane shows lower permeation compared to Nanoflex barriers and composite hood. To demonstrate the effect of the outside facing knit on permeation, the Kermel/Viscose outer knit is added. The cumulative permeation of the chemical is similar which means a similar amount of chemical permeates through the material. However, the breakthrough time is higher.

Both hood composite configurations show lower cumulative permeation compared to the barrier only. The Kermel/Viscose has a higher basis weight, thickness, and barrier against VOC.

The hydrophilic films have shown a lower permeation to tetralin compared to the porous ePTFE and PI. The improvement can be explained by the difference in structure and gas transport. The porous structure of ePTFE and PI nonwoven allows for transport of gas in air through the interconnected pore. For the hydrophilic membrane, the chemical must permeate through the membrane by a slower diffusion mechanism. The hydrophilic membrane must combine the slow permeation to chemicals for protection with a high permeation to water vapour for comfort. The permeation to water is critical for the evaporative cooling to prevent heat stress of firefighters. The selective permeation to water is possible by a selective sorption and diffusion of water due to specific intermolecular interaction with water such as hydrogen bonding.

Flow resistance evaluation

To better understand the difference of VOC permeation between the two porous barriers, the resistance to liquid penetration and gas penetration was evaluated. The liquid resistance was tested by using a water column. The gas resistance was evaluated by measuring the permeation to air.

Table 7-2. Evaluation of hood barriers air permeation and water resistance.

Hood	PGI BarriAire™ Gold	LION's RedZone™
Barrier	- Nomex® Nano Flex -	- STEDAIR® PREVENT -
Water contact angle, degrees	95.58±9.82	132.74±7.78
Water penetration pressure, Pa	83	662
Air permeability, $cm^3/s/cm^2$	8.85±2.03	5.74±0.74

The water penetration was observed at the quilting for PGI's hood. The water requires eight-time higher pressure to penetrate the ePTFE compared to the polyimide. Therefore, the resistance to water penetration of the polyimide is lower than the ePTFE. The high-water contact angle and low surface tension of the PTFE explains this difference. The permeation to air of the ePTFE is lower than that of the polyimide nanofiber due to its unique structure. Overall, the polyimide nanofiber offers less resistance to liquid and gas flow, which is also in agreement with the lower resistance to volatile organic compound.

7.6 Conclusion

Chemicals permeation through the firefighter's hood is a plausible source of exposure to VOC by dermal absorption. The NFPA 1971 has yet to implement a testing method for VOC penetration in the firefighting garment. The penetration of the chemical is evaluated against liquid chemicals for the garment and by particulate matter for the optional hood barrier.

The objective of this work was to evaluate the permeation to VOC of two commercial hoods with the optional particulate barrier and to propose a new barrier. The developed method allowed to study the permeation of hood barriers.

The polyimide nanofiber allows for a lighter hood construction and a PFAS free product. However, the nanoflex nonwoven has a worse barrier property to tetralin compared to the ePTFE.

The study shows significant variation of protection against VOC between the two certified hoods. The addition of a minimum breakthrough time requirement in the new NFPA 1970 would create a baseline protection during a firefighting operation. The current knowledge does not make it possible to determine a safe level of protection against dermal absorption of VOC in firefighting.

The composition of the outside facing knit was found to impact the permeation to VOC. It is recommended to develop the barrier hood has a composite, considering all layers and lamination method in the development. The effect of knit composition, thickness and basis weight should be studied.

The hydrophilic membrane can be a path to an improved hood barrier property to the current "pick your poison" situation between PFAS and VOC. The development of such protective clothing will require a balance between multiple properties, often contradictory. In further development of hydrophilic barrier, resistance to flame, heat, insulation and heat loss should be considered. The hood barrier should allow sufficient water vapour transmission for an adequate comfort, and also be resistant to flame and heat to meet all the requirements of the hood composite in the NFPA 1971.

An analytical method using a sorbent tube analyzed by GC-MS such as NIOSH 1550 with would be more suitable for a standard test method where interlaboratory reproducibility is most critical. The setup used in this publication allowed high resolution time to better understand the permeation of VOC of firefighters' hood.

CHAPTER 8 CONCLUSION AND PERSPECTIVES

The regulatory changes and the current issues surrounding firefighting gear constitutes a good moment to revise the design of the hood barrier. The uses of ePTFE as a filtration barrier for hood may be limited in the next years with the proposal to ban their non-essential use by REACH. There is a need for an alternative material to ePTFE with reduced impact on the environment. Moreover, the current hood barrier does not test nor protect against penetration of harmful VOC&PAH generated in the structural fire. The porous structure used in the barrier allows for penetration of chemicals and dermal absorption. The dermal absorption of the chemical is the most plausible exposure route to rationalize the increased chemicals in biological samples after firefighting (Mayer et al., 2023; Stec et al., 2018). Finally, the material should meet a balance between the protection and the comfort; the resistance to permeation against harmful chemical should protect the wearer from chemical exposition while having sufficient permeation to water vapor to avoid the accumulation of sweat between the skin and the hood for comfort.

To address those issues, the primary objective of this project was to develop a PFAS free barrier for firefighters' hood, the secondary objectives were to use reclaimed aramid fibre to reduce dependence on new material, to obtain a balance between protection and comfort and to compare the permeation to VOC of the developed hydrophilic coating with the current offering of hood barrier on the market.

Two methods of fabrication were evaluated to improve on the design of the hood barrier. The first method evaluated was the electrospinning of nanofiber on a nonwoven to prepare a filtration barrier. The electrospinning method was used to coat an aramid nonwoven with aramid nanofiber to improve the filtration efficiency of standard aramid nonwoven. The nanofiber mat was consolidated with a standard nonwoven to improve the mechanical properties of material and for ease of handling of nanofiber nonwoven. Different consolidation methods were evaluated in this project, namely, the uses of a binder, a corona treatment and of a solvent pretreatment were evaluated. The uses of a binder resulted in a sufficient adhesion between the nanofiber and the nonwoven. The nanofiber nonwoven was evaluated for the protection against fine particles and against flame. The vertical flame resistance of the composite was evaluated against the method ASTM D6413. The flame retardancy of the nonwoven material was conserved with the nanofiber coating. The after flames was identical and the char length was only 8 mm longer. The filtration

efficiency of 0.3 microns particles was of 11.93%. The filtration efficiency was not acceptable due to the low coating weight and poor process stability. The poor process stability was attributed to the high conductivity of the aramid solution. A highly conductive solution should be avoided for electrospinning. For future trial, the selected polymer for electrospinning must be soluble in a suitable solvent for electrospinning, while meeting the requirement for the hood barrier.

The second method of preparation of nanofiber by knife coating. A selective permeation membrane was developed from a blend of aramid and polyurethane. An optimized deprotonation reaction on the aramid was used to prepare a nanofiber dispersion of aramid. The nanofibre preparation reduced the L/D ratio and the quality of the fibre, efforts should be done to improve the L/D ratio to improve the quality of aramid as a nanofiller. The nanofibers were blended with polyurethane amd coated on an aramid knit to produce a flexible hood barrier. The addition of aramid nanofiber improved the resistance to heat and flame and polyurethane improved the adhesion and flexibility of the coating. A cross linker was used to improve the heat resistance and wash durability of the barrier. Additives were used to improve the coating behaviour such as wetting, defoaming and dispersion stability.

A balance between protection and comfort was obtained with the coated knit. In fact, a high filtration efficiency is obtained with over 99.8% of particle blocked, surpassing the requirement of 90% filtration efficiency. Moreover, the water vapor transmission rate of the barrier allows for evacuation of the sweat. The total heat loss of the coated knit is over the requirement, but should be evaluated as a hood composite to meet the criteria of the NFPA 1971 standards. The stiffness of the coated knit is higher than the conventional ePTFE. The flexibility of the barrier could be improved by a reduction in coating thickness or lamination method. Finally, the material is expected to be durable for at least five washes cycles as per the NFPA 1971 requirement.

The protection was evaluated by VOC permeation and particle filtration efficiency. The developed coating has an improved protection against VOC compared to other commercial barriers. The difference in permeation could be from the different transport mechanism in porous and non-porous membrane. The filtration efficiency is similar.

A pilot trial should be pursued for the polyurethane/aramid coating. The thickness could be optimised in the trial to improve the balance between protection and comfort. The coated fabric will be used to develop prototype hood with the outer layer from different protective equipment

manufacturers. Those prototypes will be tested according to the NFPA 1971 standard for structural firefighter hood. This study was limited to study the hood in flat material form, confectioned hood form will allow to validate the technology readiness of the barrier hood component. If the hood prototypes are successful, the next step would be an industrial trial, the validation in operational environment and certification of the material.

REFERENCES

Anandhan, S., Ponprapakaran, K., Senthil, T., & George, G. (2012). Parametric study of manufacturing ultrafine polybenzimidazole fibers by electrospinning. *International Journal of Plastics Technology, 16*, 101-116.

Aramid, T. Recycling used aramids. Retrieved from https://www.teijinaramid.com/en/customer-focus/recycling/

Austin, C., Wang, D., Ecobichon, D. J., & Dussault, G. (2001). Characterization of volatile organic compounds in smoke at municipal structural fires. *Journal of Toxicology and Environmental Health Part A, 63*(6), 437-458.

Barbeau, C., Lozier, F., & Rousse, S. (2018). Firefighter protective hood and gloves with regenerated cellulose fiber. In: Google Patents.

Bartkowiak, G., Frydrych, I., & Greszta, A. (2016). Fabric selection for the reference clothing destined for ergonomics test of protective clothing: physiological comfort point of view. *Autex Research Journal, 16*(4), 256-261.

Bhattacharyya, D., & Fakirov, S. (2012). *Synthetic polymer-polymer composites*: Carl Hanser Verlag GmbH Co KG.

Blake, H., Harper, S., Maples, A., Riley, S., Zischka, B., & Stübiger, W. (2021). Hood including particle barrier. In: Google Patents.

Brydon, A., Pourmohammadi, A., & Russell, S. (2022). Drylaid web formation. In *Handbook of nonwovens* (pp. 89-180): Elsevier.

Burch, R. R., Sweeny, W., Schmidt, H. W., & Kim, Y. H. (1990). Preparation of aromatic polyamide polyanions: a novel processing strategy for aromatic polyamides. *Macromolecules, 23*(4), 1065-1072.

Chang, Y., & Liu, F. (2023). Review of Waterproof Breathable Membranes: Preparation, Performance and Applications in the Textile Field. *Materials, 16*(15), 5339.

Chen, H.-J., Bai, Q.-Y., Liu, M.-C., Wu, G., & Wang, Y.-Z. (2021). Ultrafast, cost-effective and scaled-up recycling of aramid products into aramid nanofibers: mechanism, upcycling, closed-loop recycling. *Green Chemistry, 23*(19), 7646-7658.

Chen, M.-R., Tsai, P.-J., & Wang, Y.-F. (2008). Assessing inhalatory and dermal exposures and their resultant health-risks for workers exposed to polycyclic aromatic hydrocarbons (PAHs) contained in oil mists in a fastener manufacturing industry. *Environment international, 34*(7), 971-975.

Chen, X., Wang, W., & Jiao, C. (2017). A recycled environmental friendly flame retardant by modifying para-aramid fiber with phosphorus acid for thermoplastic polyurethane elastomer. *Journal of hazardous materials, 331*, 257-264.

Cloupeau, M., & Prunet-Foch, B. (1990). Electrostatic spraying of liquids: Main functioning modes. *Journal of electrostatics, 25*(2), 165-184.

Corbett, G. P. (2009). *Fire engineering's handbook for firefighter I and II*: Fire Engineering Books.

Crown, E., & Batcheller, J. (2016). Technical textiles for personal thermal protection. *Handbook of technical textiles*, 271-285.

Dennes, T. J., Simmonds, G. E., Arora, P., & Levit, N. V. (2013). Polyimide nanoweb. In: Google Patents.

Dolan, J., Murphy, M., Minor, R., Shahkarami, S., & Krummel, J. (2016). Protective undergarment. In: Google Patents.

Dupont. (2017). Kevlar® Aramid Fiber Technical Guide.

Dupont. (2019). Nomex® fiber Technical guide.

DuPont. (2023). Nomex® Nano Next generation of firefighter protection. Retrieved from https://www.dupont.com/content/dam/dupont/amer/us/en/personal-protection/public/documents/en/DSF23_2301-0268_3-8793_Nomex_Nano_Sell_Sheet_me01_02_Digital-FINAL.pdf

Eisenberg, J., Methner, M., Dowell, C. H., & Mueller, C. (2015). Evaluation of heat stress, heat strain, and rhabdomyolysis during structural fire fighter training.

Evonik. Evonik P84® Polyimide Fiber. Retrieved from https://www.p84.com/en/polyimide-fibres-chemistry

Faccini, M., Vaquero, C., & Amantia, D. (2012). Development of protective clothing against nanoparticle based on electrospun nanofibers. *Journal of Nanomaterials, 2012*.

Fent, K. W., Eisenberg, J., Evans, D. E., Sammons, D., Robertson, S., Striley, C., . . . Pleil, J. D. (2013). Evaluation of dermal exposure to polycyclic aromatic hydrocarbons in fire fighters.

Fent, K. W., Mayer, A. C., Toennis, C., Sammons, D., Robertson, S., Chen, I.-C., . . . Smith, D. L. (2022). Firefighters' urinary concentrations of VOC metabolites after controlled-residential and training fire responses. *International journal of hygiene and environmental health, 242*, 113969.

Fent, K. W., Toennis, C., Sammons, D., Robertson, S., Bertke, S., Calafat, A. M., . . . Smith, D. (2020). Firefighters' absorption of PAHs and VOCs during controlled residential fires by job assignment and fire attack tactic. *Journal of exposure science & environmental epidemiology, 30*(2), 338-349.

Fink, J. K. (2014). *High performance polymers*: William Andrew.

Godwin, A. D., & Kutz, M. (2017). Applied plastics engineering handbook. *William Andrew Applied Science Publishers*.

Grafe, T. H., & Graham, K. M. (2003). *Nanofiber webs from electrospinning.* Paper presented at the Nonwovens in filtration-fifth international conference.

Gupta, B., Agarwal, R., & Alam, M. (2010). Textile-based smart wound dressings.

Gutoff, E. B., & Cohen, E. D. (2006). *Coating and drying defects: troubleshooting operating problems*: John Wiley & Sons.

Horn, G. P., Kerber, S., Andrews, J., Kesler, R. M., Newman, H., Stewart, J. W., . . . Smith, D. L. (2021). Impact of repeated exposure and cleaning on protective properties of structural firefighting turnout gear. *Fire Technology, 57*, 791-813.

Horrocks, A. (2016). Technical fibres for heat and flame protection. In *Handbook of technical textiles* (pp. 237-270): Elsevier.

Huang, J. (2006). Sweating guarded hot plate test method. *Polymer Testing, 25*(5), 709-716.

Huang, L., Zhang, M., Nie, J., Yang, B., Tan, J., & Song, S. (2022). Ultrafast formation of ANFs with kinetic advantage and new insight into the mechanism. *Nanoscale Advances*.

Inovenso. (2022, May 25 2022). The Difference Between ElectroSpinning and Electrospraying. Retrieved from https://www.azonano.com/article.aspx?ArticleID=5060

Jaworek, A., & Sobczyk, A. T. (2008). Electrospraying route to nanotechnology: An overview. *Journal of electrostatics, 66*(3-4), 197-219.

Karlsson, J., Gatenholm, P., Blachot, J. F., & Peguy, A. (1996). Improvement of adhesion between polyethylene and regenerated cellulose fibers by surface fibrillation. *Polymer composites, 17*(2), 300-304.

Kasebi, A. (2022). *Investigating the Continuing Performance of Firefighter Hoods Following On-The-Job Exposures*: North Carolina State University.

Kasebi, A., Gaskill, M., & Ormond, R. (2020). Assessing the Durability of Firefighter Protective Hoods Following Exposure to Ultraviolet Light. *Performance of Protective Clothing and Equipment: 11th Volume, Innovative Solutions to Evolving Challenges*, 64-80.

Kim, H. B., Lee, W. J., Choi, S. C., Lee, K. B., & Lee, M.-H. (2019). Dependence of the fiber diameter on quality factor of filters fabricated with meta-aramid nanofibers. *Separation and Purification Technology, 222*, 332-341.

Kim, J. S., & Reneker, D. H. (1999). Polybenzimidazole nanofiber produced by electrospinning. *Polymer Engineering & Science, 39*(5), 849-854.

Koga, K., Ueta, S., & Takayanagi, M. (1988). The structure and physical properties of aramid film prepared by electrodeposition of poly (p-phenylene terephthalamide) polyanion. *Polymer journal, 20*(8), 639-647.

Koukoulas, A. (2022). Wetlaid web formation. In *Handbook of Nonwovens* (pp. 181-216): Elsevier.

Lee, D. J., Koru-Sengul, T., Hernandez, M. N., Caban-Martinez, A. J., McClure, L. A., Mackinnon, J. A., & Kobetz, E. N. (2020). Cancer risk among career male and female Florida firefighters: Evidence from the Florida Firefighter Cancer Registry (1981-2014). *American journal of industrial medicine, 63*(4), 285-299.

Leung, W. W. F. (2021). *Nanofiber Filter Technologies for Filtration of Submicron Aerosols and Nanoaerosols*: Elsevier Science.

Li, L., Shang, L., Li, Y., & Yang, C. (2017a). Three-layer composite filter media containing electrospun polyimide nanofibers for the removal of fine particles. *Fibers and Polymers, 18*(4), 749-757.

Li, L., Shang, L., Li, Y., & Yang, C. (2017b). Three-layer composite filter media containing electrospun polyimide nanofibers for the removal of fine particles. *Fibers and Polymers, 18*, 749-757.

Lomax, G. R. (2007). Breathable polyurethane membranes for textile and related industries. *Journal of Materials Chemistry, 17*(27), 2775-2784.

Lu, T., Cui, J., Qu, Q., Wang, Y., Zhang, J., Xiong, R., . . . Huang, C. (2021). Multistructured Electrospun Nanofibers for Air Filtration: A Review. *ACS Applied Materials & Interfaces*.

Lu, Z., Dang, W., Zhao, Y., Wang, L., Zhang, M., & Liu, G. (2017). Toward high-performance poly (para-phenylene terephthalamide)(PPTA)-based composite paper via hot-pressing: the key role of partial fibrillation and surface activation. *RSC advances, 7*(12), 7293-7302.

Lv, J., Guo, L., Xie, C., Xu, W., Ye, J., Li, X., . . . Tuo, X. (2021). Engineering all-aromatic polyamide surface from hydrophilic to superhydrophobic and the accelerated strategy. *Journal of Applied Polymer Science, 138*(44), 51316.

Manoharan, S., Krishnaraj, V., Vijay, R., Singaravelu, D. L., & Suresha, B. (2017). Development and characterization of novel fiber reinforced hybrid friction composites. *Green Composites: Materials, Manufacturing and Engineering; Walter de Gruyter Gmbh: Berlin, Germany*, 69-114.

Manoharan, S., Shihab, A. I., Alemdar, A. S. A., Babu, L. G., Vijay, R., & Singaravelu, D. L. (2019). Influence of recycled basalt-aramid fibres integration on the mechanical and thermal properties of brake friction composites. *Materials Research Express, 6*(11), 115310.

Mastrangelo, G., Fadda, E., & Marzia, V. (1996). Polycyclic aromatic hydrocarbons and cancer in man. *Environmental health perspectives, 104*(11), 1166-1170.

Mather, R. R., Rana, S., & Wardman, R. H. (2023). *The chemistry of textile fibres*: Royal Society of chemistry.

Mayer, A. C., Fent, K. W., Bertke, S., Horn, G. P., Smith, D. L., Kerber, S., & La Guardia, M. J. (2019). Firefighter hood contamination: Efficiency of laundering to remove PAHs and FRs. *Journal of occupational and environmental hygiene, 16*(2), 129-140.

Mayer, A. C., Fent, K. W., Wilkinson, A., Chen, I.-C., Kerber, S., Smith, D. L., . . . Horn, G. P. (2022). Characterizing exposure to benzene, toluene, and naphthalene in firefighters wearing different types of new or laundered PPE. *International journal of hygiene and environmental health, 240*, 113900.

Mayer, A. C., Fent, K. W., Wilkinson, A. F., Chen, I.-C., Siegel, M. R., Toennis, C., . . . Kerber, S. (2023). Evaluating Exposure to VOCs and Naphthalene for Firefighters Wearing Different PPE Configurations through Measures in Air, Exhaled Breath, and Urine. *International Journal of Environmental Research and Public Health, 20*(12), 6057.

Mazumder, N.-U.-S., Hossain, M. T., Jahura, F. T., Girase, A., Hall, A. S., Lu, J., & Ormond, R. B. (2023). Firefighters' exposure to per-and polyfluoroalkyl substances (PFAS) as an occupational hazard: A review. *Frontiers in Materials, 10*, 1143411.

McCullough, E. A., Kwon, M., & Shim, H. (2003). A comparison of standard methods for measuring water vapour permeability of fabrics. *Measurement Science and Technology, 14*(8), 1402.

Meena, M., Kerketta, A., Tripathi, M., Roy, P., & Jacob, J. (2022). Moisture barrier layer with supplemental chemical and biological protective functionality for firefighting clothing applications. *Journal of Industrial Textiles, 51*(4_suppl), 6110S-6133S.

Miao, L., Wu, Y., Hu, J., Wang, P., Liu, G., Lin, S., & Tu, Y. (2019). Hierarchical aramid nanofibrous membranes from a nanofiber-based solvent-induced phase inversion process. *Journal of Membrane Science, 578*, 16-26.

Montefusco, A. s. F. (2005). The use of Nonwovens in air filtration. *Filtration and Separation, 42*(2), 30-31.

Myers, D. (1999). *Surfaces, interfaces, and colloids* (Vol. 415): Wiley New York.

Nakamori, M., Maeda, S., Kitagawa, T., Kobayashi, H., & Ohta, Y. (2016). Polyimide nonwoven fabric and process for production thereof. In: Google Patents.

Nan, Z., Xiang-yu, J., Chen, H., & Qin-fei, K. (2017). Improved filtration properties of hydroentangled PTFE/PPS fabric filters caused by fibrillation.

Nazare, S., Madrzykowski, D., & Nazare, S. (2015). *A review of test methods for determining protective capabilities of fire fighter protective clothing from steam*: US Department of Commerce, National Institute of Standards and Technology ….

NFPA1971. (2018). Standard on protective ensembles for structural fire fighting and proximity fire fighting.

Oh, H. J., Pant, H. R., Kang, Y. S., Jeon, K. S., Pant, B., Kim, C. S., & Kim, H. Y. (2012). Synthesis and characterization of spider-web-like electrospun mats of meta-aramid. *Polymer international, 61*(11), 1675-1682.

Paris-Davila, T., Gaines, L. G., Lucas, K., & Nylander-French, L. A. (2023). Occupational exposures to airborne per-and polyfluoroalkyl substances (PFAS)—A review. *American journal of industrial medicine, 66*(5), 393-410.

Park, H., Park, J., Lin, S.-H., & Boorady, L. M. (2014). Assessment of Firefighters' needs for personal protective equipment. *Fashion and Textiles, 1*(1), 1-13.

PARKER, E. T., & Kasper, D. (2020). Protective Fabric And Process Of Manufacturing Same. In: Google Patents.

Peaslee, G. F., Wilkinson, J. T., McGuinness, S. R., Tighe, M., Caterisano, N., Lee, S., . . . Mitchell, K. (2020). Another pathway for firefighter exposure to per-and polyfluoroalkyl substances: Firefighter textiles. *Environmental Science & Technology Letters, 7*(8), 594-599.

Peshoria, S., Nandini, D., Tanwar, R., & Narang, R. (2020). Short-chain and long-chain fluorosurfactants in firefighting foam: a review. *Environmental Chemistry Letters, 18*, 1277-1300.

Sawka, M. N., Wenger, C. B., Young, A. J., & Pandolf, K. B. (1993). Physiological responses to exercise in the heat. *Nutritional needs in hot environments: applications for military personnel in field operations, 55*.

Science, I. (2021). ION Science MiniPID 2 Sensor Guide. Retrieved from https://ionscience.com/en/news/ion-science-minipid-2-sensor-guide/

Shiels, B. P., Copeland, G. S., & Qin, F. (2017). Phosphonated pbi fiber. In: Google Patents.

Shults, R. A., Noonan, G., Turner, N. L., & Ronk, R. (1992). Investigation of a heat stress-related death of a fire fighter. *Fire Technology, 28*, 317-331.

Sjöström, M., Julander, A., Strandberg, B., Lewné, M., & Bigert, C. (2019). Airborne and dermal exposure to polycyclic aromatic hydrocarbons, volatile organic compounds, and particles among firefighters and police investigators. *Annals of Work Exposures and Health, 63*(5), 533-545.

Sloan, M. S. (2008). Eco-efficient friction materials.

Smith, D. L., Horn, G. P., Goldstein, E., & Petruzzello, S. J. (2008). Firefighter fatalities and injuries: the role of heat stress and PPE.

Song, G., & Wang, F. (2018). *Firefighters' Clothing and Equipment: Performance, Protection, and Comfort*: CRC Press.

Sonntag, J. A. (2020). Firefighter hood. In: Google Patents.

Stec, A. A., Dickens, K. E., Salden, M., Hewitt, F. E., Watts, D. P., Houldsworth, P. E., & Martin, F. L. (2018). Occupational exposure to polycyclic aromatic hydrocarbons and elevated cancer incidence in firefighters. *Scientific reports, 8*(1), 1-8.

Takayanagi, M., & Katayose, T. (1981). N-substituted poly (p-phenylene terephthalamide). *Journal of Polymer Science: Polymer Chemistry Edition, 19*(5), 1133-1145.

Tan, J., Luo, Y., Zhang, M., Yang, B., Li, F., & Ruan, S. (2021). Dissolving and regeneration of meta-aramid paper: converting loose structure into consolidated networks with enhanced mechanical and insulation properties. *ACS Applied Materials & Interfaces, 13*(14), 16895-16905.

Thomas, D., Charvet, A., Bardin-Monnier, N., & Appert-Collin, J. C. (2018). *La filtration des aérosols*: ISTE editions.

Tracton, A. A. (2005). *Coatings technology handbook*: CRC press.

Wang, Q., Bai, Y., Xie, J., Jiang, Q., & Qiu, Y. (2016). Synthesis and filtration properties of polyimide nanofiber membrane/carbon woven fabric sandwiched hot gas filters for removal of PM 2.5 particles. *Powder Technology, 292*, 54-63.

Wikol, M., Hartmann, B., Brendle, J., Crane, M., Beuscher, U., Brake, J., & Shickel, T. (2007). Expanded polytetrafluoroethylene membranes and their applications. In *Filtration and purification in the biopharmaceutical industry* (pp. 643-664): CRC Press.

Wikol, M., Hartmann, B., Brendle, J., Crane, M., Beuscher, U., Brake, J., & Shickel, T. (2008). Expanded polytetrafluoroethylene membranes and their applications. *Drugs and the Pharmaceutical Sciences, 174*, 619.

Wu, K., Wang, X., Xu, Y., & Guo, W. (2020). Flame retardant efficiency of modified para-aramid fiber synergizing with ammonium polyphosphate on PP/EPDM. *Polymer Degradation and Stability, 172*, 109065.

Xiang, J., & Blankenbeckler, N. (2020). Evaluation of Inherently Flame-Resistant Nanofiber Nonwovens in Firefighter Protective Clothing. *Performance of Protective Clothing and Equipment: 11th Volume, Innovative Solutions to Evolving Challenges*, 154-175.

Xu, K., Deng, J., Lin, R., Zhang, H., Ke, Q., & Huang, C. (2020). Surface fibrillation of para-aramid nonwoven as a multi-functional air filter with ultralow pressure drop. *Journal of Materials Chemistry A, 8*(42), 22269-22279.

Xu, K., Zhan, L., Yan, R., Ke, Q., Yin, A., & Huang, C. (2022). Enhanced air filtration performances by coating aramid nanofibres on a melt-blown nonwoven. *Nanoscale, 14*(2), 419-427.

Yang, B., Li, W., Zhang, M., Wang, L., & Ding, X. (2021). Recycling of high-value-added aramid nanofibers from waste aramid resources via a feasible and cost-effective approach. *ACS nano, 15*(4), 7195-7207.

Yang, B., Wang, L., Zhang, M., Luo, J., & Ding, X. (2019). Timesaving, high-efficiency approaches to fabricate aramid nanofibers. *ACS nano, 13*(7), 7886-7897.

Yang, B., Zhang, M., Lu, Z., Luo, J., Song, S., & Zhang, Q. (2018). From poly (p-phenylene terephthalamide) broken paper: high-performance aramid nanofibers and their application in electrical insulating nanomaterials with enhanced properties. *ACS Sustainable Chemistry & Engineering, 6*(7), 8954-8963.

Yang, M., Cao, K., Sui, L., Qi, Y., Zhu, J., Waas, A., . . . Kotov, N. A. (2011). Dispersions of aramid nanofibers: a new nanoscale building block. *ACS nano, 5*(9), 6945-6954.

Yao, L., Lee, C., & Kim, J. (2010). Fabrication of electrospun meta-aramid nanofibers in different solvent systems. *Fibers and Polymers, 11*, 1032-1040.

Zaarour, B., Tina, H., Zhu, L., & Jin, X. (2022). Branched nanofibers with tiny diameters for air filtration via one-step electrospinning. *Journal of Industrial Textiles, 51*(1_suppl), 1105S-1117S.

APPENDIX A : VALIDATION METHOD FOR VOC ANALYSIS

The sweeping gas is sent to dump after detection to prevent saturation (poisoning) of the detector. The sensor is calibrated using standard isobutylene at three concentrations. The lamp is heated and purged with nitrogen for 30 minutes before testing. The cells are cleaned with methanol and dried in a vacuum oven between each test. Three test specimens are evaluated. Dry nitrogen is used as a carrier gas. Nitrogen is inert and gives a stable baseline for the sensor. The chemical challenge is injected manually in the permeation cell by using a 10-microlitre gas chromatography syringe.

Methanol is used for diluting the analyzed VOC before the manual injection. Methanol has a higher ionization potential of 10.9 eV than the lamp of 10.6 eV (Science, 2021). Consequently, the methanol is not ionized by the lamp and is not detected at the sensor.

Conditioning

The cells, test materials and chemicals are maintained in a controlled temperature and humidity environment by a low-profile enclosure heater to control the temperature and an ultrasonic humidifier to control the humidity of the test environment.

The conditioning of the sample is chosen to simulate the condition of use of the barrier. The temperature and humidity are similar to the area around the skin during intense physical effort. In fact, these conditions are used in testing protective ensembles against chemicals in NFPA1994 Standard on Protective Ensembles for First Responders to Hazardous Materials Emergencies and CBRN Terrorism Incidents. The stability of the condition is important, diffusion rate is influenced directly by the temperature. Humidity and temperature can affect the sample. For example, humidity can swell hydrophilic membranes and increase the permeation rate of VOC.

Calibration

The detector is calibrated at a flow rate of 0,3 liter per minutes by using Isobutylene gas in nitrogen at 0, 0.1, 10, 40 ppm.

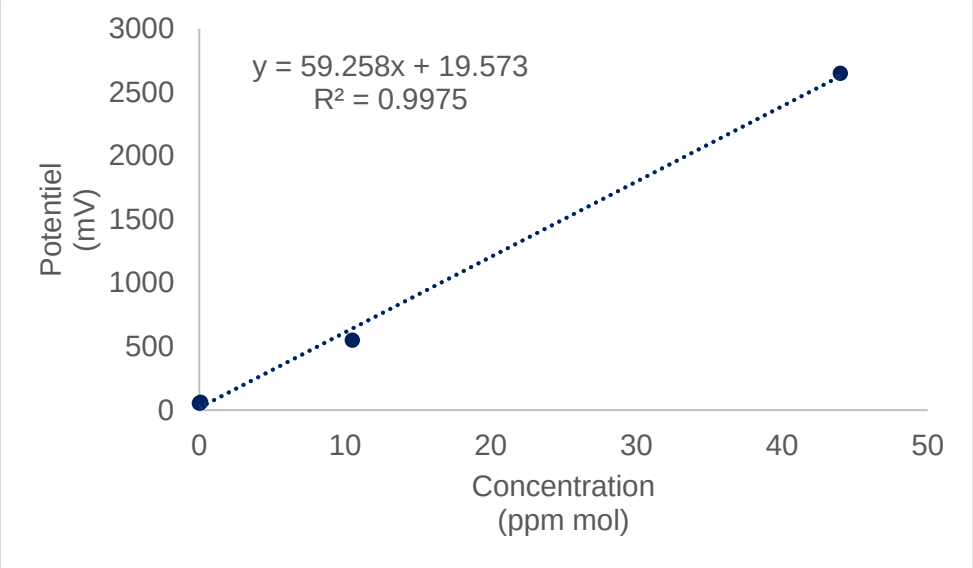

Figure A.1 PID PPB Calibration against Isobutylene

Detector: 10.6 eV PID PPB – Ion Science

LD: 1 ppb – 40 ppm (Ion Science)

R^2: 0.9975

Carrier gas: Nitrogen – 0.3 LPM

Tetralin correction factor: 0.4

Validation method

To validate the method, the recovery of the chemical is validated by the spike method. A known quantity of analyte is injected in the test side of the cell. An aluminum foil is placed as an impermeable sample. The spike of the analyte is measured by the detector. The recovery of the chemical is calculated by the following equation:

$$\% \, Recovery \, = \frac{(C_f - \, C)}{C_a} \qquad (A.1)$$

Where C_f is the fortified concentration, C the unfortified concentration and Ca the added concentration. A recovery of 96% is obtained which is acceptable. A recovery of 95 to 100% is expected for the method to be valid.

Method discussion

A method to detect the permeation of VOC was developed. The detector analyzes the concentration of collected VOC in the chamber with a near real-time response. A minimal delay is expected due to dead volume and detector response time. The method gives a high time resolution with a resolution of only 10 seconds. The range of detection is acceptable for the application. The minimal detection limit and range are acceptable. Finally, the detector has the flexibility to detect multiple types of VOC.

The analytical method has a linear response to a certified calibration gas, with a coefficient of 0.998 between 0 and 44 ppm. The detector response is acceptable. The recovery of spiked chemical is of 96%. The recovery rate is acceptable.

The drawbacks from this method are the lack of steady state from the depletion of chemical overtime, lack of mixing and lower detection limit compared to chromatography. The method uses a single manual injection to inject a chemical concentration on the challenge side. The chemical depletes over time which means the steady state is not reached, Fick's first law does not apply and the diffusion rate cannot be calculated. Second, the diffusion is dependent on the gradient of the chemical. A good mixing could ensure a uniform concentration gradient across the challenge side of the cell. Thermal desorption gas chromatography is often used in VOC testing. The PID detection method was preferred for the higher time resolution which can give insight on the diffusion mechanism. Chromatography method can be more precise and reproducible, especially with the uses of internal calibration.

Permeation is defined as the diffusion of gas species through a material surface.

$$P = D\,S \qquad (A.2)$$

Where P is the permeation, D the diffusion and S the surface. In this test, the permeation of the hood barrier is evaluated against tetralin. The permeation rate is calculated based on the ASTM F739 method for a open loop cell:

$$P_i = \frac{C_i F}{A} \qquad (A.3)$$

Where P is the permeation at the given time, C the detected concentration on the collection side, F the flow rate of the collection side and A the area of the coated fabric exposed to the chemical challenge.

The cumulative permeation is defined as a sum:

$$K_t = \sum_{i=1}^{n} \left[P_{i-1}(T_i - T_{i-1}) + \frac{1}{2}(P_i - PC_{i-1})(T_i - T_{i-1}) \right] \quad (A.4)$$

Where T is the specified time.

The driving force for diffusion is the chemical concentration gradient. The nitrogen gas sweep has a zero VOC concentration and the challenge side has a non-zero VOC concentration. Fick's first law is often used to model the diffusion in steady state. However, the concentration of the gas varies through time in this experiment. First, the gas concentration is high and over time, the gas concentration is depleted as the gas permeates through the barrier. A steady state is not reached in this test and Fick's first law of diffusion cannot be used to model the diffusion. Instead, Fick's second law of diffusion can be used.

$$\frac{\partial C}{\partial t} = D \frac{\partial^2 C}{\partial x^2} \quad (A.5)$$

Where D is the diffusion coefficient, t is time, x is the thickness and C the concentration. The

$$\frac{\partial C}{\partial t} = D \Delta C \quad (A.6)$$

APPENDIX B : SEM, UV-VIS AND FTIR SPECTRUM

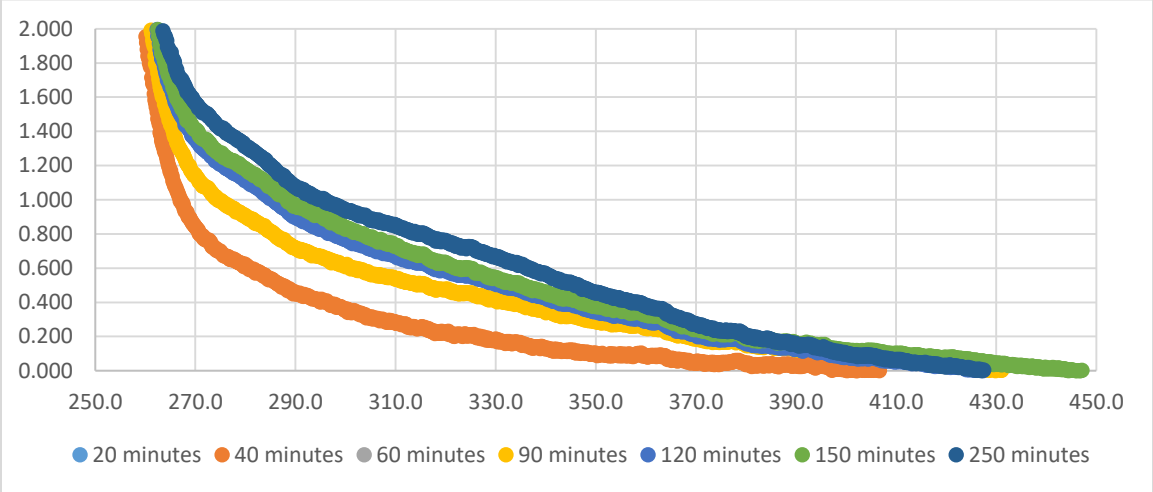

Figure B.1. Aramid deprotonation as function of time

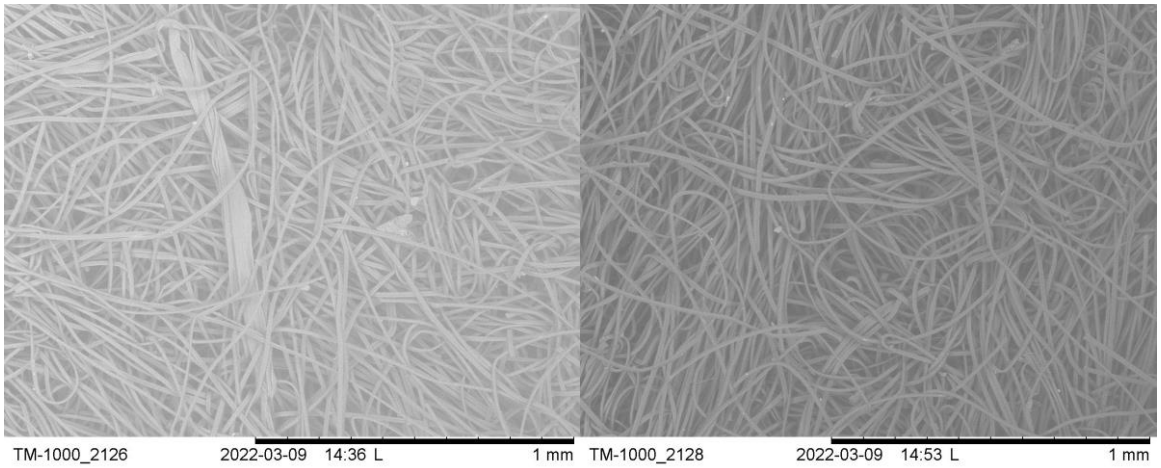

Figure B.2. Nonwoven before and after scouring

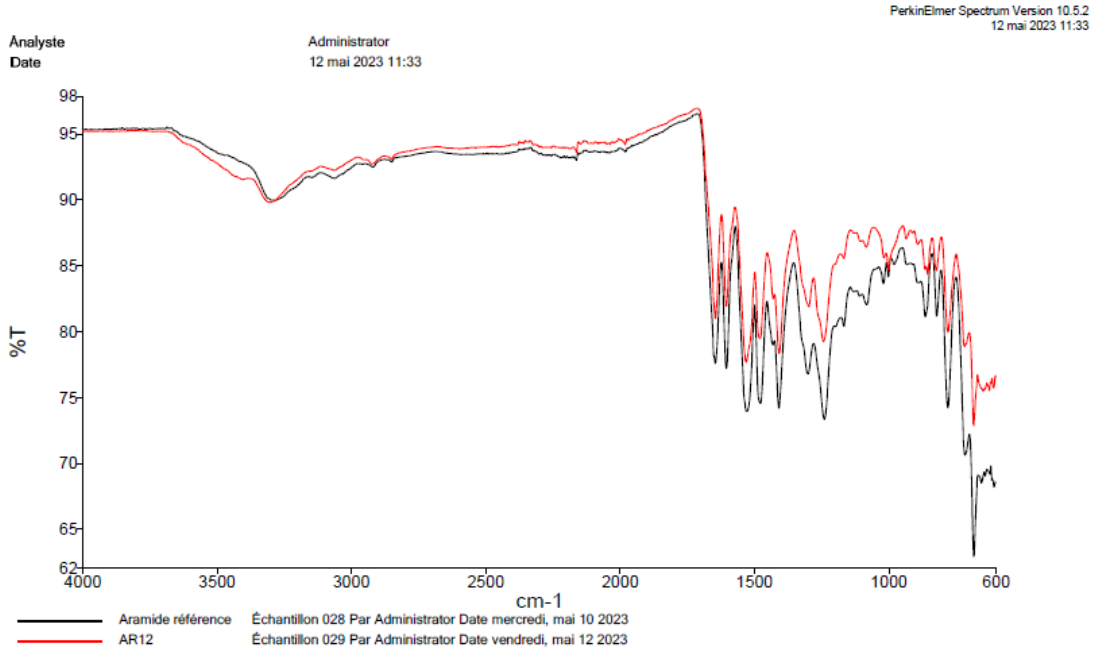

Figure B.3 FTIR of aramid before (black) and after (red) scouring

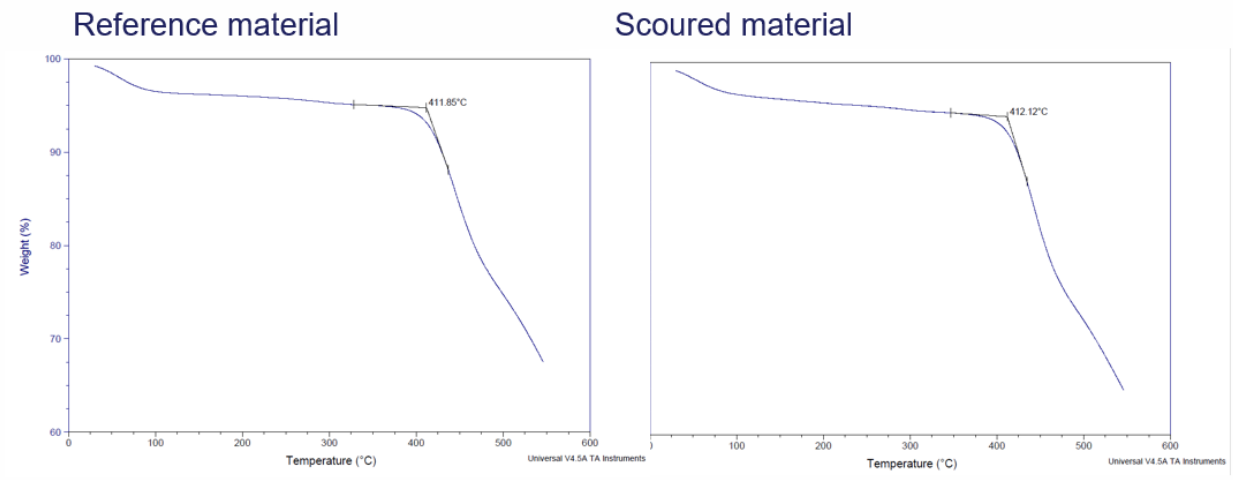

Figure B.4. Thermogravimetric analysis before and after scouring